Contrails

WADC TECHNICAL REPORT 59-337
PART III

SYNTHESIS AND PURIFICATION OF DIELECTRIC MATERIALS

W. C. DIVENS
D. H. HOGLE
D. W. LEWIS
P. A. TIERNEY
T. W. DAKIN
D. BERG

WESTINGHOUSE ELECTRIC CORPORATION
RESEARCH LABORATORIES
BEULAH ROAD, PITTSBURGH 35, PA.

JUNE 1961

DIRECTORATE OF MATERIALS & PROCESSES
CONTRACT No. AF 33(616)-5979
PROJECT No. 7371

AERONAUTICAL SYSTEMS DIVISION
AIR FORCE SYSTEMS COMMAND
UNITED STATES AIR FORCE
WRIGHT-PATTERSON AIR FORCE BASE, OHIO

McGregor & Werner, Inc., Dayton, O.
400 - November 1961 - 7-189 & 190

Approved for Public Release

Contrails

FOREWORD

This report was prepared by the Research Laboratories of Westinghouse Electric Corporation under USAF Contract No. AF 33(616)-5979. This contract was initiated under Project No. 7371, "Applied Research in Electrical Electronic, and Magnetic Material," Task No. 73710, "Applied Research on Dielectric Materials." The work was administered under the direction of the Materials Central, Directorate of Advanced Systems Technology, Wright Air Development Division, with Mr. W. G. D. Frederick acting as project engineer.

This report covers work conducted from 1 July 1960 to 31 December 1960.

Persons engaged on this project include: Scientists, W. C. Divens, D. H. Hogle, D. W. Lewis, P. A. Tierney; Technicians, V. DeNunzio, M. H. Ihrig, Miss M. M. Rutter, E. G. Tirk, P. F. Walsh; Supervisory and Advisory Scientists, T. W. Dakin, Daniel Berg.

We should like to acknowledge the contribution of Mr. John Kijowsky of the Central Technical Services, Central Laboratories, for the electron micrographs of anodized aluminum surfaces.

Approved for Public Release

Contrails

ABSTRACT

This is the final report on a contract to synthesize and purify inorganic dielectrics to achieve better dielectric properties at high temperatures up to 500°C. The research program has concentrated particularly on boron nitride and aluminum oxide, with some work on several other materials. During the last year, effort has concentrated on preparing thin films of these materials and evaluating their dielectric properties at high temperature. Thin films of boron nitride and anodically formed alumina have been developed with quite satisfactory dielectric properties at 500°C. Work on arc plasma jet sprayed inorganic films starting with high purity materials has yielded only films with inferior dielectric properties, indicating contamination from the arc electrodes.

PUBLICATION REVIEW

This report has been reviewed and is approved.

FOR THE COMMANDER:

Jules I. Wittebort

JULES I. WITTEBORT
Chief, Thermophysics Branch
Physics Laboratory
Materials Central

Approved for Public Release

Contrails

TABLE OF CONTENTS

	Page
GENERAL INTRODUCTION	1
SECTION I. BORON NITRIDE	3
A. ELECTRICAL PROPERTIES OF BORON NITRIDE SAMPLES	3
1. CABAL GLASS BONDED BORON NITRIDE PRESSED BODIES	3
2. COMMERCIAL SAMPLE OF BORON NITRIDE ROD	4
3. EFFECT OF HEATING AT 600°C ON THE ELECTRICAL PROPERTIES AT LOWER TEMPERATURES	4
4. ELECTRICAL PROPERTIES OF BORON NITRIDE PRESSED FOR SHORTER TIMES AT LOWER TEMPERATURES	4
5. GRADATION OF IMPURITIES IN BORON NITRIDE SAMPLES	5
B. REACTION OF BORON HALIDES AND AMMONIA	5
1. REACTION OF AMMONIA WITH EXCESS BORON TRICHLORIDE	6
2. REACTION OF BORON TRICHLORIDE WITH EXCESS AMMONIA	6
3. REACTION OF BORON TRIBROMIDE WITH EXCESS AMMONIA	9
4. PREPARATION OF BORON NITRIDE	9
C. REACTION OF BORON WITH NITROGEN AT 1200°C	10
D. BORON NITRIDE CAPACITORS	10
E. SUMMARY	12
SECTION II. BORON PHOSPHIDE	24
A. PREPARATION OF BORON PHOSPHIDE BY REACTION OF THE ELEMENTS	24
B. REACTION OF BORON TRICHLORIDE WITH HYDROGEN AND PHOSPHOROUS	25
C. THERMAL DECOMPOSITION OF THE PHOSPHINE-BORON TRICHLORIDE ADDITION COMPOUND	25
D. THERMAL DECOMPOSITION OF THE PHOSPHINE-BORON TRIBROMIDE ADDITION COMPOUND	27
E. CONCLUSIONS	27
SECTION III. APPLICATION OF INORGANIC DIELECTRICS BY PLASMA JET	37
A. INTRODUCTION	37
B. ALUMINA	37
C. MAGNESIA	40

Approved for Public Release

Contrails

	Page
D. SILICA	40
E. FLUOROPHLOGOPITE MICA	41
F. BORON NITRIDE	41
G. BORON NITRIDE + 30% CABAL GLASS	41
H. CONCLUSIONS	41
SECTION IV. ANODIZED ALUMINUM	56
A. INTRODUCTION	56
B. APPARATUS	57
1. ANODIZING EQUIPMENT	57
a. PROTECTIVE ENCLOSURE	57
b. ANODIZING CELLS	58
c. CELL SCREENS	58
d. POWER SUPPLIES	58
2. TEST FACILITIES	59
a. TESTING OVENS	59
b. LIFE TEST OVEN	59
c. MEASURING INSTRUMENTS	59
C. FOIL PREPARATION	60
1. CHEMICAL POLISHING	60
2. HEAT TREATING OF ALUMINUM FOIL	61
D. ELECTRODES	63
1. SPUTTERED GOLD	63
2. EVAPORATED ALUMINUM	63
E. ANODIZING CONDITIONS	63
1. THE POROUS LAYER	63
2. THE BARRIER LAYER	67
F. DIELECTRIC PROPERTIES	68
G. LIFE TESTS	71
H. SUMMARY	73
GENERAL CONCLUSIONS AND SUGGESTIONS FOR FUTURE WORK	100

Approved for Public Release

Contrails

LIST OF ILLUSTRATIONS

Figure		Page
1	Boron Nitride (90%), Cabal Glass (10%) Hot-pressed 2 hrs. at 1800°C and 2000psi. N_2 Envelope.	13
2	Boron Nitride (80%), Cabal Glass (20%) Hot-pressed 2 hrs. at 1800°C and 2000 psi. N_2 Envelope.	14
3	Boron Nitride (70%), Cabal Glass (30%) Hot-pressed 1 hr. at 2000 psi and 1800°C.	15
4	Boron Nitride (Supplier X) Rod.	16
5	Boron Nitride (Supplier X) Hot-pressed in Degassed Graphite Die at 3000 psi and 1600°C for 3 hrs.	17
6	Boron Nitride (Supplier X) Hot-pressed in High Purity Graphite Die for 3 hrs. at 1800°C and 2550 psi. Sample Measured at 30% and 50% Relative Humidity (Room).	18
7	Boron Nitride (Supplier X) Hot-pressed for 45-min. at 1600°C and 2000 psi Graphite Die, N_2 Envelope.	19
8	Measurements on a Boron Nitride Sample at 500°C with Successively Larger Electrodes.	20
9	Boron Nitride (Supplier X) Hot-pressed at 1600°C and 3000 psi for 3 hrs. Measured After Heating for 7 Days at 500°C at a Pressure of 1 x 10^{-4} mm Hg.	21
10	Boron Nitride (Supplier Y) Hot-pressed at 1800°C and 2550 psi for 3 hrs. Measured after Heating for 7 Days at 500°C at a Pressure of 1 x 10^{-4} mm Hg.	22
11	Construction of a Boron Nitride Capacitor.	23
12	Photograph of Needle Growth of Boron Phosphide (50X).	24
13	Photograph of Growth Center of Boron Phosphide Crystals on Wall of Quartz Tube (50X).	25
14	Photograph of an Individual Boron Phosphide Crystal (100X).	26
15	Photograph of Cross Section of Boron Phosphide Crystal (1150X).	27
16	X-Ray Diffraction Pattern of Boron Phosphide Prepared from the Elements.	28

Approved for Public Release

Contrails

Figure		Page
17	X-Ray Diffraction Pattern of an Individual Crystal of Boron Phosphide.	29
18	X-Ray Diffraction Pattern of Boron Phosphide Vapor Deposited on Tantalum Foil.	30
19	X-Ray Diffraction Pattern of Boron Phosphide Vapor Deposited on Molybdenum.	31
20	IR Spectrum of $B Cl_3$ Gas.	32
21	IR Spectrum of PH_3 Gas.	33
22	IR Spectrum of H_3P:$B Cl_3$ Gas.	34
23	X-Ray Diffraction Pattern of Thin Film of Boron Phosphide.	35
24	Photograph of Alumina Coating Applied by Flame Spray (50X).	36
25	Photograph of Alumina Coating Applied by Plasma Jet (50X).	43
26	Schematic of Plasma Jet Gun.	44
27	Photograph of Aluminum Disc Coated with Alumina by Plasma Jet.	45
28	Photograph of Jig Holding Four Aluminum Discs in Path of Plasma Flame.	45
29	Electrical Properties of Alumina Applied to Aluminum Foil by Plasma Jet.	46
30	Electrical Properties of Magnesia Applied to Aluminum Foil by Plasma Jet.	47
31	Resistivity and RC Factor of Sintered and Plasma Jet Sprayed Alumina.	48
32	Dissipation Factor of Sintered and Plasma Jet Applied Alumina, (60 cy).	49
33	Resistivity of Fluorophlogopite Mica Paper and Plasma Jet Applied Film.	50
34	60 Cycle Properties of Fluorophlogopite Mica Paper and Plasma Jet Applied Film.	51
35	Two-minute Resistivity of Hot-pressed Boron Nitride Disc and Plasma Sprayed Film.	52
36	Dissipation Factor and Dielectric Constant of Hot-pressed Boron Nitride and Plasma Sprayed Film (60 Cy.).	53

Approved for Public Release

Contrails

Figure		Page
37	Two-minute Resistivity of Hot-Pressed Disc and Plasma Sprayed Film Composed of 70% Boron Nitride and 30% Cabal Glass.	54
38	Electrical Properties of Hot-Pressed Disc and Plasma Sprayed Film Composed of 70% Boron Nitride and 30% Cabal Glass (60 Cy.).	55
39	Anodizing Equipment.	74
40	Anodizing Cell.	75
41	Screen Separator Used in Cell.	76
42	Placement of Test Capacitors in Oven.	77
43	Life Test Oven and Samples.	78
44	Test Equipment.	79
45	Cross Section of Sample Capacitor.	80
46	Cross Section of Thick Oxide Section of Capacitor in Figure 45.	80
47	Large Grain Capacitor.	81
48	Effect of Grain Size on the Electrical Properties of Anodically Formed Al_2O_3 Film Capacitors.	82
49	Capacitor from Highly Cold Worked Aluminum.	83
50	Cross Section of a Sample Capacitor Showing Uneven Oxide Film.	83
51	Temperature Effects on the Solvation of the Oxide Barrier Layer.	84
52	Schematic Cross Section of Cell Base Pattern for 60 Volt, 2% Oxalic Acid Solution at 23°C and 500 V Tartaric Anodization. [After Keller etal., J. Electrochem. Soc. 100, 411 (1953)].	85
53	Initial Formation Voltage-Time Behavior with Various Anodizing Conditions.	86
54	Dielectric Loss as a Function of Frequency and D.C. Bias Voltage of a Micron Capacitor.	87
55	Capacitance as a Function of Frequency and D.C. Bias Voltage of a 5 Micron Capacitor.	88
56	Resistance Voltage Characteristics of a 5 Micron Capacitor.	89
57	Frequency Characteristics of the Loss and Capacitance for Capacitor LT-2C at 500°C.	90

Approved for Public Release

Contrails

Figure		Page
58	Resistance Voltage Characteristics of Capacitor LT-2C at 500°C.	91
59	Effects of Aging Time Under a Voltage Stress of 45 D.C. Volts for Capacitor LT-2C at 500°C.	91
60	Effects of Anodizing Temperature on the Electrical Properties of Anodized Aluminum Capacitors.	92
61	Development of Apparent Strain Lines Under the Counterelectrode of a Sample Capacitor Aged Under Electrical Stress.	93
62	Development of Bubbles Under the Counterelectrode for a Sample Capacitor Aged Under Electrical Stress.	94
63	Reverse Side of Capacitor in Figure 62.	94
64	Dielectric Properties of a 1.3 Micron Anodized Aluminum Capacitor. (No. 02)	95
65	Resistance-Voltage-Temperature Characteristics of a 1.3 Micron Anodized Aluminum Capacitor No. 02.	96
66	Electron Micrograph of High Purity, Large Grained and Polished Aluminum Anodized in 2% Oxalic Acid at 17°C and 5.8 ma/cm^2.	97
67	Electron Micrograph of High Purity, Annealed and Polished Aluminum Anodized in 2% Oxalic Acid at 0°C and 11.6 ma/cm^2.	98
68	Electron Micrograph of High Purity, Large Grained and Polished Aluminum Anodized in 0.1% Oxalic Acid, 0.1% Tartaric Acid at 0°C and 5.8 ma/cm^2.	99

Approved for Public Release

Contrails

Approved for Public Release

Contrails

GENERAL INTRODUCTION

During the later stages of this contract, the research effort has concentrated largely on preparing and evaluating thin films or coatings of inorganic dielectrics to achieve the best possible dielectric properties at high temperatures up to 500°C. It had been shown in the earlier stages of the contract that excellent properties could be achieved in molded blocks of materials such as boron nitride and alumina, if high purity materials were used to start with, and scrupulous care was used in maintaining their purity during fabrication. The same problems of maintaining purity were encountered, even to a greater degree, in preparing thin films of these same materials in a useable and measureable form. The most obvious use of such thin films with good dielectric properties is in a high temperature capacitor. Therefore simple capacitors have been made and evaluated during the course of the investigation.

Thin dielectric films are particularly subject to the effect of defects on their properties since the size of such defects whether they are projections of the metal electrodes, or impurity particles, may be as thick as the film. For this reason the dielectric properties measured on these films may be grossly affected by these imperfections, in addition to any more generally distributed impurities. Another characteristic of thin film dielectrics is the greater prominence of interfacial ionic polarization effects. This has been noticed particularly in the anodized aluminum studies, which have been about half of the effort during the later stages of the contract work. With this material, it has not been possible to duplicate the properties of the high purity sintered block material in a thin film. However relatively good dielectric properties have been achieved in these thin films.

A second phase of the investigation has been concerned with the study of thin films prepared by the relatively new technique of arc plasma jet spraying. Here the problem of contamination from the arc electrodes and nozzle were encountered. A variety of high purity starting materials were evaluated with this technique.

A third part of the investigation has been concerned with extended studies of hot molded boron nitride and the effects of added bonding agents on the high temperature dielectric properties. Preparation of the material in thin films of the order of 0.001" thick, suitable for capacitor construction has also been part of the program.

A side line of the boron nitride program has been a detailed study of the chemical reaction of boron trichloride or boron tribromide with ammonia. This reaction is of interest because it is one which could lead to a synthetic boron nitride of extreme purity.

In a fourth phase of the investigation, boron phosphide has been prepared by several methods, each of which has lead to a crystalline product of poor electrical insulation properties. It had been hoped that this III-V compound might have some of the excellent character of its analog, boron nitride.

Manuscript released for publication 27 February 1961 as a WADC Technical Report.

Approved for Public Release

Contrails

Throughout the program there has been an attempt to analyze and understand the results of the experimental investigations, particularly the high temperature dielectric properties of the materials prepared.

Approved for Public Release

Contrails

SECTION I. BORON NITRIDE

(P. A. Tierney)

A. ELECTRICAL PROPERTIES OF BORON NITRIDE SAMPLES

Because of the increased interest in insulation that can operate at temperatures even in excess of 500°C it was decided that measurement of electrical properties of boron nitride samples would be extended to include 600°C values. All samples of boron nitride were obtained from outside suppliers. Powdered samples were hot pressed into cylinders and then machined into discs 30-50 mils thick in order to measure electrical properties. All samples were left in the furnace at the highest temperature at which measurements were to be made for at least 16 hours before measurement. Values at lower temperatures were obtained as the sample was cooled. Some samples measured previously were remeasured in order to determine the effect of heating for 16 hrs. at 600°C on the electrical properties at lower temperatures. Table I contains a summary for all samples of the pressing conditions and densities, along with a cross reference to the figures which summarize the electrical properties.

TABLE I. PRESSED SAMPLES OF BORON NITRIDE

Supplier	Temp. (°C)	Pressure (psi)	Time (hrs.)	Die	Atmosphere	Den. (gm/cc)	Fig. No.
X[a]	1800	2000	2	Used Graphite[d]	N_2	2.1	1
X[b]	1800	2000	2	Used Graphite[d]	N_2	1.9	2
X[c]	1800	2000	2	Used Graphite[d]	N_2	1.8	3
X	--	--	-	-- --	--	2.2	4
X	1600	3000	3	Degassed Graphite	N_2	1.9	5,9
X	1800	2550	3	Degassed Graphite	N_2	1.6	6,10
X	1600	2000	0.75	Used Graphite[d]	N_2	2.0	7

a) 90% BN, 10% Cabal Glass.
b) 80% BN, 20% Cabal Glass.
c) 70% BN, 30% Cabal Glass.
d) A graphite die which had been degassed and used for pressing a sample of boron nitride was reused in pressing this sample, without further degassing.

1. Cabal Glass-Bonded Boron Nitride Pressed Bodies

Even though the electrical properties of boron nitride are outstanding at elevated temperatures, it is weak mechanically. Attempts to increase its mechanical strength and its pressability by using admixtures of boric acid lead to higher dissipation factors and lower volume resistivities. It was reasoned that other additives, particularly Cabal ($CaO-B_2O_3-Al_2O_3$) glasses which have relatively low losses at high temperature might increase physical strength without seriously affecting the electrical properties. The electrical properties of two boron nitride bodies containing 4% cabal glass were reported in WADC TR 59-337, Part I, Figs. 14 and 15. Boron nitride bodies containing 10, 20 and 30

Approved for Public Release

Contrails

percent cabal glass were prepared. Their electrical properties are summarized in Figs. 1, 2 and 3. All three samples have comparable electrical properties and these in turn are quite similar to those reported previously for the 4% cabal glass samples. Although the electrical properties of BN-cabal glass bodies do not change in the composition range, 4% - 30% cabal glass, there is no unambiguous proof as yet that the addition of cabal glass has no detrimental effect on the electrical properties of boron nitride.

2. Commercial Sample of Boron Nitride Rod

In WADC TR 59-337 Part I, Fig. 10, the electrical properties of a rod of boron nitride from supplier X were reported. The rod contained 10% ethanol-soluble boron (as % B_2O_3). Because of the high ethanol-soluble boron content supplier X agreed to send another sample of boron nitride to replace the first. The second sample contained 6% ethanol-soluble boron (as % B_2O_3). Its electrical properties, summarized in Fig. 4, are quite similar to the first sample in the temperature range 100-500°C. At 600°C the losses and dielectric constant were too high to measure.

3. Effect of Heating at 600°C on the Electrical Properties at Lower Temperatures

A sample of boron nitride which had shown excellent electrical properties at 500°C (cf. WADC TR 59-337 Part II, Fig. 5) was remeasured starting at 600°C after being heated at 600°C overnight. The electrical measurements are shown in Fig. 5. The resistivity is an order of magnitude higher at 500°C than that reported previously. The tan δ values at 60 cy, 1 KC and 100 KC are in contrast a factor of 10 higher than those reported previously. The reason for these contradictory differences from the results obtained on the previous measurement are not understood.

The above result contrasts with the very good agreement of successive measurements on another sample of boron nitride which was measured at 600°C and lower temperatures after being heated overnight at 600°C. The results are shown in Figure 6. This sample has been measured on two previous occasions and those results were reported in WADC TR 59-337, Part II, Fig. 2. The three sets of data are in good agreement in the range 100-500°C.

4. Electrical Properties of Boron Nitride Pressed for Shorter Time at Lower Temperature

It has been shown in previous reports that an upper time-temperature limit exists above which hot-pressing detracts from the electrical properties of boron nitride. The best electrical properties were obtained on samples pressed only for 2 hours at 1800°C or 3 hours at 1600°C. Hence it was of interest to shorten the time of pressing at the lower temperature. Fig. 7 shows the electrical properties of a boron nitride sample pressed for only 45 minutes at 1600°C. The losses are higher and the resistivity is lower than the sample pressed for 3 hours at 1600°C (cf. WADC TR 59-337, Part II, Fig. 5).

Approved for Public Release

Contrails

However, it should be pointed out that the graphite die used in pressing this sample was one that had been used before in pressing another sample of boron nitride. Therefore, it is possible that re-use of these high purity graphite dies introduces some impurity into the sample.

5. Gradation of Impurities in Boron Nitride Samples

The variation in volume resistivity and tan δ as the electrode diameter was increased on a pressed sample of boron nitride was shown in WADC TR 59-337, Part II, page 8. There it appeared that the resistivity went through a maximum and the tan δ went through a minimum at an electrode diameter of about 1 in. This work was repeated, but no such maximum or minimum was observed. The results of the second run are summarized in Figure 8. The values of tan δ at all frequencies decrease markedly with increasing electrode diameter, and the resistivity increases so rapidly as to be out of proportion to the increase in electrode diameter. Therefore, this improvement in electrical properties must be attributed, at least in part, to some factor other than a decrease in impurities with increase in electrode diameter.

One explanation of these unusual results was that a volatile impurity was being removed during the application of the gold electrodes by vapor deposition. In order to test this explanation two samples of boron nitride whose electrical properties had been measured previously were placed in a quartz tube furnace and heated to 500°C. while being evacuated to 10^{-5} mm Hg. After seven days of heating in vacuum the samples were removed. Their electrical properties were measured in the temperature range 100°C - 500°C beginning at the higher temperature. The data are shown in Figs. 9 and 10. The data before treatment of the sample of Fig. 9 are shown in Fig. 5. The resistivity curves for the two sets of data are practically identical. At temperatures above 300°C the values for tan δ are in good agreement, but at temperatures of 300°C and lower the values of tan δ are higher for the sample after it was heated in vacuum.

The previous data obtained on the sample of Fig. 10 are shown in the same figure. Here again the curves cross each other between 300 and 400°C.

There is no evidence from the information above that heating boron nitride under high vacuum improves the electrical properties. And consequently, the improvement in electrical properties observed with increasing electrode diameter still remains unexplained.

B. REACTION OF BORON HALIDES AND AMMONIA

In WADC TR 59-337, Part I, the preparation of boron nitride from the reaction of boron trichloride and ammonia was described. It was observed that a compound 2 $NH_3 \cdot BCl_3$ was formed in excess boron trichloride while another compound was formed in excess ammonia. No report of the compound $2NH_3 \cdot BCl_3$ was found in the literature, and the existence and stoichiometry of compounds of higher ammonia content has not been clearly stated. This work was carried out between 50 and 150 years ago and since then the reactions of boron halides with amines has received more attention than the reactions of boron halides with the simple ammonia molecule. Hence it was of interest to investigate the compound $2NH_3 \cdot BCl_3$ in more detail and to extend the study to higher ammonia contents.

Approved for Public Release

Contrails

1. The Reaction of Ammonia with Excess Boron Trichloride

In order to establish the stoichiometry of the reaction of boron trichloride and ammonia in the presence of excess boron trichloride, the reactants were measured into a break-tip ampule from the standard bulb of a high vacuum system and sealed off. Equimolar amounts of the reactants to 400% excess of boron trichloride were used so that in the cases of large excesses liquid boron trichloride remained in the tube after it had warmed to room temperature. The reactions were carried out either by allowing the reactants to warm to -80°C or to room temperature. After standing at room temperature for 2 weeks the tubes were attached to the vacuum system, cooled with liquid nitrogen and then opened. The excess boron trichloride was recovered as the tube warmed to room temperature and transferred to the standard bulb for measurement. The only volatile product recovered in this manner was boron trichloride. The ratio of ammonia to boron trichloride in the white solid product was 2:1 whether the reaction was carried out by warming to room temperature or only to -78°C. This final ratio was independent of the initial mole ratio of reactants and pressure of the excess boron trichloride.

X-ray diffraction patterns on the white solid product were obtained by carrying out the reaction in a tube which was constricted near the top and fitted with a side arm which lead through a pyrex-quartz graded seal to a quartz x-ray diffraction capillary. Six pyrex glass beads were placed in the tube. The tube was then sealed to the vacuum system. After condensing the reactants in the tube as before, the reaction was allowed to take place by warming to -78°C or to room temperature. The excess boron trichloride was removed after reaction. The tube was removed from the line by sealing off the constriction. The reaction product was pulverized by shaking the tube and glass beads. Then it was tapped into the capillary tube and sealed off again under vacuum. The results of a typical diffraction pattern on the product are shown in the second column of Table II. These patterns also showed a sharp pattern for NH_4Cl but those lines are not included in Table II.

X-ray diffraction patterns were obtained on products formed under different reaction times and pressures. However, the patterns for products formed in excess boron trichloride, like their ratios of NH_3 to BCl_3, remained essentially the same.

No evidence for the compound, $3NH_3 \cdot 2BCl_3$, reported by Berzelius[1] was obtained. It has been established, however, that the compound, $2NH_3 \cdot BCl_3$, is not a simple addition compound but rather a mixture consisting of ammonium chloride and at least one other compound.

2. The Reaction of Boron Trichloride with Excess Ammonia

One mmole of boron trichloride and six mmoles of ammonia were condensed into a reaction flask fitted with a manometer on the vacuum line. Upon warming to room temperature from -196°C a vigorous reaction took place with the formation of a white solid material. In cases where the excess ammonia was recovered immediately after the flask reached room temperature the mole ratio of

Approved for Public Release

Contrails

TABLE II

X-RAY DIFFRACTION DATA FOR BORON HALIDES AND AMMONIA*

d spacing	2 $NH_3 \cdot BCl_3$	4 $NH_3 \cdot BCl_3$	4 $NH_3 \cdot BBr_3$
6.8	VW		
6.2		VVW	
5.3	VW		
4.2	MS	VVW	
3.91			W
3.40			MW
3.30	VVW		
2.87	MS		
2.69	W		
2.55	VVW		
2.45	VVW		
2.43			W
2.40		W	
2.16		MW	
2.11	VVW		
2.06			VVW
2.05	VVW		
1.96			VVW
1.87	VW		
1.54		VW	
1.53			VVW
1.49	VVW		
1.44	VVW		
1.33	VVW		
1.27	VVW		
1.25		VW	

* The patterns contained lines corresponding to the ammonium halides in each case, but these lines are not reported here. The "d" spacings were measured on Nies chart and the intensities of the lines were measured visually.

S strong
W weak
M moderate
V very

Approved for Public Release

Contrails

ammonia to boron trichloride in the product was 4:1. If, however, the product was allowed to stand at room temperature in the presence of ammonia gas, the ammonia was slowly and irreversibly taken up by the white solid, eventually forming a product corresponding to the empirical formula, $9NH_3 \cdot 2BCl_3$. Reactions carried out in sealed tubes with large excesses of ammonia also formed $9NH_3 \cdot 2BCl_3$ after standing for 2 weeks at room temperature. Again the final mole ratio in the product was independent of the mole ratio of reactants, temperature, and presence of ammonia.

X-ray diffraction patterns on the compounds $4NH_3 \cdot BCl_3$ and $9NH_3 \cdot BCl_3$ were obtained in the same way as the pattern on $2NH_3 \cdot BCl_3$ described previously. The compound $9NH_3 \cdot 2BCl_3$ gave a pattern containing only lines corresponding to NH_4Cl. If the reaction may be represented by an equation similar to the one proposed by Joannis[7] for the compound $9NH_3 \cdot 2BBR_3$,

$$2BCl_3 + 9NH_3 \longrightarrow B_2(NH)_3 + 6NH_4Cl$$

then it must be concluded that $B_2(NH)_3$ gives no x-ray diffraction pattern. On the other hand, the 4:1 addition compound in addition to lines corresponding to NH_4Cl gave lines belonging to at least one other crystalline product. (cf. 3rd column of Table II). In Table II it is apparent that the crystalline product, other than NH_4Cl, present in $2NH_3 \cdot BCl_3$ and $4NH_3 \cdot BCl_3$ are not the same.

X-ray diffraction patterns on compounds containing a mole ratio of NH_3 to BCl_3 of 3:1 gave diffraction patterns corresponding to a mixture of the 2:1 and 4:1 compounds. No lines corresponding to B-trichloroborazole were obtained. Brown and Laubengayer[2] reported the formation of trace amounts of B-trichloroborazole from the reaction of ammonia and boron trichloride but no experimental details were given. Since they did prepare the compound by heating NH_4Cl and BCl_3 to 110°C it is likely that B-trichloroborazole could be formed when an excess of BCl_3 is heated with ammonia to the same temperature. In this case the reaction would be between the NH_4Cl formed from the BCl_3 and NH_3 and the excess BCl_3, and not according to the simple equation:

$$3\ BCl_3 + 9\ NH_3 \longrightarrow B_3\ N_3\ Cl_3\ H_3 + 6\ NH_4\ Cl$$

McDowell and Keenan[3] studied the reaction of BI_3 and ammonia and wrote the equation:

$$2\ BI_3 + 9\ NH_3 \longrightarrow B_2(NH)_3 + 6\ NH_4I.$$

X-ray diffraction patterns on the product showed only lines corresponding to the ammonium iodide. This equation is consistent with the equation:

$$2\ BCl_3 + 9\ NH_3 \longrightarrow B_2(NH)_3 + 6\ NH_4Cl$$

which represents the products formed from BCl_3 and excess ammonia. The absence of lines other than those for ammonium chloride in the x-ray diffraction

Approved for Public Release

Contrails

patterns in this case, together with the absence of lines other than NH_4I in the case of BI_3 and excess ammonia indicate that boron imide, $B_2(NH)_3$, is not crystalline. It may be polymeric, i.e.,

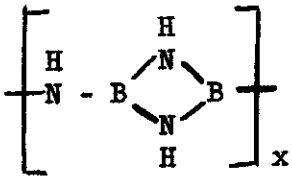

No evidence for the compound, $BCl_3 \cdot 6NH_3$ reported by Joannis[4] was obtained. However, Joannis carried out his reactions at 0°C, where there is the possibility of solvating the products with ammonia.

3. Reaction of Boron Tribromide with Excess Ammonia

The reaction of boron tribromide with excess ammonia was studied, using the same techniques as those employed in the study of boron trichloride with excess ammonia. The reaction was observed to proceed in a similar manner. X-ray diffraction patterns on the compound $2BBr_3 \cdot 9NH_3$ again showed only lines corresponding to ammonium bromide. The equation consistent with the ones for BCl_3 and BI_3 is the one proposed by Joannis for this reaction:

$$2\ BBr_3 + 9\ NH_3 \longrightarrow B_2(NH)_3 + 6NH_4Cl$$

X-ray diffraction patterns for the compound $4NH_3 \cdot BBr_3$ showed lines corresponding to ammonium bromide and at least one other crystalline compound. (cf. last column Table II). From the table it is evident that the crystalline products other than the ammonium halides formed from $4NH_3 \cdot BCl_3$ and $4NH_3 \cdot BBr_3$ are not the same. It seems reasonable then to conclude that these crystalline compounds contain chlorine atoms in one case and bromine atoms in the other case. Both compounds react with ammonia to form boron imide.

Besson[5] studied the reaction of boron tribromide and ammonia, and reported the formation of a white solid of empirical formula, $4NH_3 \cdot BBr_3$ at 0°C. Upon warming to 10°C the compound absorbed ammonia slowly to form $9NH_3 \cdot 2BBr_3$, but Besson considered this absorption to be of a physical nature.

In reviewing the literature on the reaction of boron halides with ammonia, Martin[6] suggested that any molecular addition compounds formed were easily dissociated into boron imide and ammonium halide. This certainly seems to be the case when an excess of ammonia was used in the reaction, but the existence of compounds other than boron imide and ammonium halide was demonstrated here when the mole ratio of reactants was lowered to 4:1. It has also been shown that at room temperature, the product of the reaction depends only on the mole ratio of the reactants.

4. Preparation of Boron Nitride

One of the difficulties encountered in the preparation of boron nitride from boron trichloride and ammonia was in separating the by-product,

Approved for Public Release

Contrails

ammonium chloride. Vacuum sublimations resulted in loss of the flocculent boron nitride and removal of ammonium chloride by washing with water lead to contamination of the boron nitride with boric acid. The similarity of the reaction of boron tribromide with ammonia to that of the trichloride and ammonia, together with the solubility of ammonium bromide in anhydrous ethyl ether, suggested the following method of preparation.

A mixture of ammonia and boron trichloride in a ratio of 4:1 was sealed in a quartz tube and heated at 950-1000°C for 16 hrs. The tube was then cooled and opened. The white solid was washed with anhydrous ethyl ether to remove the ammonium bromide. X-ray diffraction patterns on the residue contained only lines corresponding to boron nitride. Attempts to press the boron nitride into discs for electrical measurement however were unsuccessful.

C. REACTION OF BORON WITH NITROGEN AT 1200°C

G. W. Rowe [Wear 3, #4, 274 (1960)] reported the preparation of a film of boron nitride on boron by heating the boron to 1200°C and passing nitrogen over it for a period of 4-5 hours. Measurements were made on the frictional behavior of the deposited film but no measurements of electrical properties were reported. The film was reportedly hard and durable even though it was not visible to the naked eye. Its identity as boron nitride was established by electron diffraction patterns.

Samples of crystalline boron which had been heated in the course of our investigation in a stream of nitrogen at 1200°C for 6 hours appeared to be more conducting than the original boron. Electron diffraction patterns on other samples of boron which had been heated under the same conditions did not show the presence of BN.

D. BORON NITRIDE CAPACITORS

Previous capacitors made from aluminum foil and boron nitride by cold pressing and heating to 500°C had an RC factor at 500°C of 0.59 sec., but shorted after 8 hours at 500°C.

Capacitors which do not short after 100 hours at 500°C have been prepared from boron nitride and aluminum, molybdenum and platinum metal foils. This has been accomplished in part by careful chemical and physical polishing of the metal discs after cutting. In addition, the boron nitride content of the deposited film was increased to 7-10 times the amount by weight of organic binder material. Such a low organic content made possible the use of n-butyl-iso-butyl methracrylate as the binding material. Finally, in order to decrease further the probability of flaws in the dielectric film the metal was either coated on both sides or a piece of boron nitride - methracrylate film was placed between the metal discs. The film was prepared by spraying a slurry of boron nitride and methracrylate in acetone onto a piece of Teflon and then stripping it off.

Typical electrical properties of boron nitride capacitors are shown in Table III. The lower RC factors in the case of molybdenum foil capacitors may be attributed to the formation of molybdenum oxides on the metal surface at 500°C. In these experimental capacitors the number of cubic inches per microfarad is ca. 40 in the case of molybdenum capacitors and ca. 70 in the

Approved for Public Release

Contrails

case of aluminum or platinum capacitors. The volume of the case is excluded in these calculations.

TABLE III. ELECTRIC PROPERTIES OF BORON NITRIDE CAPACITORS[a]

Metal	No. of Plates[b]	Dissipation Factor (%)[c]	Capacitance (μμf)	RC Factor (megohm-μf)	Temp. (°C)	Time at Temp. (hrs.)
Mo	3	7	740	0.7	500	75
Mo	5	9	1320	0.6	500	100
Pt	4	2.5	640	12.5	500	24
Pt	4	2.5	600	0.2	600	75
Al	4	0.3	650	14.3	500	100

a) Approximate thickness of the dielectric film is 3 to 5 mils. All capacitors withstood 300 volts DC at temperature and were aged with an applied DC voltage of 225.
b) Area of each plate is 2.4 $in.^2$, foil thickness 1 mil.
c) 1 Kc

Figure 11 shows an unassembled and assembled boron nitride capacitor. Two foil discs have been coated with a boron-nitride slurry in n-butyl-iso-butyl methracylate. The capacitor is assembled by interleaving the coated discs with the uncoated discs and placing them on the supporting boron nitride disc. The boron nitride powder near the top of the photograph is either cold pressed into another disc and placed on top of the stacked foils or cold pressed onto the foil and bottom boron nitride disc in a die. Stainless steel plates are placed on the top and bottom of the boron nitride encased discs and bolted together. The silver wire leads are silver-soldered to the tabs protruding from each side of the capacitor.

A significant improvement was made in the construction of boron nitride capacitors by using the following technique for obtaining a coating of BN on the metal foil. The 2 in. diameter foil discs were taped to a piece of metal plate and placed under a 5 in. diameter 325 mesh screen. A small amount (ca. 0.1 gm.) of finely divided boron nitride powder was placed on the screen and then blown through it by a blast of air from an air gun. The boron nitride so blown through the screen formed a thin, smooth layer on the metal foil. The foil was removed and dipped in a dilute (1 gm. of n-butyl-isp-butyl methracylate in 100 ml. of acetone) acrylic lacquer solution. The spraying operation was repeated before the lacquer was completely dry. In this way coatings less than 1 mil thick could be obtained. Some data obtained on capacitors prepared in this manner are shown in Table IV.

Two pieces of aluminum metal which had been lapped smooth and flat were coated with boron nitride powder using the same techniques described above. The area of the blocks was 4 in^2 and the thickness of the boron nitride coating was 1 mil. The two pieces of coated metal were pressed together and held in place by bolting them between two stainless steel plates in the same manner as the capacitor plates were held together in the capacitors. After 168 hrs. at 500°C the capacitance of this test fixture was 1340 μμf. The resistance was 9,000 megohms. The dielectric constant was 1.54, calculated from the area and thickness of the dielectric and the capacitance of the test fixture. Such a low dielectric constant indicates that the boron nitride coating is of low density.

Approved for Public Release

Contrails

TABLE IV. ELECTRICAL PROPERTIES OF IMPROVED BN CAPACITORS AT 500°C

No. of Plates[a]	Capacitance (μμf)	Resistance (megohms)	RC Factor	Power Factor (% @ 1 KC)	Electric Strength	Hrs.@ 500°C 225 V DC
2	660	70,000	46.2	0.3	>300	168
3	1660	25,000	41.5	0.5	175	0
2	860	50,000	43.0	0.2	550	168
5	3050	16,000	48.8	0.4	>300	400
3	2330	10,000	23.3	0.6	100	0
3	1730	18,000	30.6	0.3	>300	1300
3	1610	5,600	9.0	0.4	>300	1200
3	1350	12,000	16.2	0.5	>300	168
3	1490	50,000	74.5	<0.1	>300	168

a 2 in. diameter discs of aluminum foil

Attempts to improve the dielectric constant of the boron nitride coatings by evaporating or sputtering gold or aluminum metal onto the surface were unsuccessful. The gold did not form continuous coatings on the surface at all. The application of 7 or 8 coatings of gold through vapor deposition may lead to continuous coatings as it did in the case of low density cold pressed samples of boron nitride, but only one vapor deposition or sputtering was tried in each case. After many attempts with the evaporation of aluminum metal onto the boron nitride coating, one film of aluminum that was electrically continuous was obtained. However, it did not improve the dielectric constant of the boron nitride.

E. SUMMARY

Additions of 4-30% cabal ($CaO-B_2O_3-Al_2O_3$) glasses have been added to improve the mechanical strength of pressed BN bodies. The strength increases while the electrical properties seem insensitive to the percentage of cabal glass in the 4-30% range. It has not been proved unambiguously whether the cabal glass affects the electrical properties of the mixture.

Capacitors have been prepared using BN as the dielectric. These capacitors have R-C factors as high as 74 at 500°C and have been life tested up to 1000 hours at this temperature. They have been able to withstand a 300 volt dc test. It is concluded that BN capacitors could be built having a volume of less than 10 cu. in per microfarad excluding the case.

The preparation of boron nitride from boron tribromide and ammonia instead of boron trichloride and ammonia offers the advantage of easy separation of the by-product ammonium halide while maintaining anhydrous conditions.

Studies of the reaction of boron trichloride and ammonia have shown that at room temperature simple addition compounds between boron trichloride and ammonia are not formed. The existence of compounds of stoichiometry, $2NH_3 \cdot BCl_3$, $4NH_3 \cdot BCl_3$ and $9NH_3 \cdot 2BCl_3$ is shown, and in each case the product is actually a mixture of ammonium chloride and another compound. The stoichiometry of the product obtained at room temperature depends only upon the mole ratio of the reactants if the temperature is not allowed to exceed 25°C.

Approved for Public Release

Contrails

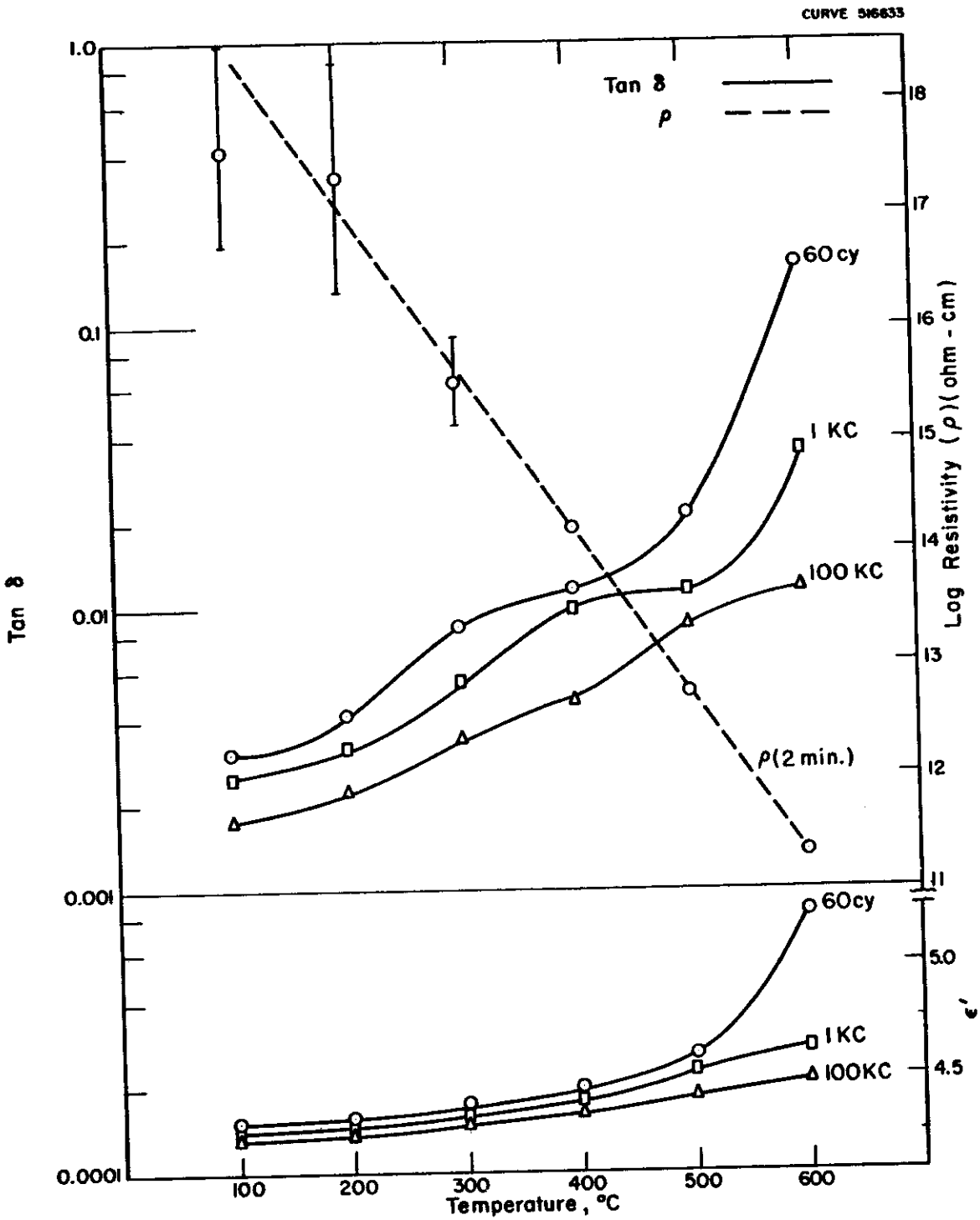

Fig. 1—Boron nitride (90%), Cabal glass (10%) hot-pressed 2 hrs. at 1800°C and 2000 psi. N_2 envelope.

Approved for Public Release

Contrails

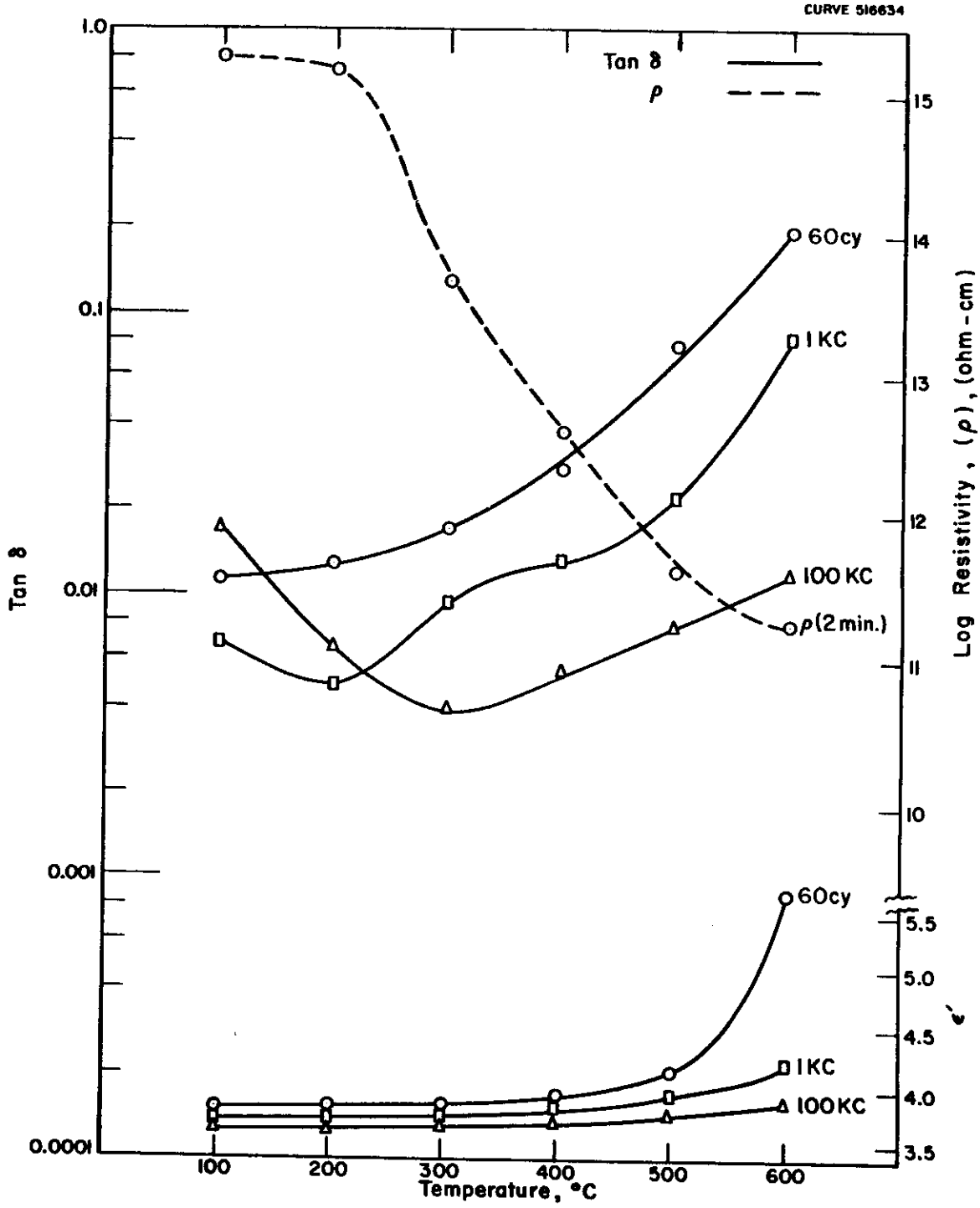

Fig. 2—Boron nitride (80%), Cabal glass (20%) hot-pressed 2 hrs. at 1800°C and 2000 psi. N_2 envelope.

Approved for Public Release

Contrails

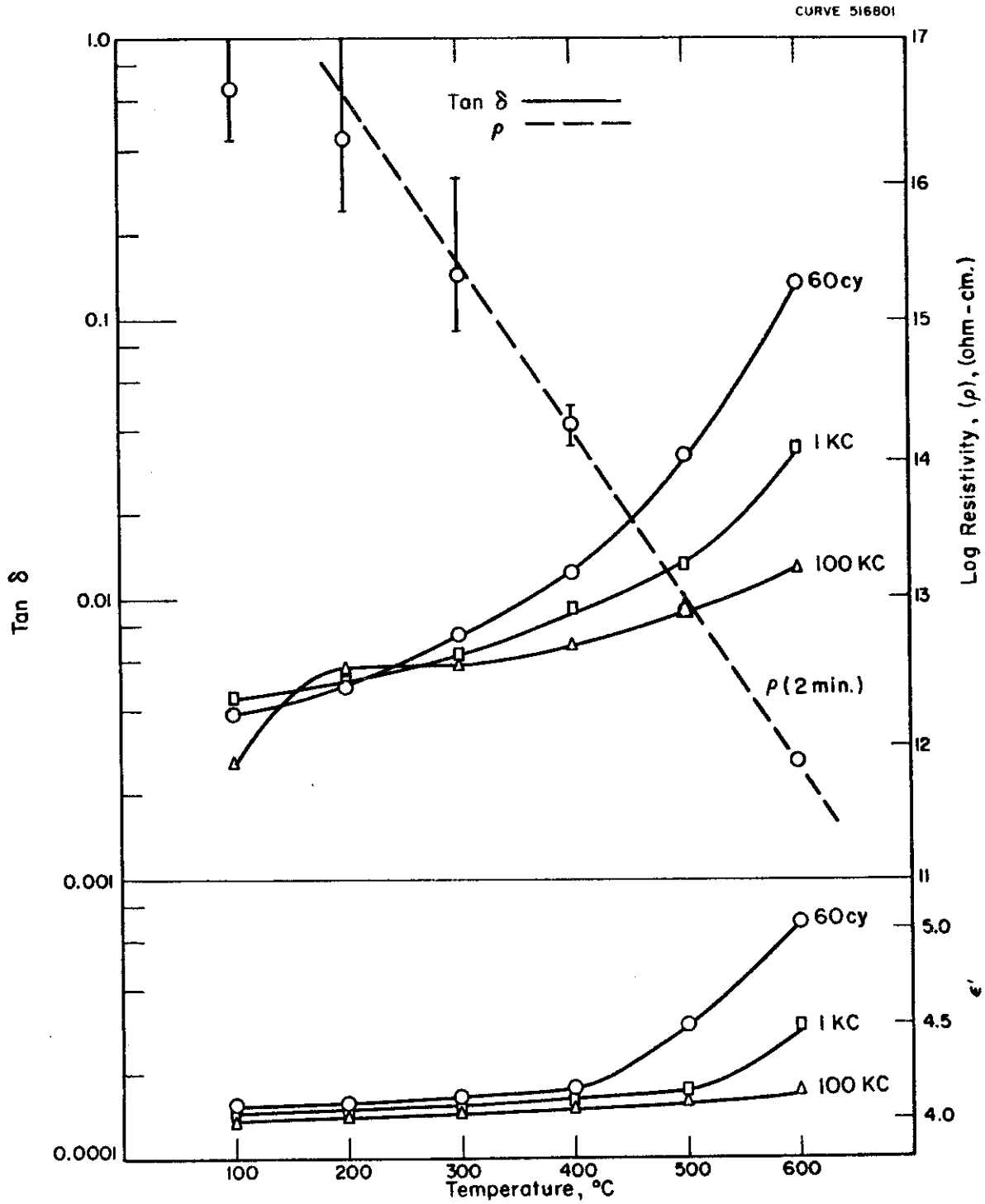

Fig. 3 – Boron nitride (70%) - cabal glass (30%) hot pressed 1 hr at 2000 psi and 1800 °C.

Approved for Public Release

Contrails

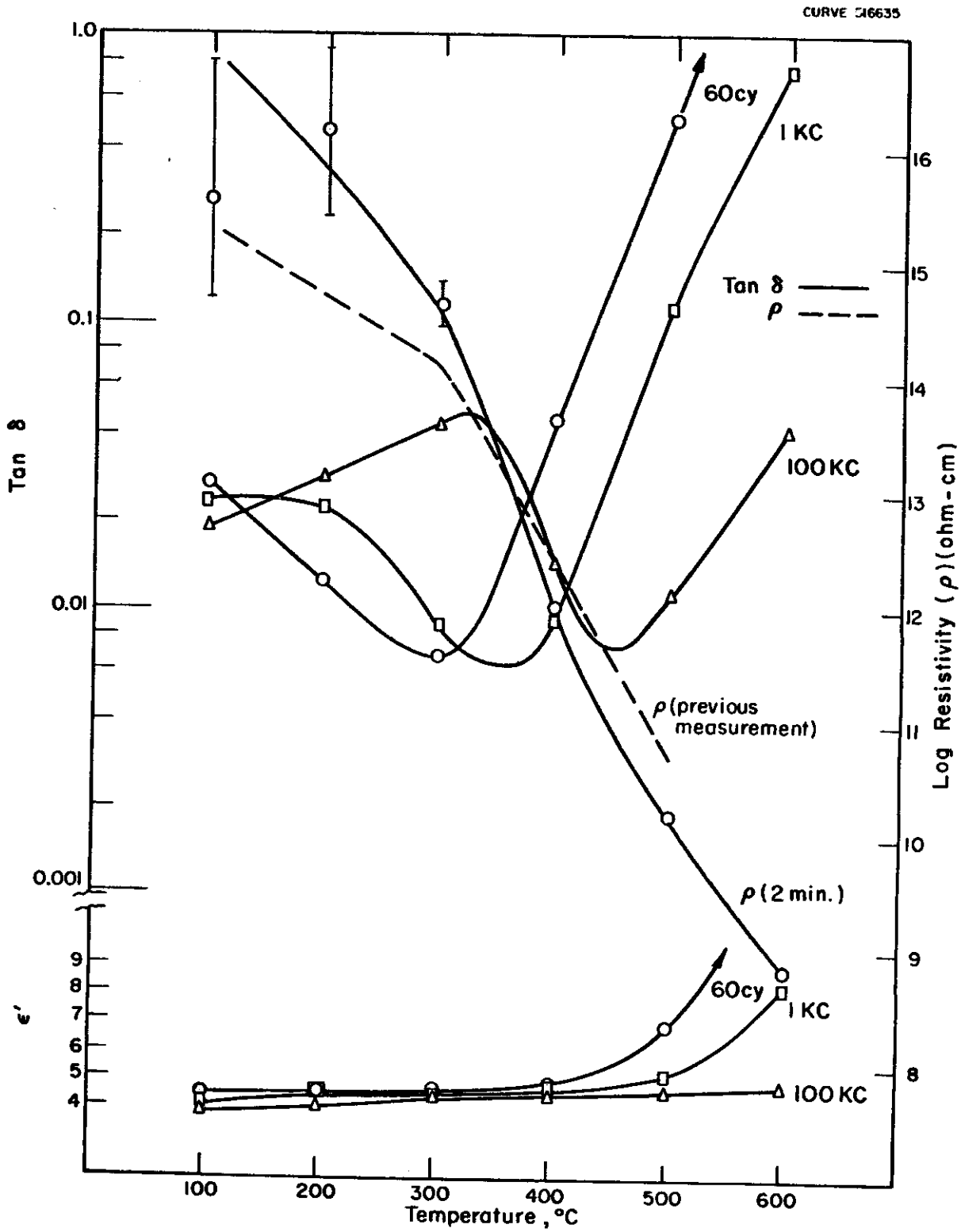

Fig. 4—Boron nitride (supplier X) rod.

Approved for Public Release

Contrails

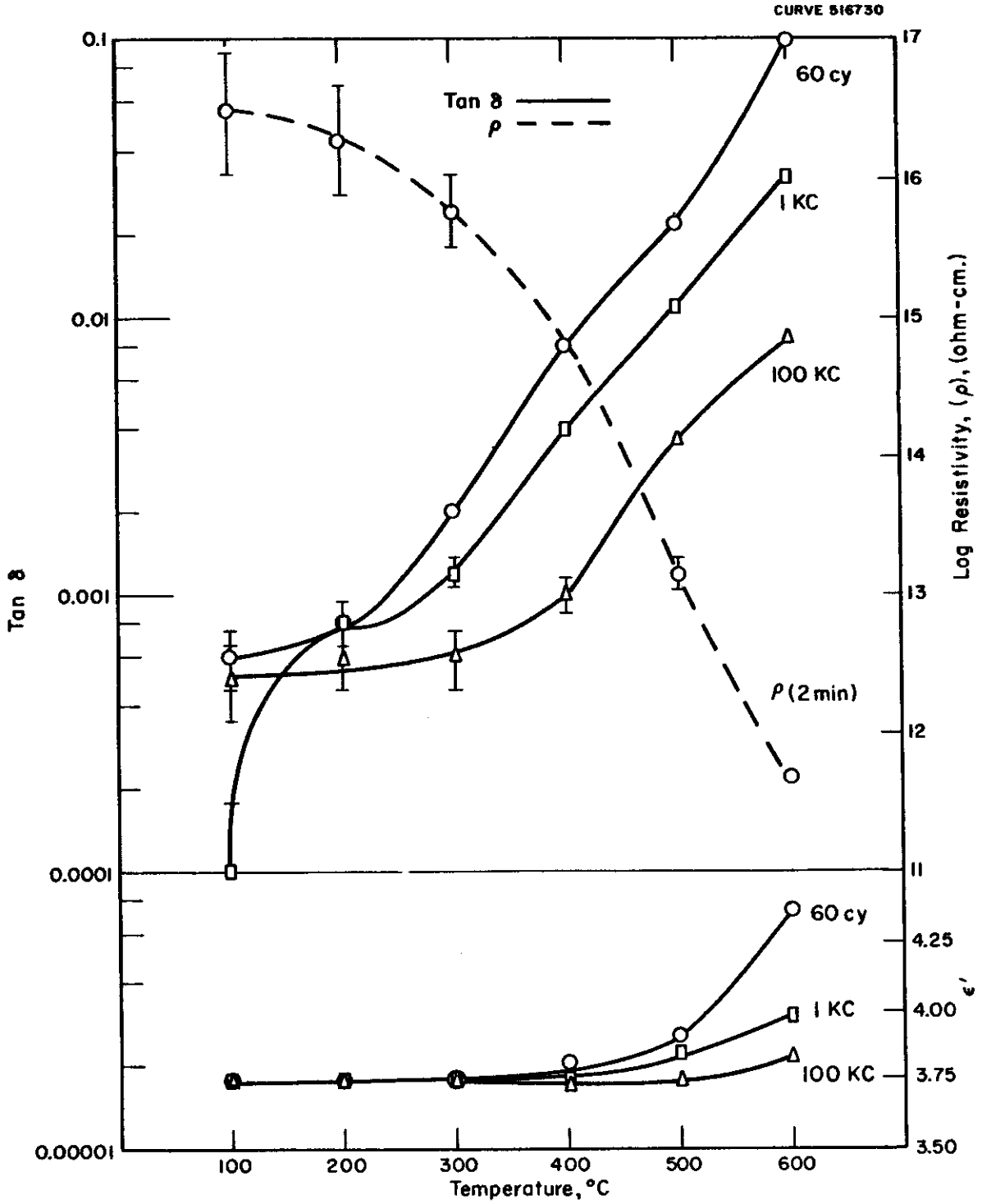

Fig. 5 - Boron nitride (supplier X) hot pressed in degassed graphite die at 3000 psi and 1600°C for 3 hours.

Approved for Public Release

Contrails

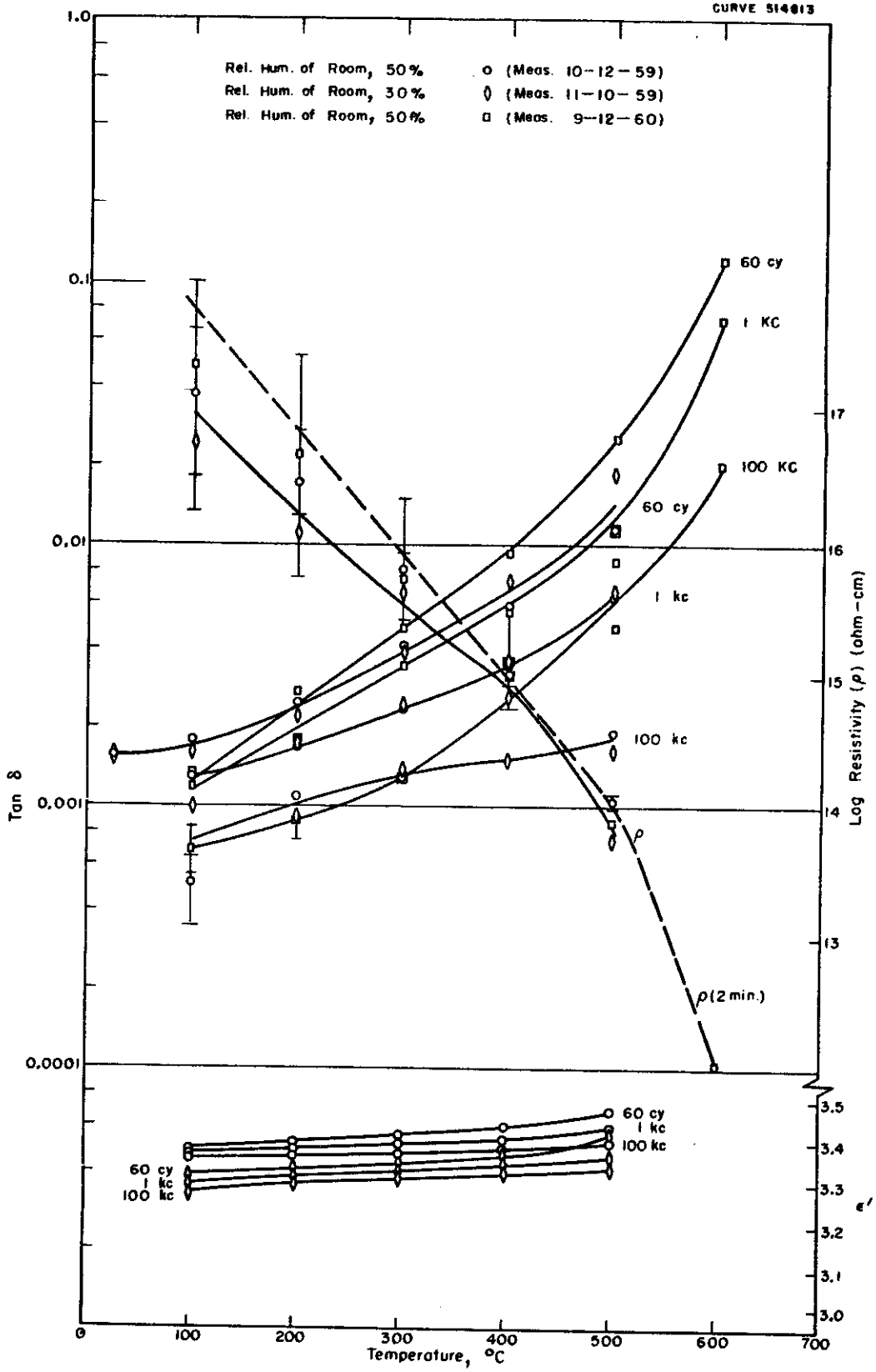

Fig. 6 – Boron Nitride (supplier x) hot pressed in high purity graphite die for 3 hrs. at 1800 °C and 2550 psi. Sample measured at 30 % and 50 % relative humidity (room).

Approved for Public Release

Contrails

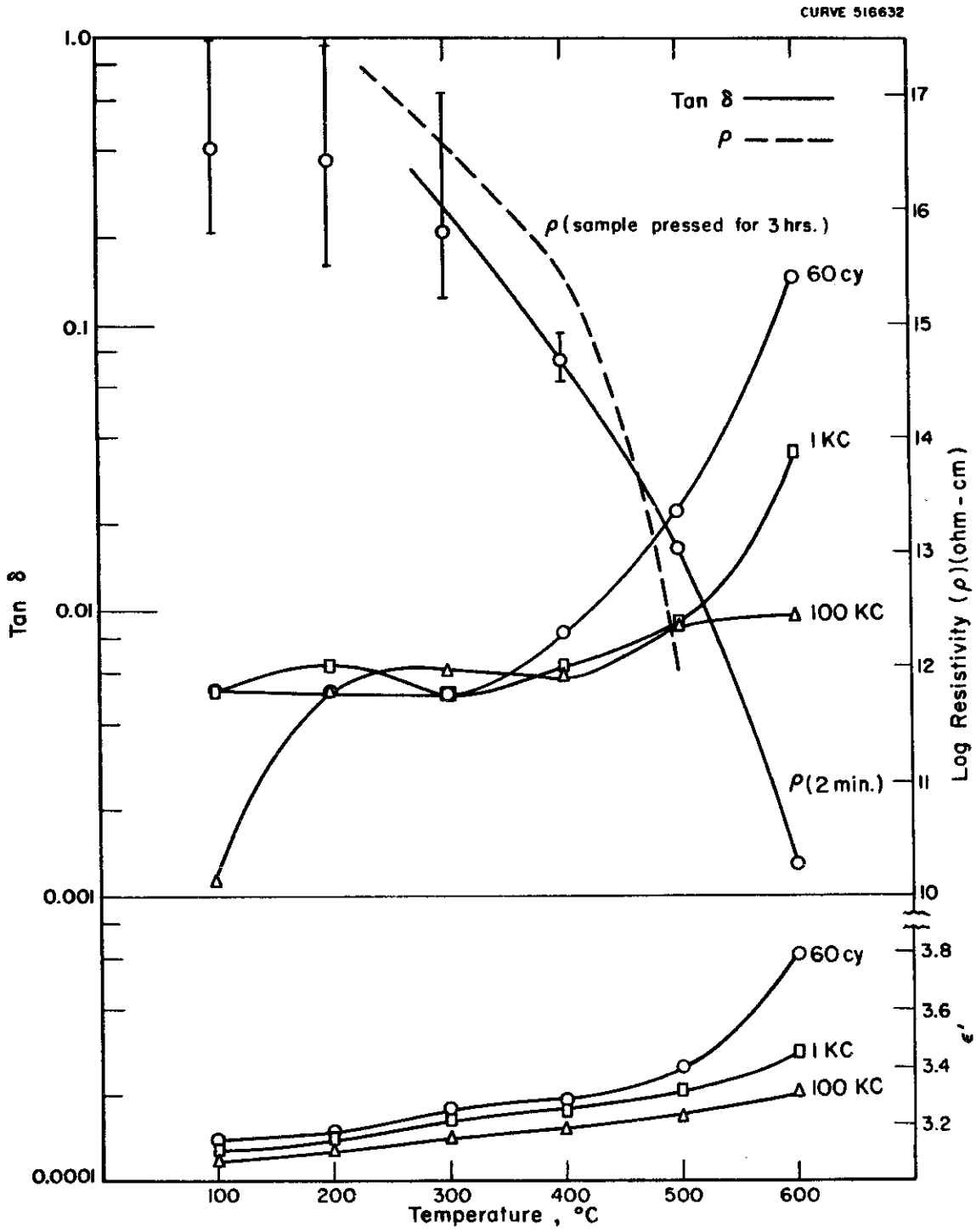

Fig. 7— Boron nitride (supplier X) hot pressed for 45 min at 1600°C and 2000 psi, graphite die, N_2 envelope.

Approved for Public Release

Contrails

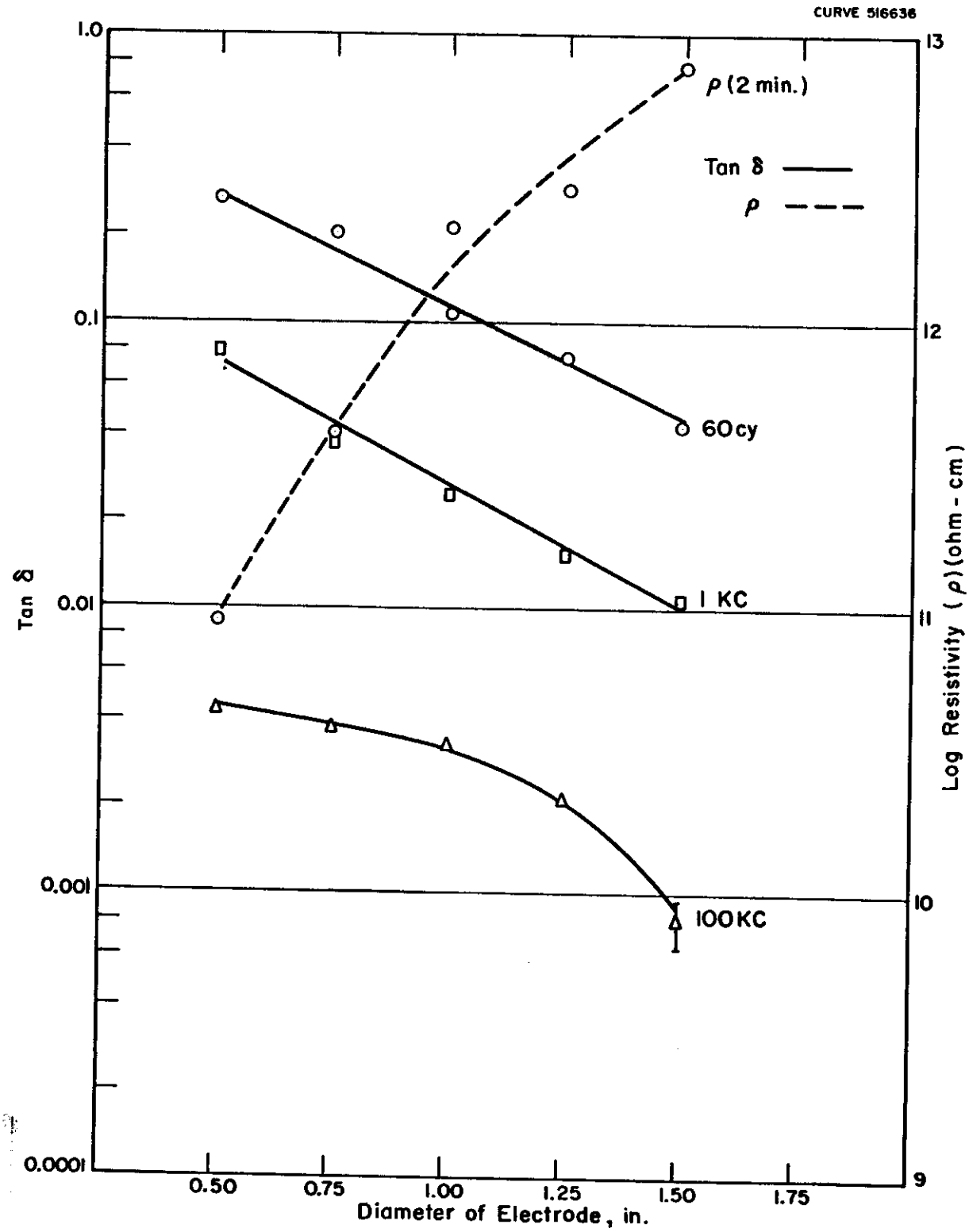

Fig.8—Measurements on a boron nitride sample at 500 °C with successively larger electrodes.

Approved for Public Release

Contrails

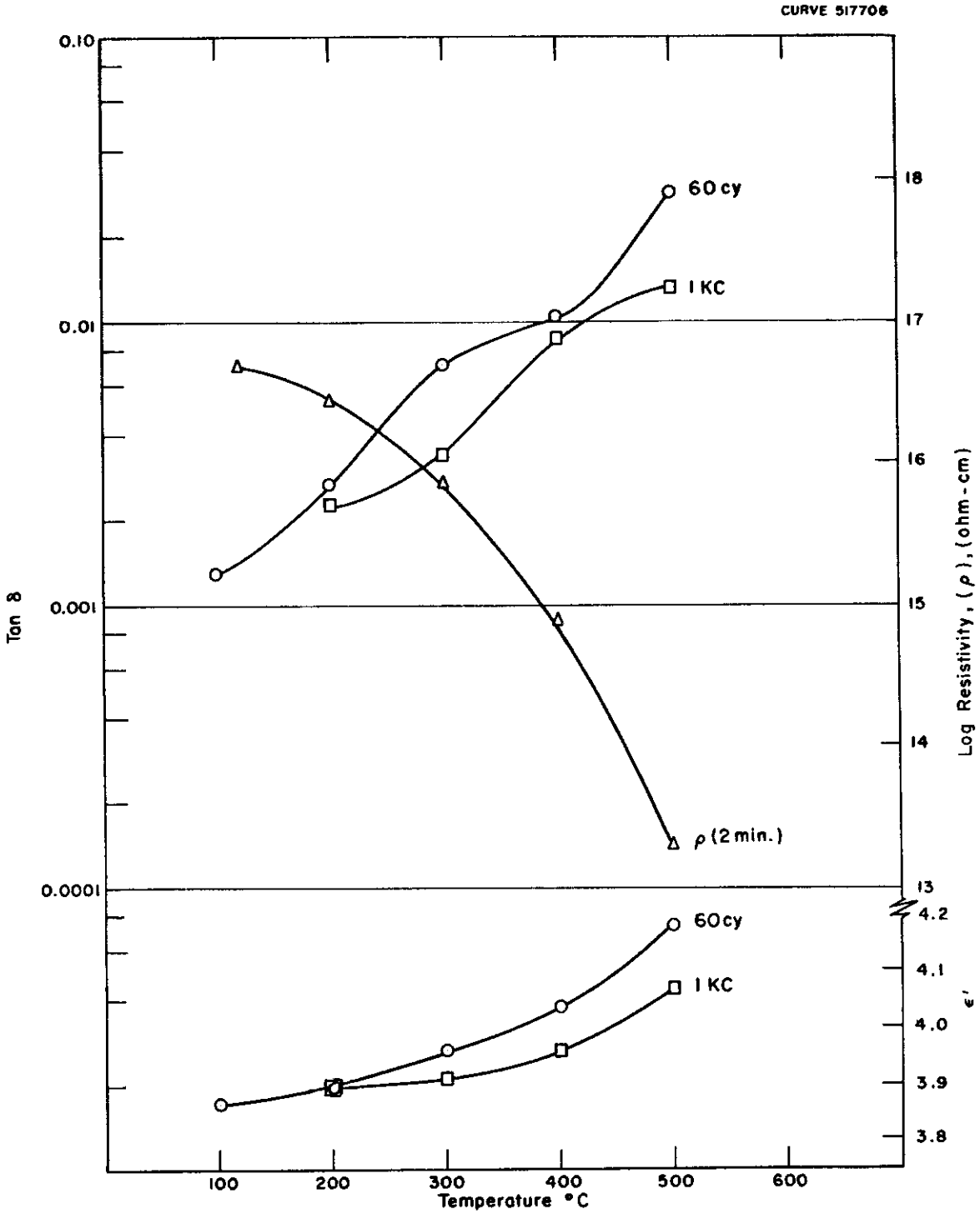

Fig. 9 - Boron nitride (supplier X), hot pressed at 1600°C and 3000 psi for 3 hrs. Measured after heating for 7 days at 500°C at a pressure of 1×10^{-4} mm Hg.

Approved for Public Release

Contrails

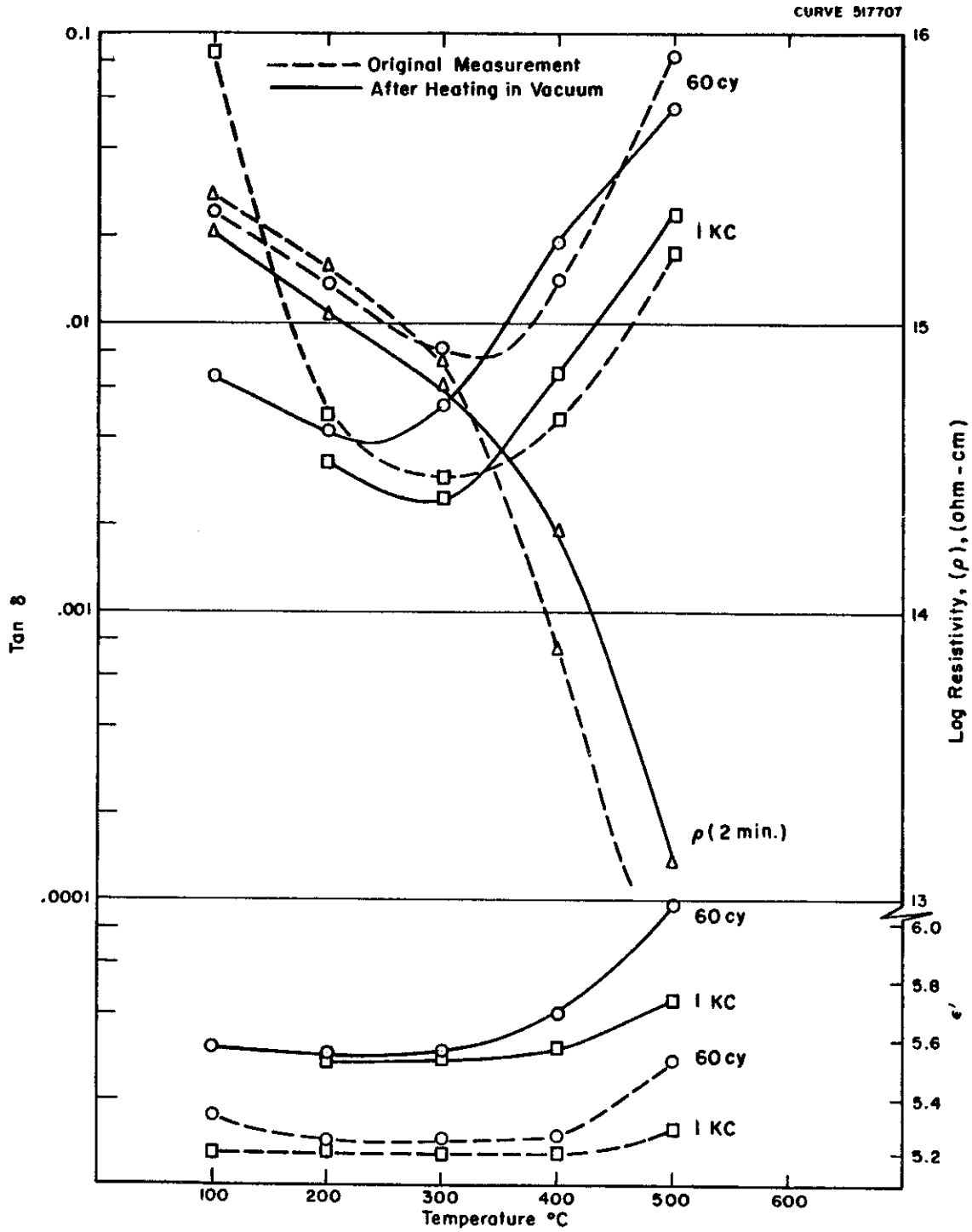

Fig. 10 - Boron nitride (supplier Y), hot pressed at 1800°C and 2550 psi for 3 hrs. Measured after heating for 7 days at 500°C at a pressure of 1×10^{-4} mm Hg.

Approved for Public Release

Contrails

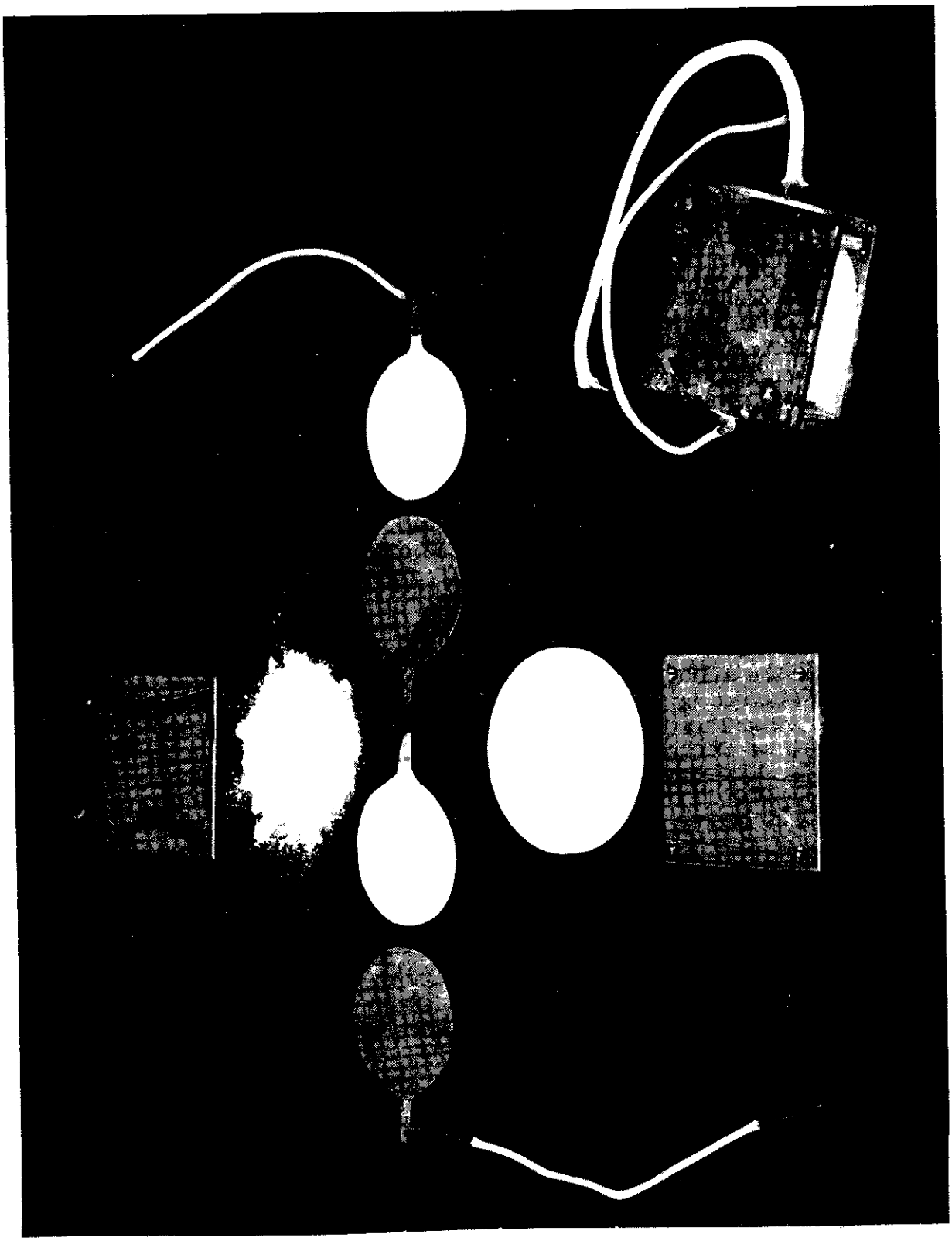

Fig. 11 Construction of a Boron Nitride Capacitor.

Approved for Public Release

Contrails

SECTION II. BORON PHOSPHIDE

(D. W. Lewis and P. A. Tierney)

As noted in a previous report (WADC TR 59-337 Part II) what little is known of the chemical properties of boron phosphide indicates that it is stable to moisture and air up to 800°C. Also, from theoretical considerations and preliminary optical transmission measurements, its energy gap is estimated to be about 5.9 electron volts. These properties suggest that boron phosphide if obtained in a pure colorless state might be a potential insulating, or possibly semi-conducting, material for use at 500°C.

A. PREPARATION OF BORON PHOSPHIDE BY REACTION OF THE ELEMENTS

Attempts were made to prepare BP in bulk form by the reaction of the elements at 1100°C. A mixture of amorphous boron powder and excess red phosphorous in an evacuated quartz tube was heated at 1100°C for 48 hours. The main portion of the reaction product was a dark, gray to black, loosely combined clinker having a metallic appearance. Growing out of this at localized points were clumps of needles 1 to 2 mm long. A picture of one such needle growth is shown in Fig. 12 Some of these crystal centers also appeared on the walls of the quartz tube as shown in Fig. 13. Figure 14 is a photograph of an individual crystal at a magnification of 100X. To get a cross sectional view of one of these crystals, one was embedded in a casting resin. The casting resin was then abraided and lapped in the appropriate direction to expose a cross section of the crystal. A view of this at a magnification of 1150X is shown in Fig. 15. The cross section is seen to be hexagonal.

The clinker of the reaction product was easily broken down to a powder which was then stirred in hot HNO_3 to remove excess reactants, followed by water to remove the acid. It was then analyzed by wet chemical analysis and by emission spectroscopy. X-ray diffraction patterns were obtained on the powdered product and on individual crystals. Fig. 16 shows an x-ray diffraction pattern of the powder. These spacings agree with those reported for the cubic boron phosphide structure. Fig. 17 is the pattern obtained on an individual crystal. In this pattern it can be seen that lines 4 and 16 are missing. This is due to the fact that the 200 and 400 planes of the rigidly held crystal were not exposed to the x-ray beam.

These x-ray diffraction patterns show that BP is present. However it is not colorless as expected from a material having an energy gap close to 6 electron volts. The fine granular product is greyish black with some particles having a metallic appearance. The crystals are maroon to dark brown and have a metallic luster in reflected light. Emission spectroscopy shows that the darker crystals contain 5 times more iron than the lighter ones. The presence of iron (about 0.1%) may be the cause of the color. This probably was introduced as an impurity in the boron used. It might also be the cause of their poor electrical resistance. When probes are touched to the ends of a crystal 2 mm long, the resistance is about 0.1 megohm. The color and poor resistance could also be due to the presence of some material having a deficiency of phosphorous; that is, a boron subphosphide such as B_6P. Boron phosphide, BP, is known to dissociate into elemental phosphorous and boron subphosphides at high temperature. This supposition is borne out by the results of chemical analysis. In all preparations of boron phosphide from the elements at 1100°C,

Approved for Public Release

Contrails

the ratio of boron to phosphorous was always greater than 1. Ratios in four runs were 1.04, 1.12, 1.2 and 1.4 boron to phosphorous.

B. REACTION OF BORON TRICHLORIDE WITH HYDROGEN AND PHOSPHOROUS

An effort was made to deposit thin films of BP on metallic substrates in order to obtain specimens suitable for measuring its electrical properties. Vapor deposition techniques were used. A mixture of boron trichloride and hydrogen was passed through a vertical quartz tubular vessel containing red phosphorous which was heated to 300°C. A metallic plate or cylinder, suspended in the quartz tube, was heated inductively to 900° - 1000°C at which the desired reaction was to take place depositing BP. Metals used were platinum, nickel, tungsten, tantalum and molybdenum in the form of a plate or a foil of cylindrical shape. Platinum and nickel foil, 0.004" thick, reacted with the BCl, H_2, P atmosphere at 900° - 1000°C. Tungsten foil was attacked by a mixture of BCl_3 + H_2 at 1350°C. Tantalum foil was inert. Since molybdenum foil could not be spot-welded to form a cylinder, a plate 0.06"thick was used. The molybdenum plate did not seem to be attacked in this atmosphere at 900° - 1000°C.

A very brittle film was formed on a tantalum foil cylinder which was heated to 1000°C for 30 minutes in a mixture of BCl_3, H_2, and phosphorous vapor. The gray film easily flaked off the metal foil. An x-ray diffraction pattern of this material contains strong lines representing the cubic BP structure. This is shown in Fig. 18. Enough of the film was obtained to carry out a chemical analysis. As in the case of boron phosphide prepared from the elements, the ratio of B to P in this film was greater than 1. Tantalum was not present in the film in concentration detectable by wet chemical analysis. Even so, the resistance of the film is very low.

This same reaction was run using a molybdenum plate as the substrate. The combined vapors were passed over the plate which was heated to 900°C. The plate became coated with a very thin, gray adherent non-insulating film. It could not be isolated from the plate but an x-ray diffraction pattern was obtained. This is shown in Fig. 19. Definite lines characteristic of the BP structure are present and intermixed with these is the molybdenum pattern. Apparently the film was quite thin allowing the x-ray beam to reach the metal substrate.

In a variation of this method, BCl_3 and H_2 were passed into the quartz reaction vessel where PCl_3 was used as the source of phosphorous in place of elemental phosphorous. This attempt was even less successful than previous ones. PCl_3 was reduced to phosphorous which was swept out of the reaction zone before coming into contact with the hot (900°C) tantalum plate. A great deal of both red and yellow phosphorous deposited on the colder portions of the apparatus. No satisfactory film was obtained.

C. THERMAL DECOMPOSITION OF THE PHOSPHINE-BORON TRICHLORIDE ADDITION COMPOUND

In the preparation of boron phosphide by heating the two elements to 1100°C there was no convenient way of bringing them together in an exact 1:1 ratio. The result was that the product was rich in boron. This same problem existed in the vapor deposition procedure where it was most difficult

Approved for Public Release

Contrails

to meter in the exact stoichiometric quantities of the reactants. The procedure attempted here for the preparation of BP was the decomposition of a 1:1 addition compound of phosphine and a boron trihalide. Use of such a compound would insure a 1:1 ratio of boron and phosphorous.

The preparation of a 1:1 addition compound of boron trichloride and phosphine was described in WADC TR 59-337, Part II. In the same report, Fig. 19 shows the variation in vapor pressure with temperature. However, measurement of the density of this vapor has shown that the number average molecular weight is 80 $\pm$ 2 gms/mole. The theoretical molecular weight for the undissociated addition compound is 151 gms/mole. Consequently, the compound is largely dissociated in the gas phase, and the value of ΔH = 11 kcal/mole for the reaction

$$H_3P{:}BCl_3\ (S) = H_3P{:}BCl_3\ (V)$$

is incorrect. Additional evidence for the dissociation of $Cl_3B{:}PH_3$ in the gas phase was obtained from the infrared spectra on the individual reactants, PH_3 and BCl_3, and on the vapors of the addition compound. The three spectra are shown in Figs. 20, 21 and 22. The absorption peaks between 7 and 7.5 microns in Fig. 20 may be attributed to the addition compound. The peaks between 4 and 4.5 microns are due to PH_3 (compare Fig. 21) and the peaks between 10 and 10.5 microns are due to BCl_3 (compare Fig. 20). The existence of the peaks between 7 and 7.5 microns in Figure 22 and the high value of the vapor density indicate that the addition compound is not 100% dissociated in the gas phase at room temperature. Even though $Cl_3B{:}PH_3$ is largely dissociated in the gas phase, it could easily be prepared and vaporized in the vacuum system and recondensed to the original compound, and an attempt was made to prepare BP from it.

Vapors of $H_3P{:}BCl_3$ were passed over a tantalum foil cylinder heated to 1000°C. After the flow of vapor was stopped, a full vacuum was pulled on the reaction vessel while the cylinder was still hot to remove any volatile materials from the foil. Gases coming out of the reaction chamber were unreacted addition compound, BCl_3, HCl and H_2. An orange-red film coated the walls of the chamber. This is probably a mixture of phosphorous and possibly a complex such as $(BPCl_2)_x$. The presence of these products can be explained by the following reactions in addition to the desired one.

$$H_3P{:}BCl_3 \longrightarrow BCl_3 + PH_3$$
$$2PH_3 \longrightarrow 2P + 3H_2$$
$$H_3P{:}BCl_3 \longrightarrow (BPCl_2) + HCl + H_2$$

Only a very thin film was formed on the foil. It was a very poor insulator either inherently or because it was very thin and porous.

This reaction was repeated with some modifications. The metal substrate in this case was a molybdenum plate in place of the tantalum cylinder. Instead of passing the vapors of the addition compound through the reaction chamber as in the previous run, a quantity of the compound was condensed in

Approved for Public Release

Contrails

the vessel which was then sealed off from the rest of the line. The plate was heated to 900°C. The gas given off in this reaction was predominantly HCl with little or no BCl_3 or H_2. An orange-yellow film formed on the walls of the vessel. This film did not ignite spontaneously or even burn very well. A small amount on a spatula gave a green color to a flame indicating the presence of boron. It is probably a boron phosphorous complex as $(BPCl_2)_x$.

An extremely thin film which had deposited on the molybdenum plate pealed off quite readily. In reflected light it appeared metallic. Looking through it at a light it resembled a somewhat transparent plastic film or possibly an extremely fine mesh screen. It is not an insulator. The x-ray diffraction pattern of the film in Fig. 23 shows that BP is present but the lines are not as sharp as in previous samples.

Boron phosphide was also prepared by heating $Cl_3B{:}PH_3$ in a sealed quartz tube for 16 hours at 1000°C. The material formed was similar to that prepared from the vapor deposition experiments.

D. THERMAL DECOMPOSITION OF THE PHOSPHINE-BORON TRIBROMIDE ADDITION COMPOUND

Since boron tribromide is a stronger Lewis acid than boron trichloride, a stronger BP bond in the addition compound is expected in the case of the tribromide. While this would lead to a less volatile complex unsuitable for vapor deposition techniques, it appeared to be a more attractive route to BP through thermal decomposition in sealed quartz tubes.

Boron tribromide forms a simple 1:1 addition compound with phosphine. The vapor pressure of the material at room temperature is less than 1 mm. At 900°C in sealed quartz tubes it formed H_2, HBr, P, and an inert solid which gave the typical cubic x-ray diffraction pattern of BP. The solid product was dark gray in color and was not an electrical insulator.

Another attempt was made to prepare BP by using an excess of phosphorus-containing reactant. Phosphine and boron tribromide in a ratio of four moles of phosphine to one of the tribromide were sealed in a quartz tube and heated for 15 hours at 900°C. The main product was a gray to black solid formed on the walls of the tube. A considerable amount of phosphorous was formed which ignited spontaneously when exposed to air. The third product, a gas which fumed in contact with moist air, was believed to be HBr. The solid looked very much like the product of the reaction of elemental boron and phosphorous at 1100°C. However, the lines in the x-ray pattern of this material are more diffuse than in previous samples. This is probably due to the presence of some amorphous material. No doubt a longer heating time and higher temperature would produce a more crystalline product having more distinct lines.

In view of the fact that the several avenues of approach to the preparation of BP have not produced a colorless product having favorable electrical properties, this effort has been discontinued.

E. CONCLUSIONS

Attempts were made to prepare colorless BP by: reaction of its elements, by reaction of BCl_3 with H_2 and P, and by thermal decomposition of

Approved for Public Release

Contrails

the $PH_3 \cdot BCl_3$ and $PH_3 \cdot BBr_3$ addition complexes. In all cases a colored product of low electrical resistivity resulted. X-ray diffraction analysis indicated that BP was probably present. In all the materials prepared, an excess of boron over that in BP was found by chemical analysis and probably accounts for the low electrical resistivity. Because of the lack of success in making high resistivity BP, this effort was discontinued in the first quarter of this period.

Approved for Public Release

Contrails

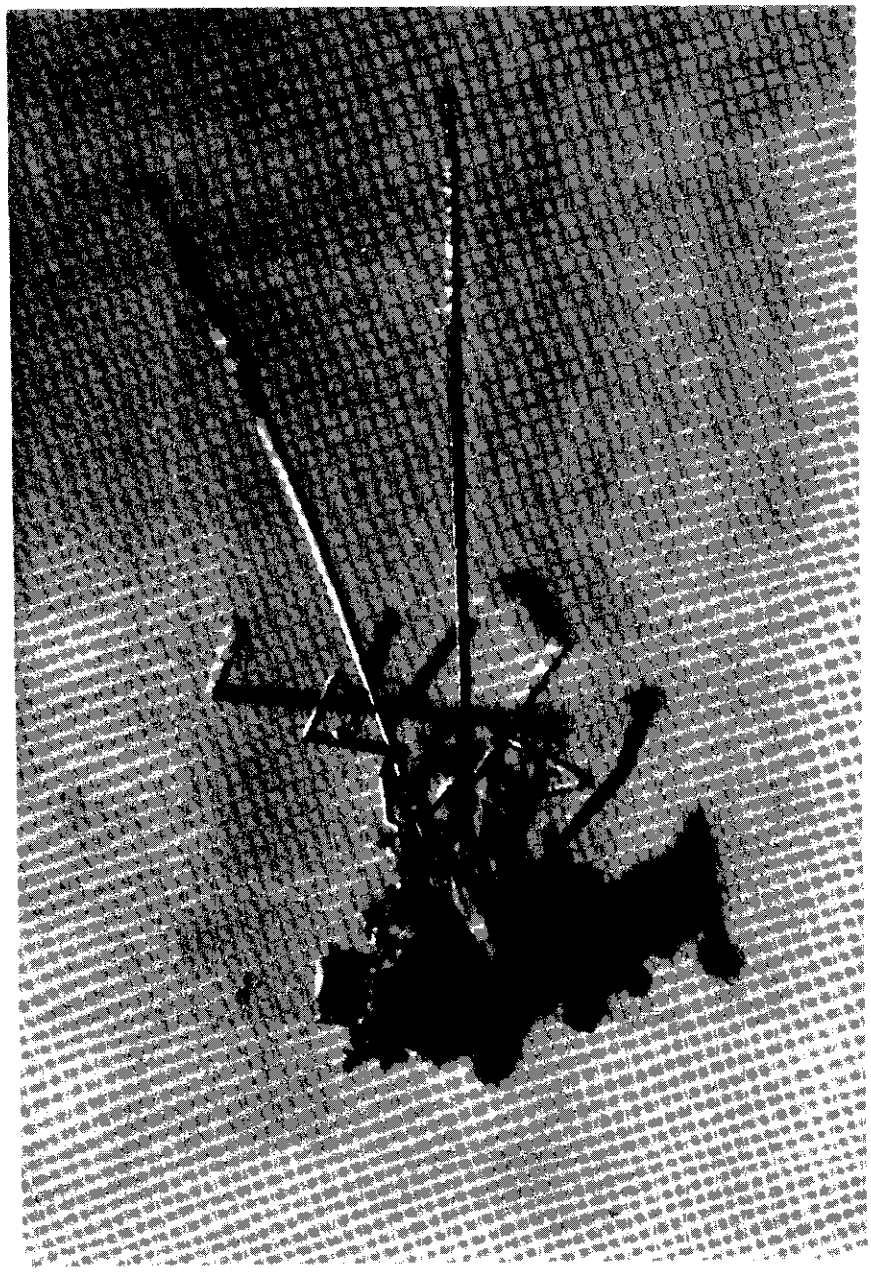

Fig. 12 Photograph of Needle Growth of Boron Phosphide (50X).

Approved for Public Release

Contrails

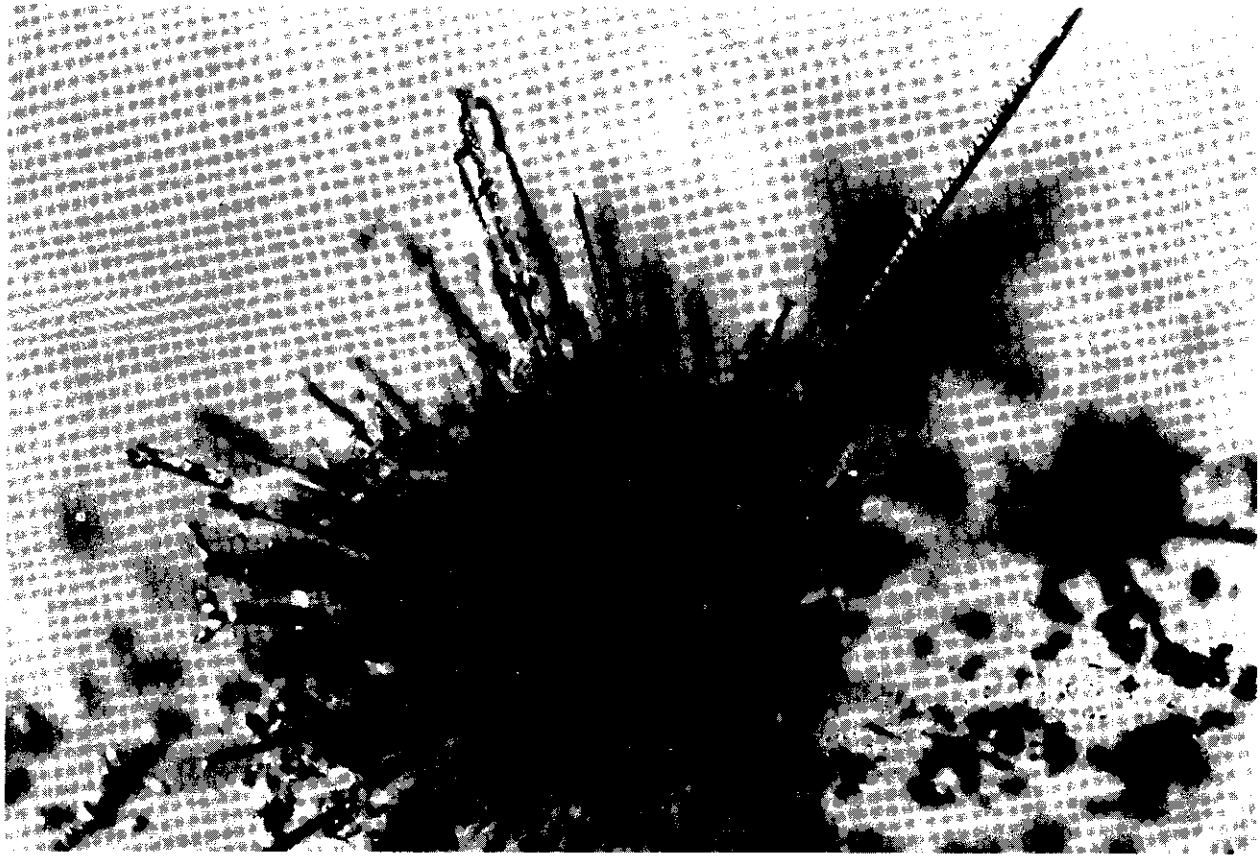

Fig. 13 Photograph of Growth Center of Boron Phosphide Crystals on Wall of Quartz Tube (50X).

Approved for Public Release

Contrails

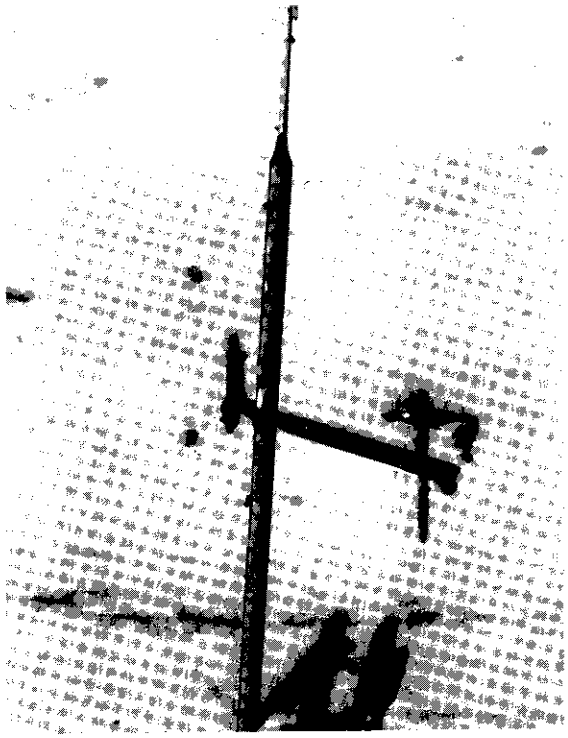

Fig. 14 Photograph of an Individual Boron Phosphide Crystal (100X).

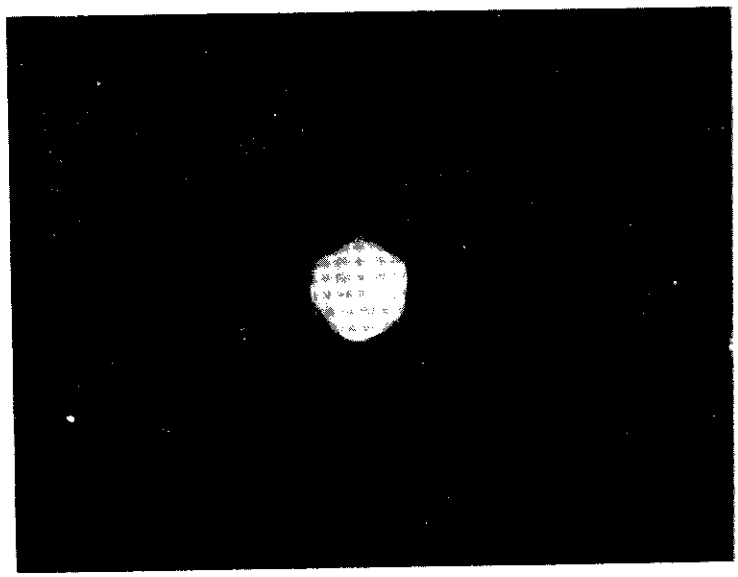

Fig. 15 Photograph of Cross Section of Boron Phosphide Crystal (1150X).

Approved for Public Release

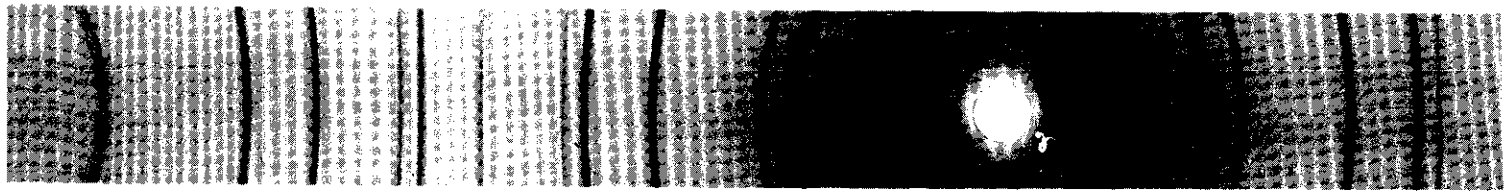

Fig. 16 X-Ray Diffraction Pattern of Boron Phosphide Prepared from the Elements.

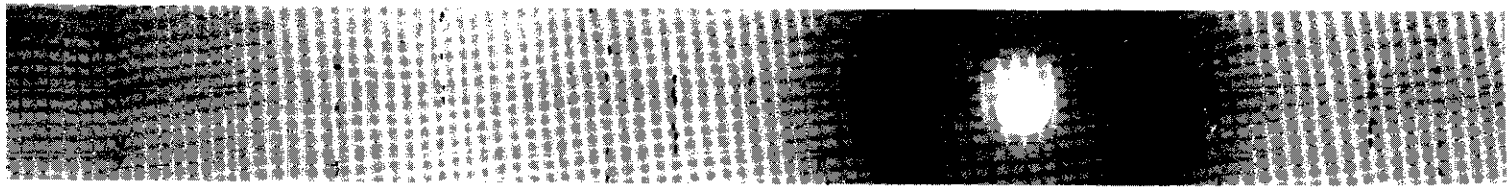

Fig. 17 X-Ray Diffraction Pattern of an Individual Crystal of Boron Phosphide.

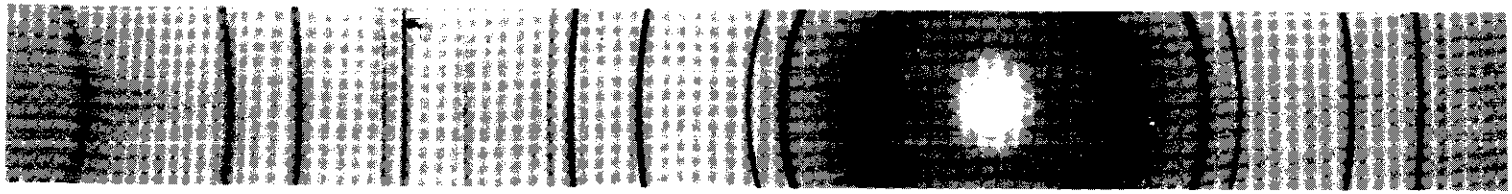

Fig. 18 X-Ray Diffraction Pattern of Boron Phosphide Vapor Deposited on Tantalum Foil.

Fig. 19 X-Ray Diffraction Pattern of Boron Phosphide Vapor Deposited on Molybdenum.

Approved for Public Release

Controlled

Contrails

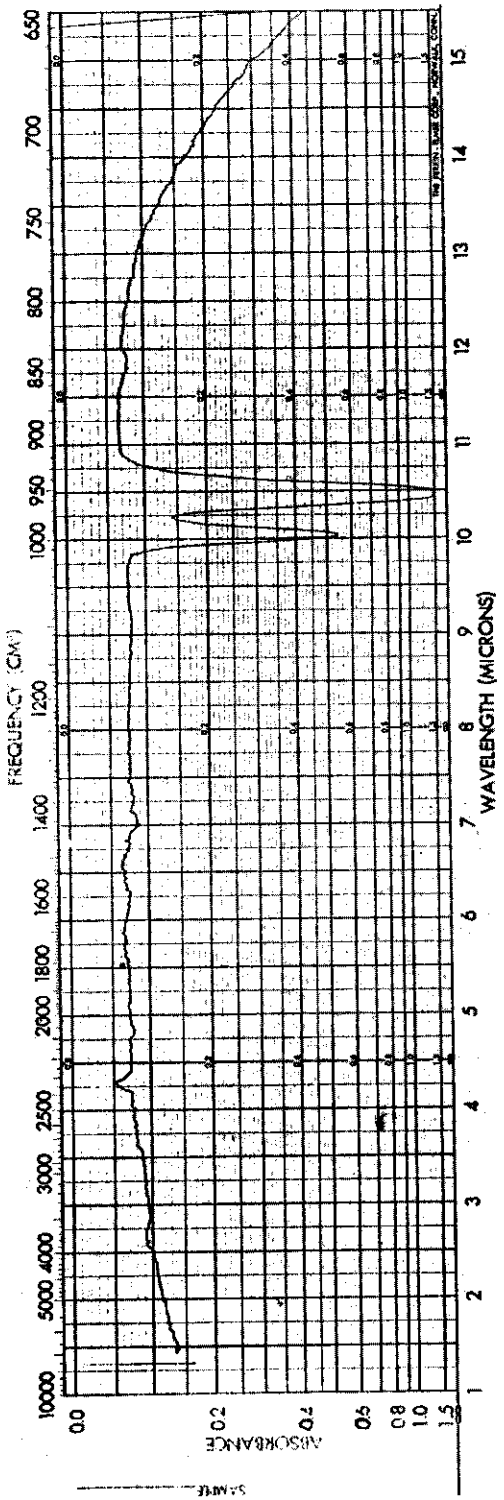

Fig. 20 - IR spectrum of BCl_3 gas

Approved for Public Release

Contrails

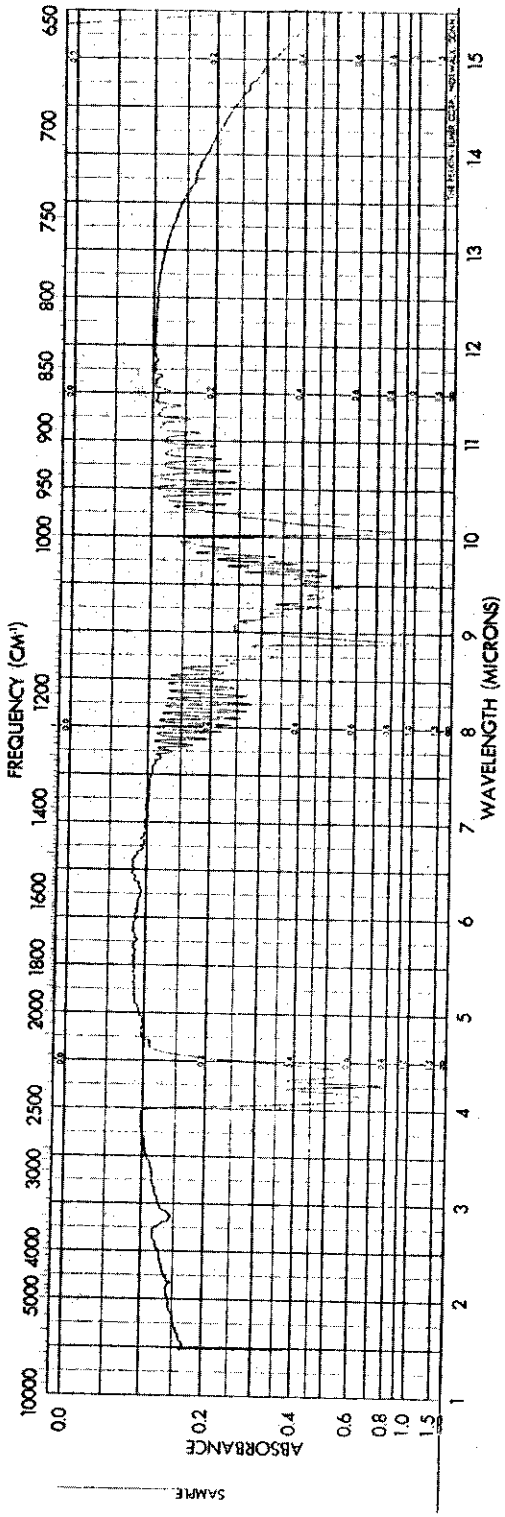

Fig. 21 - IR spectrum of PH_3 gas

Approved for Public Release

Contrails

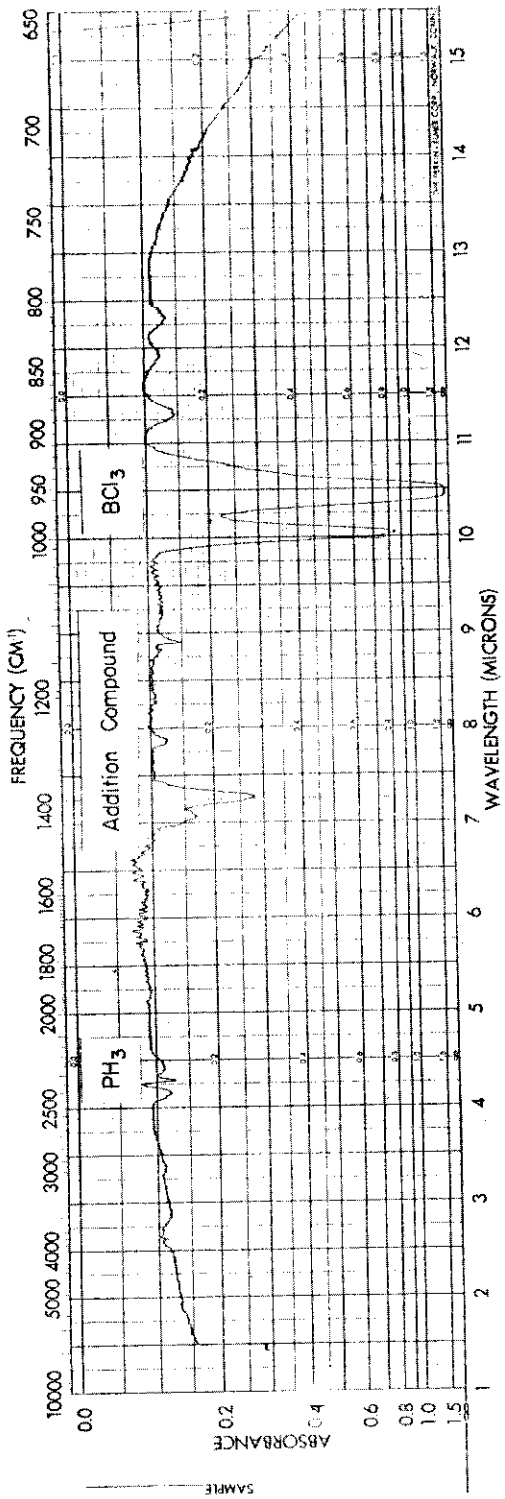

Fig. 22 - IR spectrum of H_3P: BCl_3 gas

Approved for Public Release

Approved for Public Release

Confidential

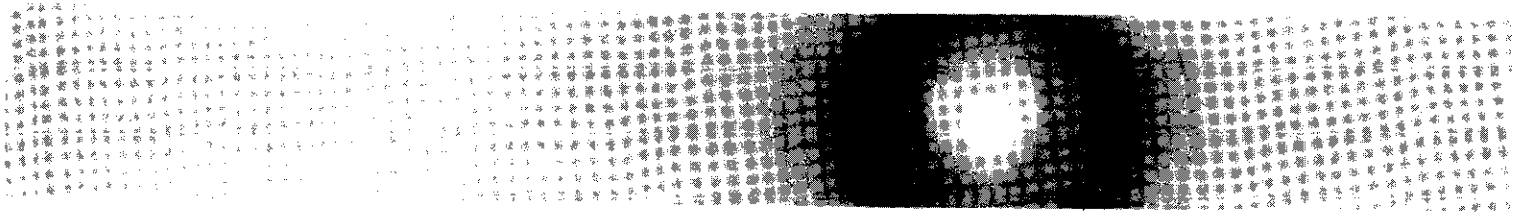

Fig. 23 X-Ray Diffraction Pattern of Thin Film of Boron Phosphide.

Contrails

SECTION III. APPLICATION OF INORGANIC DIELECTRICS BY PLASMA JET

(D. W. Lewis)

A. INTRODUCTION

In the initial Technical Report (WADC 59-337, Part I) describing the synthesis and purification of dielectric materials, it was shown that a high purity polycrystalline alumina could be prepared which has high temperature electrical properties equal to those of single crystal sapphire. This alumina was prepared by sintering a powder obtained from the hydrolysis of a highly purified aluminum isopropoxide. Part II of this report described the preparation of thin films of high purity alumina. These were obtained by spraying a solution of aluminum isopropoxide onto a metallic foil, allowing the isopropoxide to hydrolyze to aluminum hydroxide, and finally converting the hydroxide to alumina by heating. Films of magnesia were similarly prepared using magnesium methylate as the source material. These films were adherent, but unfortunately were permeable to metallic vapors, making it impossible to evaporate an electrode onto their surface without shorting through to the substrate. In the present period, inorganic coatings were applied to metallic substrates by flame spray and plasma jet techniques. The latter method provides thin adherent films which are impervious to gold vapors and to liquid gallium-indium alloy.

B. ALUMINA

Alumina powders are available which can be applied in continuous coatings by the flame spray technique, but unfortunately they contain fluxing additives which are deleterious to high temperature electrical properties of the coatings. A high purity alumina was applied to a metal surface by flame spray but this too was permeable to gold vapor. When viewed under the microscope it appeared that the particles did not get hot enough to soften so that the coating had a very loose, permeable structure. A photograph (50X) of one of these coatings is shown in Figure 24.

Since a higher temperature seemed to be required to obtain nonporous alumina films, plasma jet spraying suggested itself. In this gun a stream of gas is passed through an arc where it is ionized and heated. Argon is conveniently used in this application. Alumina powder is vibrated into the jet stream where it is heated almost to its melting point and then transported at high velocity to the metal surface where it is embedded. A schematic drawing of the plasma gun is shown in Figure 26. The arc is struck across a tungsten cathode and a copper anode, the latter which, also serves as the nozzle of the gun. Many variables must be adjusted to obtain optimum conditions for suitable application: for example, the voltage to be applied across the electrodes, the composition of the plasma gas, the rate of flow of the gas, the rate of powder flow, the particle size of the powder, the position in which the powder is to be introduced into the gun and the distance at which to place the material to be coated from the nozzle of the gun. In addition to the usual problems associated with obtaining a relatively thin, adherent, continuous insulating coating, the plasma jet spray method presents another. This is the contamination of the coating by particles of the arc electrodes. As the voltage is increased to increase the temperature of the plasma flame, so as to approach the melting point of the

Approved for Public Release

Contrails

material being sprayed, more and more of the tip of the cathode becomes molten. This increases the ease with which particles of electrode can be dislodged by the plasma stream and deposited on the foil along with the powder being sprayed.

Still considering the problem of transferring enough energy to the powder to soften it, it might be thought advisable to introduce the powder into the plasma gas in the plenum region of the gun, just before the gas reaches the arc. In this way the maximum heat would be transferred to the powder. However, this proved to be impractical in spraying alumina, for the coatings obtained were badly contaminated with electrode particles. Apparently the rapid moving stream of argon and alumina caused serious erosion of the electrode. This source of contamination is almost completely eliminated by introducing the alumina powder into the nozzle region, that is, after the gas has passed through the arc. Even so, minute particles are often found in the coatings.

High purity alumina, free of fluxing additives, has been applied to 2, 3 and 5 mil aluminum foil by the plasma jet technique. These coatings are well bonded to the substrate and to itself. They are quite smooth, having a surface finish of 65-70 microinches, r.m.s. Unlike high purity films applied by other spraying methods and those previously applied by the plasma jet, these coatings are continuous as shown by the fact that gold electrodes have been evaporated onto them without shorting through. Also, liquid gallium-indium alloy, which has excellent wetting characteristics does not penetrate the film. The electrical breakdown of a 1 mil film is about 450 volts, which is somewhat greater than that of air. When viewed at a magnification of 200X, it can be seen that at least the surface of the alumina particles had been molten. A photograph of such a coating, at a magnification of 50X, is shown in Fig. 25 to compare its fine structure with that of the flame sprayed coating shown in Fig. 24 at the same magnification. The coated foil can be bent or curled without visible harm to the coating.

The foil which was coated was in the shape of a disc having a diameter of 2-1/4 inches and containing two tabs as shown in Fig. 27. The tabs served two purposes. First they held the disc in a jig which allowed the discs to be coated completely out to the edge. The stainless steel jig containing four aluminum discs can be seen in the path of the plasma flame shown in Figure 28. The jig was rotated and moved in a horizontal direction as it passed in the path of the flame. Having been coated to the edge they could be placed on top of one another to form a capacitor. The tabs also serve as terminals for electrical connection to the capacitor.

A gold electrode was sputtered onto an aluminum coating which was 1.5 mils thick. The resistance, capacitance and tan δ of this capacitor were measured between 200° and 500°C at 60 cy to 100 Kcy. The values obtained are shown in the curves in Fig. 29. At 500°C and 60 cycles the tan δ is about 0.22, the capacitance is 185 picofarads and the RC factor is about 0.3 megohm-microfarads. These values are inferior to sintered alumina obtained from the same powder.

Various efforts have been made to improve the electrical properties of the coatings. The gun was dismantled and thoroughly cleaned as was the powder

Approved for Public Release

Contrails

flow apparatus. The power going into the arc was increased in an effort to cause increased melting of the oxide particles so as to obtain a more dense coating. However, in increasing the power, a point of diminishing return is soon encountered, for as the electrode gets hotter, the greater is the opportunity for contamination of the coating by electrode particles. This is believed to be the main source of contamination for, whether the starting material is a very high purity alumina or a magnesia of only 97% purity, the electrical properties of both coatings are about the same. Thus there appears to be a deleterious leveling of the electrical properties of the oxide as it goes through the arc. Electrical properties of these two oxide coatings are shown in Figure 29 and 30. A comparison is also made of the electrical properties of alumina discs sintered in an argon atmosphere in a graphite furnace and plasma sprayed coatings, both prepared from the same high purity powder. At 500°C and a frequency of 60 cycles, sintered alumina has a tan δ of .011 while that of the plasma sprayed coating is 0.2. This comparison is shown in Figures 31 and 32.

To determine the nature of the impurities introduced in the oxide as it passes through the arc, emission spectra were obtained on the powder and on the plasma sprayed coating. Several metallic impurities, which would be detrimental to electrical properties, were found in increased amounts in the coating over that in the original powder. There was a 50 fold increase in the concentration of silver, a 10 fold increase in copper and magnesium; a 9 fold increase in iron, and a 3 fold increase in sodium. No doubt this increase in conducting impurities is responsible for the deterioration of the high temperature electrical properties of the oxides. A compilation of the concentration of impurities present in alumina before and after spraying is found in Table V. Oddly enough, even though a tungsten electrode is used in the plasma jet gun, little or no evidence of tungsten contamination was found in the spectrum of the sprayed alumina coating.

TABLE V. PERCENT IMPURITIES IN ALUMINA BEFORE AND AFTER PASSING THROUGH THE PLASMA JET GUN

	Mg	Si	Cu	Ag	Ca	Ba	Na	Fe	Ti	Sr
Alumina Powder	.008	.02	.005	.002	.01	.01	.02	.01	.001	.001
Plasma Sprayed Alumina Coating	0.1	0.1	.05	0.1	.04	.07	.07	.09	.05	.005

A capacitor was constructed by stacking alternately four bare aluminum foil discs and three similar discs which had been coated on both sides with 1.2 mils of alumina. The stack was held under compression between two aluminum plates which had been insulated with a coating of alumina. Aluminum wire leads were spot-welded onto the tabs. It was then placed in a furnace fitted for measuring electrical properties while at temperature and under voltage. The temperature and voltage were increased over a period of 172 hours. Final conditions were 350 volts dc at 500°C for a period of 25 hours at which point the experiment was stopped. During this final period the RC factor was 1.5 MΩ -μf. Complete aging characteristics are recorded in Table VI. The capacitance is not as high as hoped but its ability to operate at such high temperature and voltage should make it useful for special applications.

Approved for Public Release

Contrails

TABLE VI. PROPERTIES OF A 6 PLATE Al-Al_2O_3 CAPACITOR

Hours	Aging* °C	Volt DC	Resistance (megohms)	Capacitance (μf)	Dissipation Factor %, 1 Kcy	KC Factor (MΩ -μf)
18	400°	7.5	2800	.0075	1.1	2.1
3	450°	7.5	920	.0076	1.6	6.8
3	500°	7.5	280	.0076	2.4	2.1
1	500°	50	355	.0076	2.4	2.7
1	500°	100	490	.0076	2.2	3.7
15	500°	150	600	.0077	2.1	4.6
2	500°	200	610	.0077	2.1	4.7
4	500°	250	700	.0077	2.1	5.4
100	500°	300	180	.0078	2.5	1.4
25	500°	350	200	.0078	2.5	1.5

*Measurements made at 7.5 volts dc after aging at this time, temp. and voltage.

C. MAGNESIA

A powdered magnesia of 97% purity was successfully applied to 5 mil aluminum foil by plasma jet. The coating was adherent and was impervious to gold vapor. It was darker than the alumina films described above. It was also darker than the MgO powder from which it was made. A 3/4 inch gold electrode was sputtered onto a 1-3/8 inch disc of this 97% MgO on aluminum foil. The thickness of the coating was 1.1 mils. Capacitance, resistance and tan δ of this sample were measured at 100° to 400°C. Curves drawn from these values are shown in Fig. 30. At 400°C and 60 cycles, the tan δ is 0.1, the capacitance is 1229 picofarads and the RC factor is about 0.3 megohm-microfarads. These values are quite encouraging considering the 97% purity of the powder. The electrical breakdown of these coatings were about the same as that of alumina, about 450 V mil, measured on a coating 1.8 mils thick.

An attempt was then made to apply a high purity magnesia to aluminum foil. But this was unsuccessful. The coating did not adhere to the foil or to itself. Apparently the softening point of MgO is too high to permit suitable coatings to be applied under the conditions employed. A fine silica powder was mixed with high purity magnesia in an attempt to lower its melting point, but this too was unsuccessful.

D. SILICA

When silica was sprayed onto aluminum foil by the plasma jet gun, it appeared as though a thin adherent coating of silica was being applied, but examination showed that silica was not adhering to the foil. The particles were striking the aluminum surface and bouncing off. What appeared to be a coating was merely a sand blasted surface. Why silica with a softening point some 500°C lower than that of alumina could not be applied in this manner is not clearly understood.

Approved for Public Release

Contrails

E. SYNTHETIC FLUOROPHLOGOPITE MICA

A powdered synthetic fluorophlogopite mica was applied to aluminum foil by plasma jet. These coatings were not as adherent as those of alumina or magnesia. They were also more porous. However, they could be made more dense and quite adherent by subjecting them to pressures of 15 tons/in^2 between steel plates. Evaporated gold electrodes were applied to these films without shorting through. Electrical measurements were made from 100° to 500°C at 60 and 1000 cy/sec. The values obtained show an improvement over similar values previously reported for reconstituted fluorophlogopite mica paper. (WADC Technical Paper 59-337, Part II, Fig. 53). In Fig. 33 and 34 there is a comparison of the high temperature electrical properties of these films and the paper.

F. BORON NITRIDE

Films of boron nitride applied to aluminum foil by plasma jet were quite rough and weakly adherent. Apparently, boron nitride with a melting point of about 3000°C, was not softened in the plasma flame. The films could be made more dense and very adherent by pressing them at 15 tons/in^2. Gold electrodes were evaporated onto several of these. Resistance, tan δ, and capacitance were measured at 100° to 500°C and frequencies of 60 and 1000 cycles. These values, shown by the curves in Fig. 35 and 36, are quite inferior to those of pure hot pressed boron nitride discs.

G. BORON NITRIDE + 30% CABAL GLASS

In Section I of this report there is described the electrical properties of relatively thick hot pressed discs of boron nitride bonded with cabal glass. This glass is known to have fairly low conductivity at high temperatures. The bonded boron nitride is mechanically stronger than without the bond and the deterioration of electrical properties is not severe. A finely powdered mixture of boron nitride with 30% cabal glass was applied to aluminum foil using the plasma gun. The coating, like that of boron nitride, had poor adhesion to itself and to the substrate. But again the film could be compacted by pressing at 15 tons/in^2. Smooth adherent coatings, 1 to 2 mils thick were obtained. Gold electrodes were evaporated onto the films. Electrical properties were measured up to 500°C at 60 and 1000 cy/sec. The values obtained are compared with the properties of the pressed discs in the curves shown in Figure 37 and 38.

H. CONCLUSIONS

A plasma jet technique has been developed for applying thin adherent films of inorganic dielectrics to metallic foils. The films are smoother and less permeable to conducting vapors than those applied heretofore by flame spray or plasma jet methods. Alumina and magnesia films, 1 to 2 mils thick are impervious to gold vapors and to liquid metallic alloys such as gallium-indium. The density of the oxide coatings is less than that of the sintered material but apparently the pores are isolated, preventing conducting liquids or vapors from shorting through to the metallic substrate. The electrical breakdown of the oxide coatings is greater than that of air. Capacitors have been constructed by stacking alternately, uncoated aluminum foil and foil coated on both sides with alumina. After aging for 100 hours at 500°C under a stress of 300 volts, it had an RC factor of 1.4 megohm-microfarads. The RC factor was practically unchanged upon further aging for 25 hours at 500°C

Approved for Public Release

Contrails

and 350 volts dc.

The electrical properties of the oxide films are poorer than those of sintered discs made from the same powder. This might be expected as a result of the lower density of the films. Another contributing factor to poorer high temperature properties is the increase in the concentration of conducting impurities in the coating over that found in the original powder. As the powder goes through the arc it apparently picks up impurities from the cathode, the tip of which is sometimes molten during operation.

A synthetic fluorophlogopite mica powder, applied to aluminum foil by the plasma jet, gave films which were less dense and less adherent than the oxide coatings. Application of pressure to the films corrected these faults and their electrical properties were somewhat better than those previously obtained on fluorophlogopite mica paper.

Boron nitride and mixtures of BN with cabal glass were applied to aluminum foil by plasma jet. The mechanical properties of these coatings were improved by pressing, but even so, their electrical properties were poorer than hot pressed discs of the same material.

Approved for Public Release

Contrails

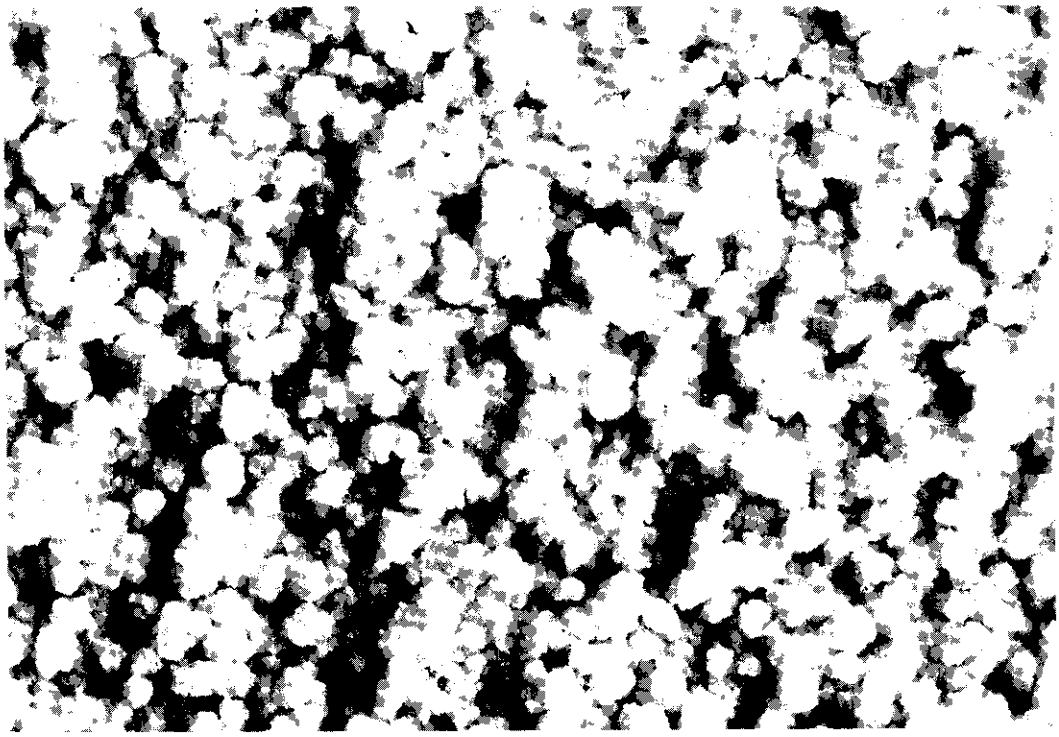

Fig. 24 Photograph of Alumina Coating Applied by Flame Spray (50X).

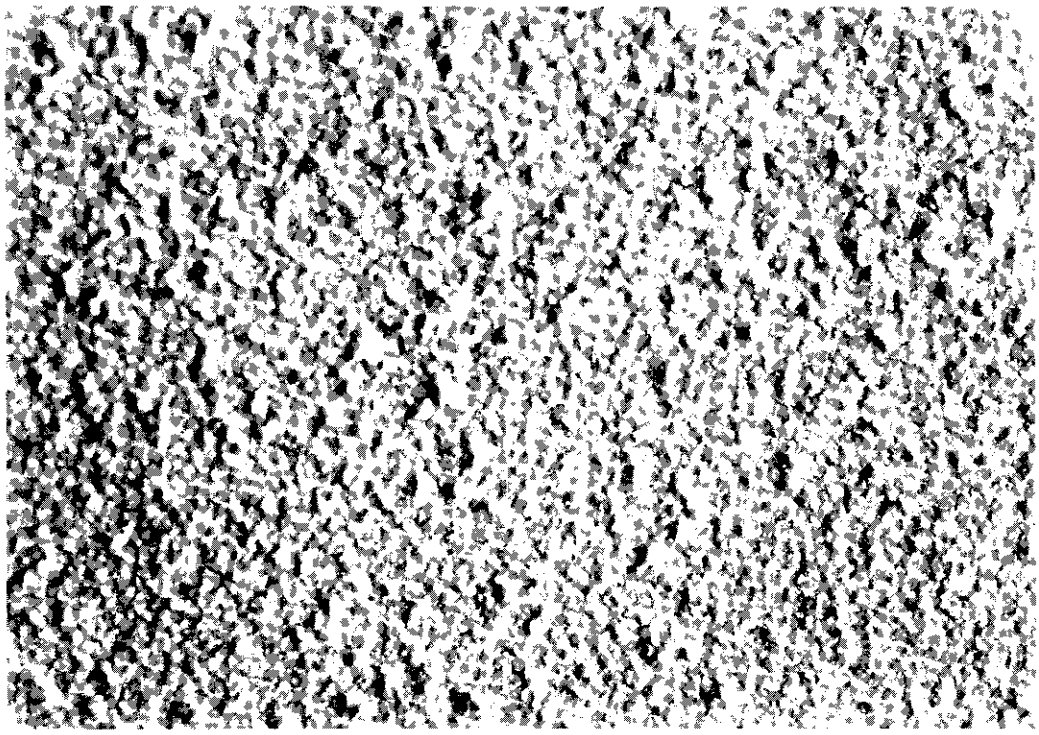

Fig. 25 Photograph of Alumina Coating Applied by Plasma Jet (50X).

Approved for Public Release

Contrails

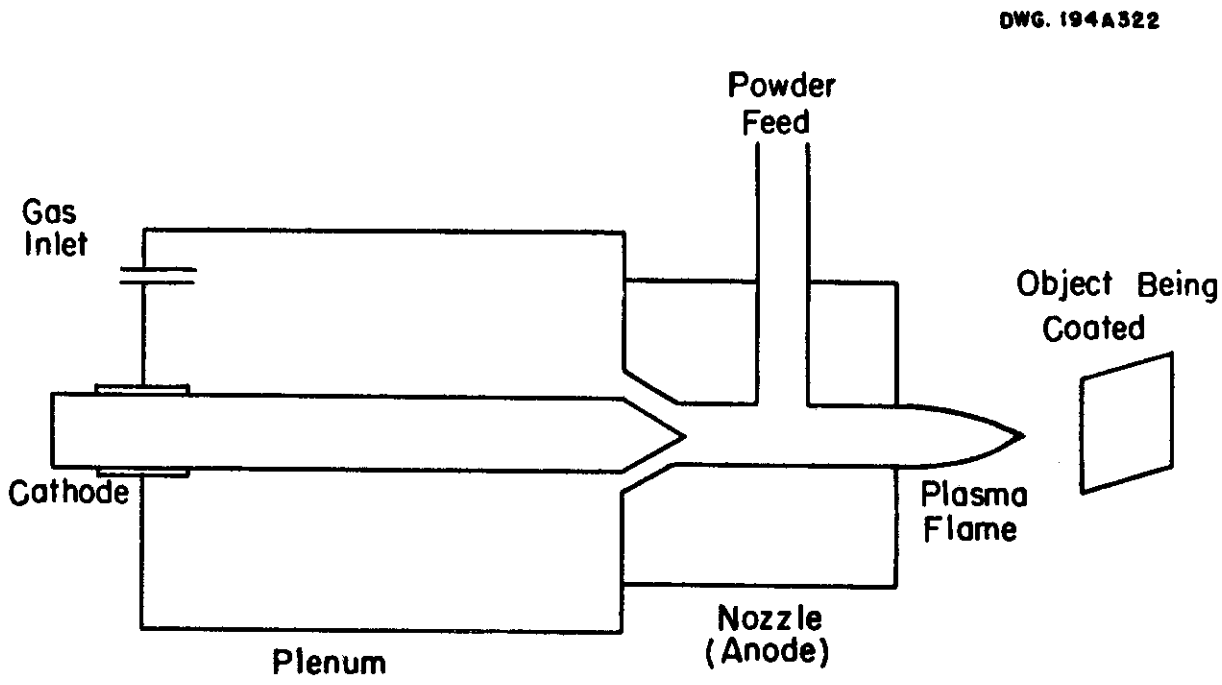

Fig. 26 - Schematic of plasma jet gun.

Approved for Public Release

Contrails

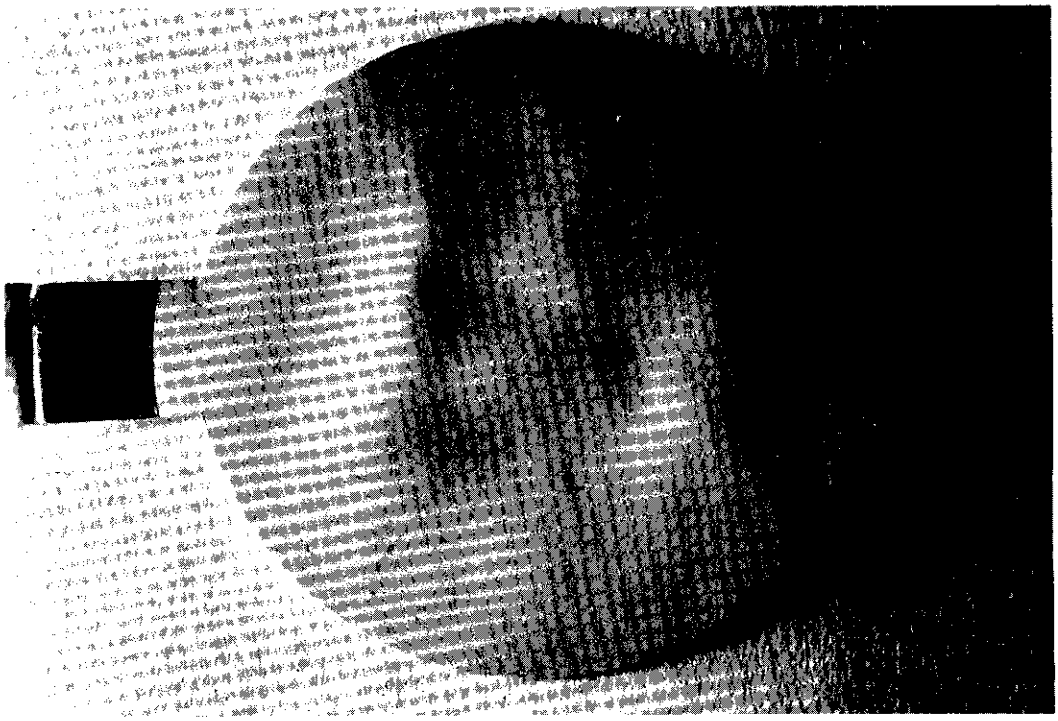

Fig. 27 Photograph of Aluminum Disc Coated with Alumina by Plasma Jet.

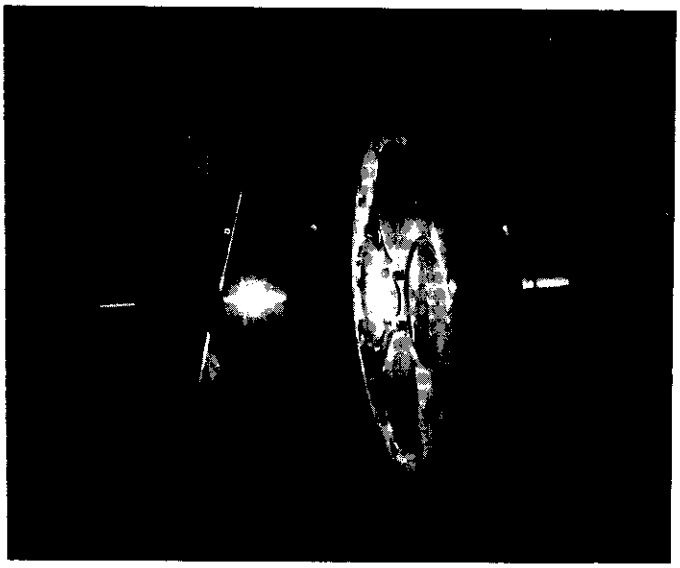

Fig. 28 Photograph of Jig Holding Four Aluminum Discs in Path of Plasma Flame.

Approved for Public Release

Contrails

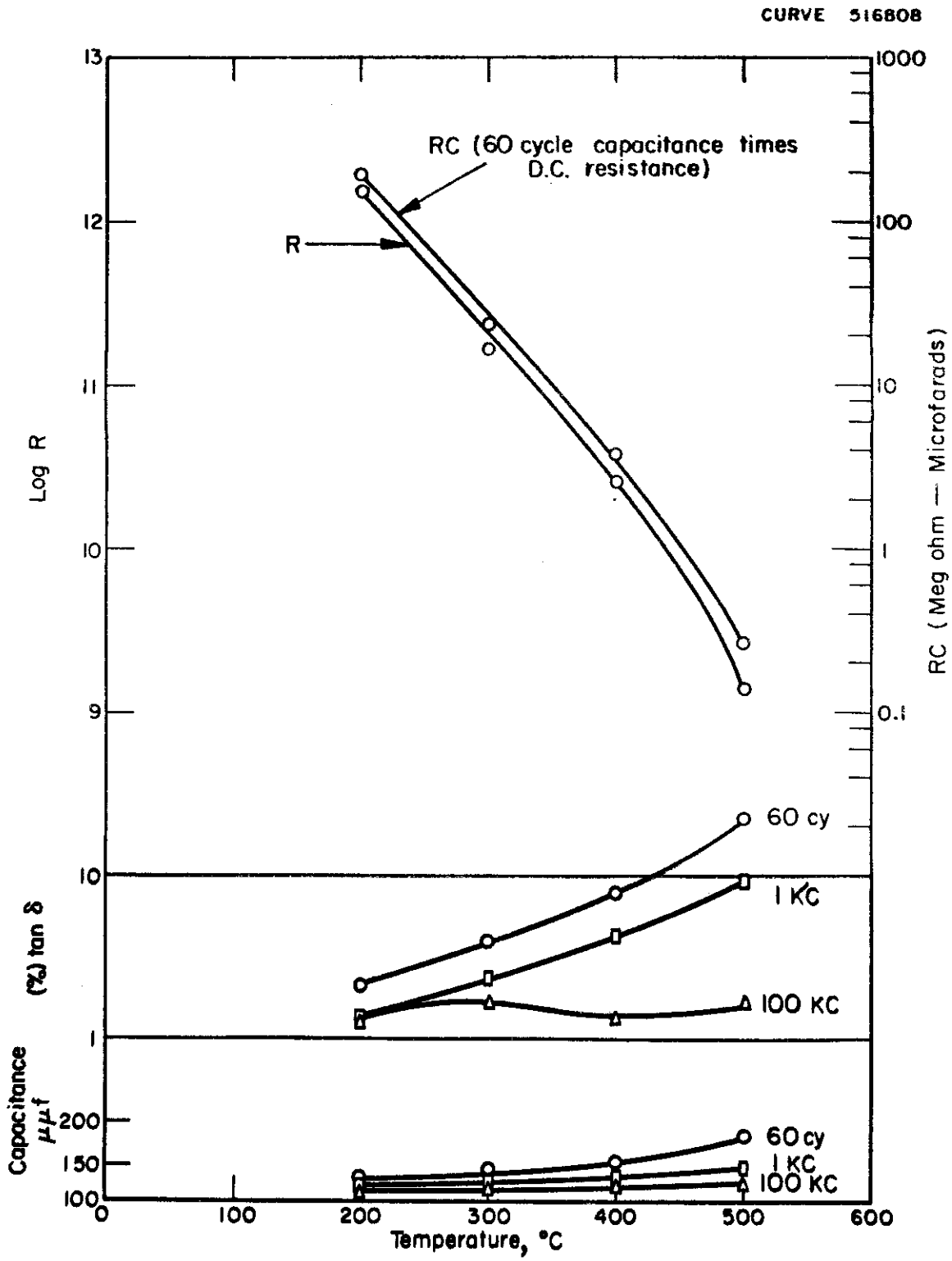

Fig.29 - Electrical properties of alumina applied to aluminum foil by plasma jet.

Approved for Public Release

Contrails

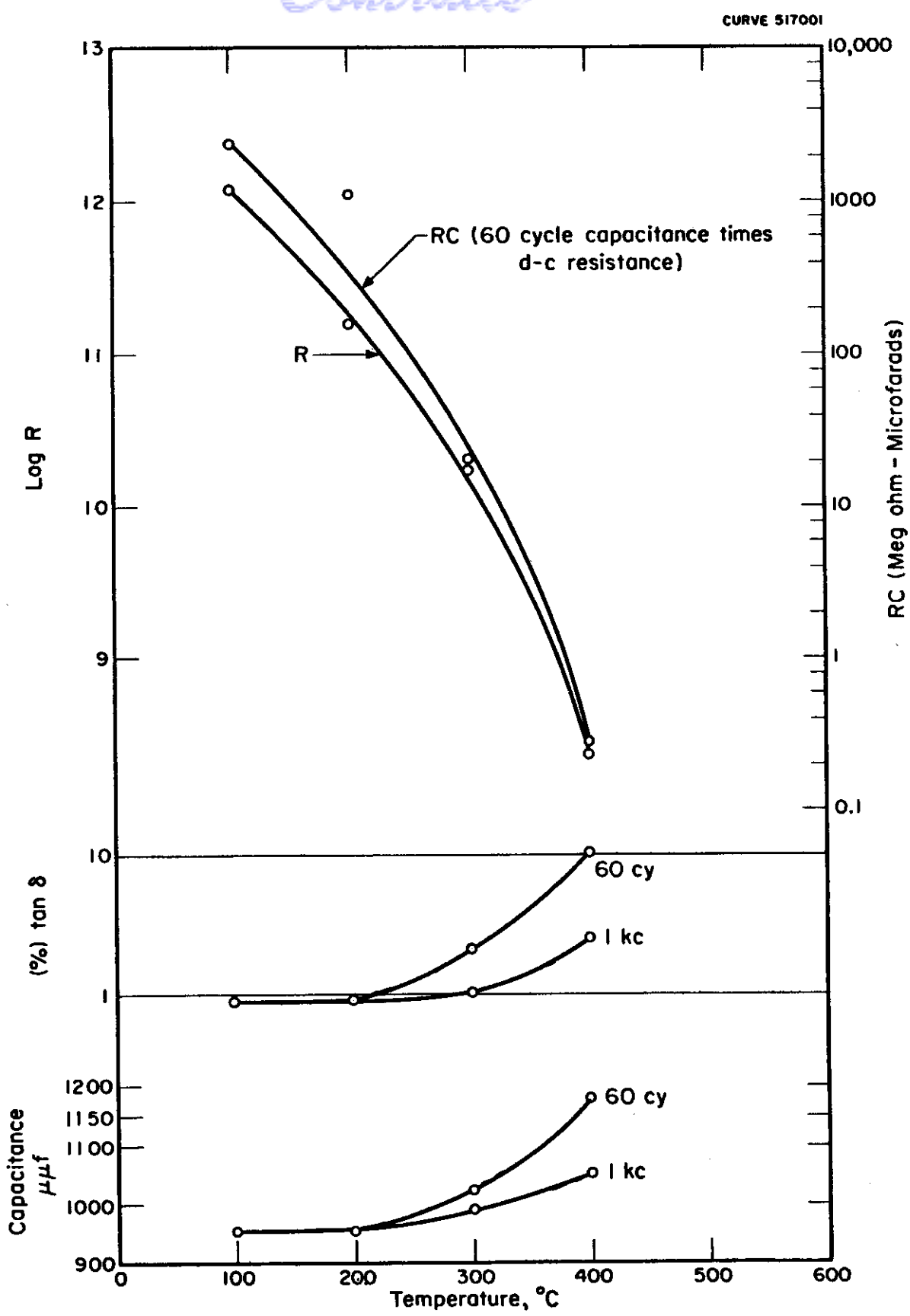

Fig.30- Electrical properties of magnesia applied to aluminum foil by plasma jet.

Approved for Public Release

Contrails

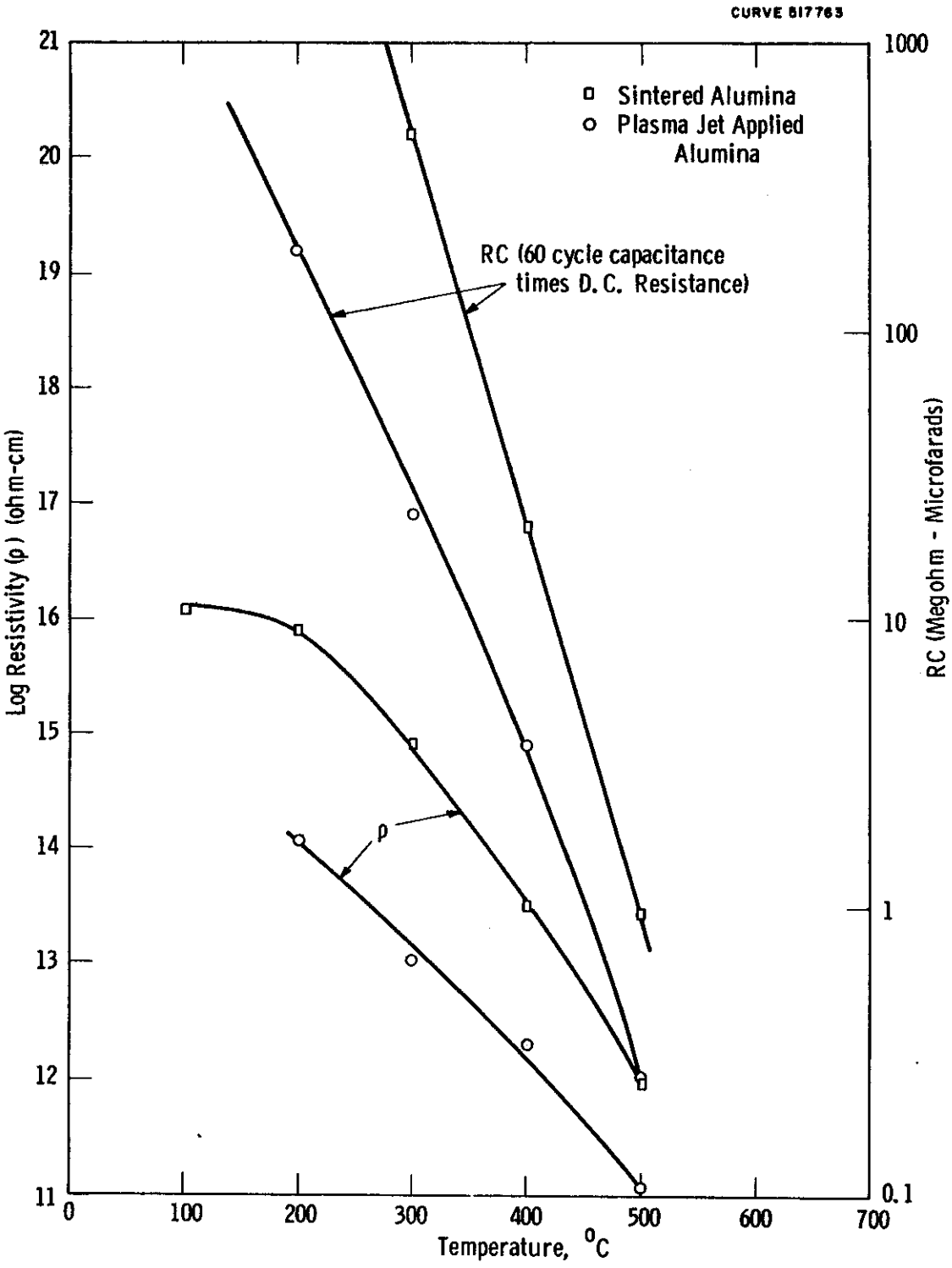

Fig. 31 --Resistivity and RC factor of sintered and plasma jet sprayed alumina

Approved for Public Release

Contrails

CURVE 517762

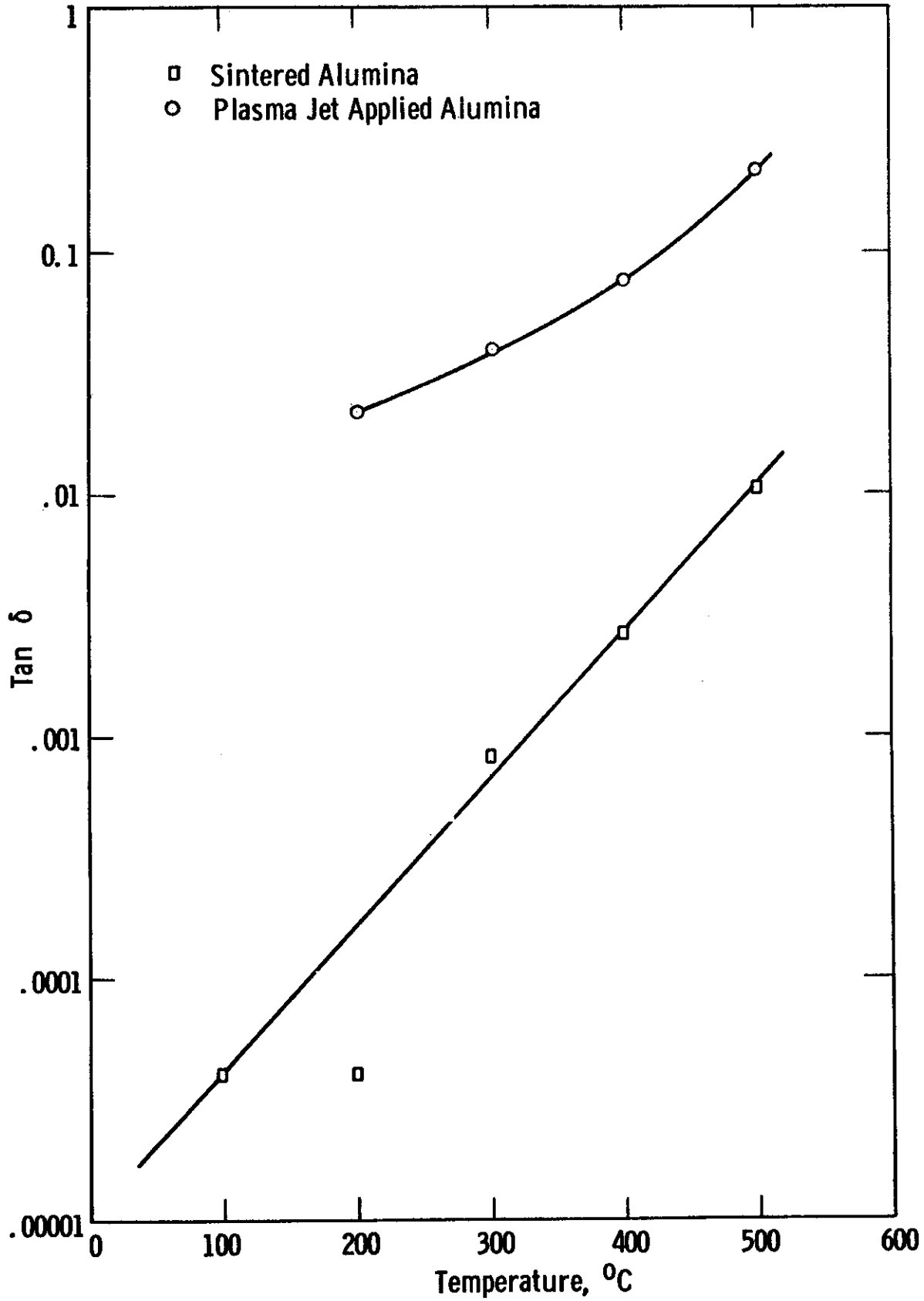

Fig. 32 --Dissipation factor of sintered and plasma jet applied alumina (60 cy)

Approved for Public Release

Contrails

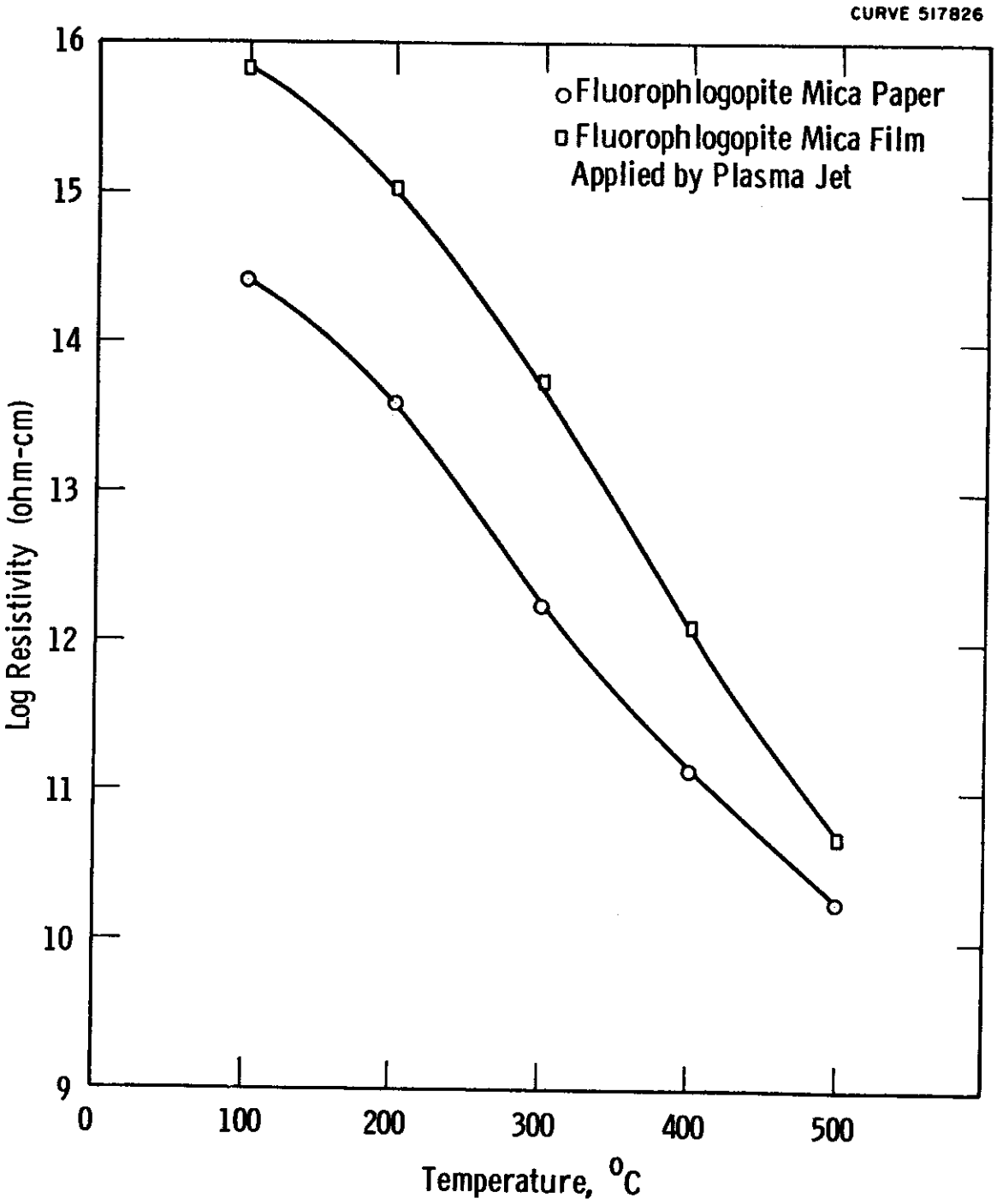

Fig. 33--Resistivity of fluorophlogopite mica paper and plasma jet applied film

Approved for Public Release

Contrails

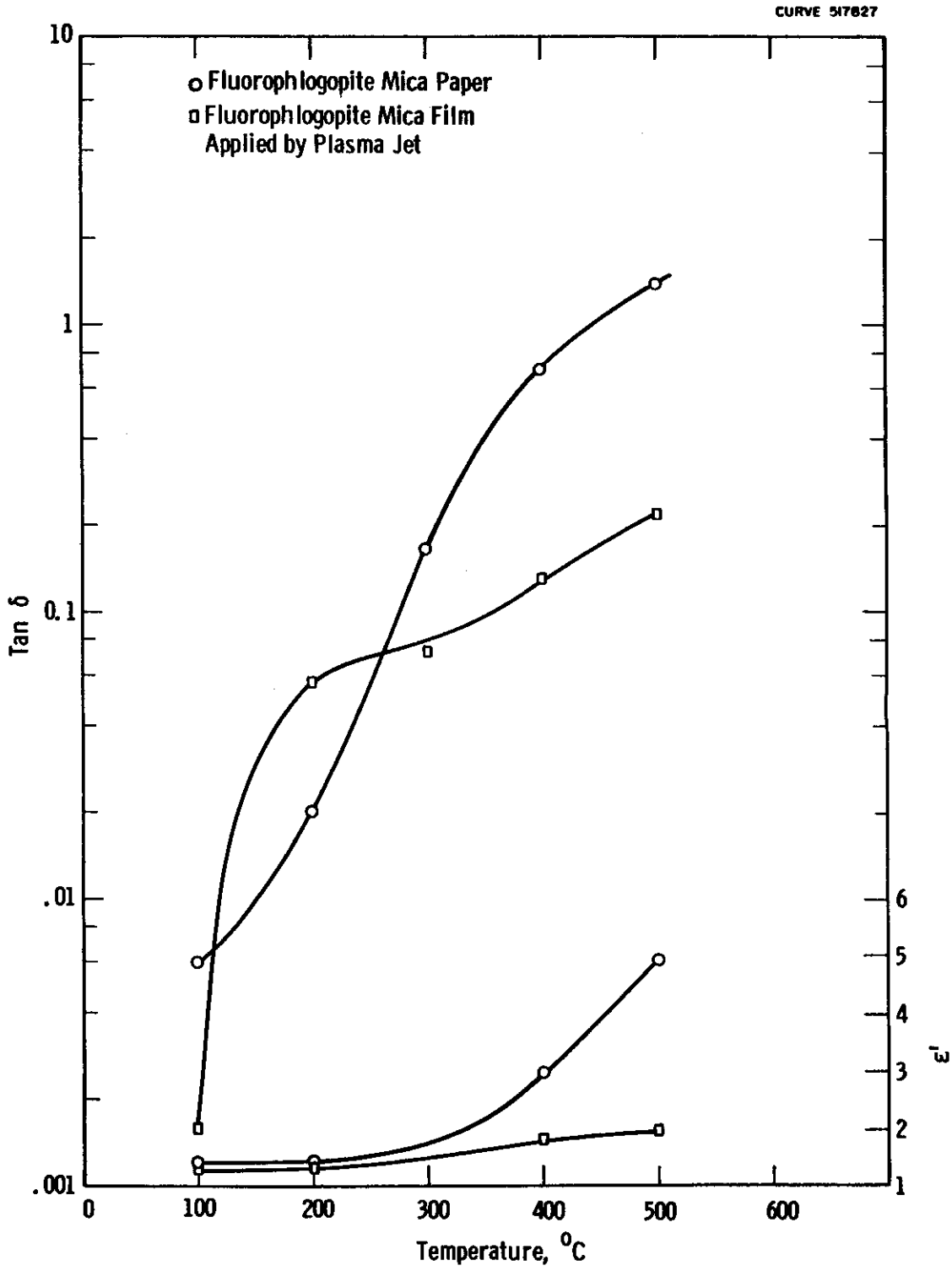

Fig. 34--60 cycle properties of fluorophlogopite mica paper and plasma jet applied film

Approved for Public Release

Contrails

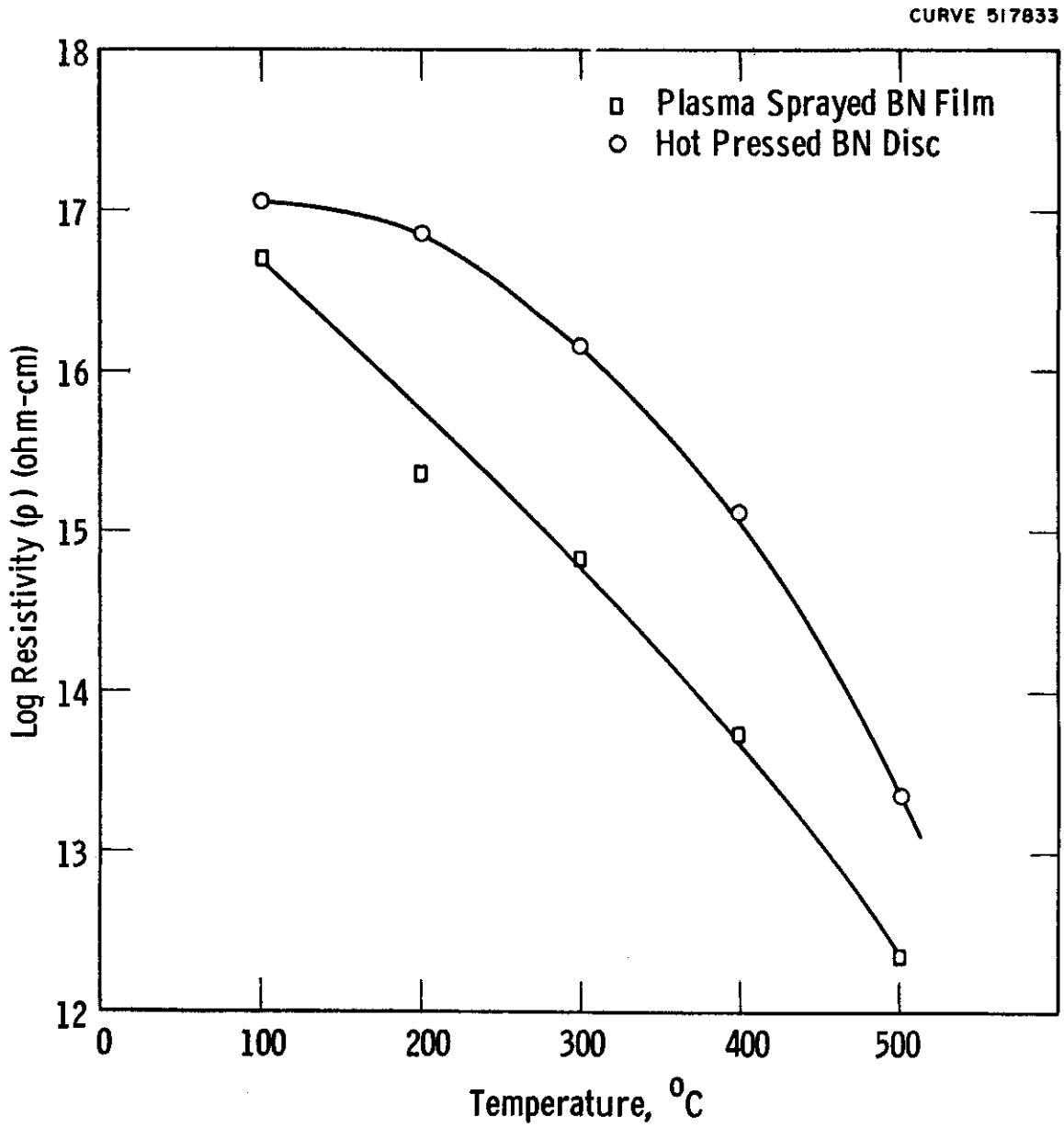

Fig. 35--Two minute resistivity of hot pressed boron nitride and plasma sprayed film

Approved for Public Release

Contrails

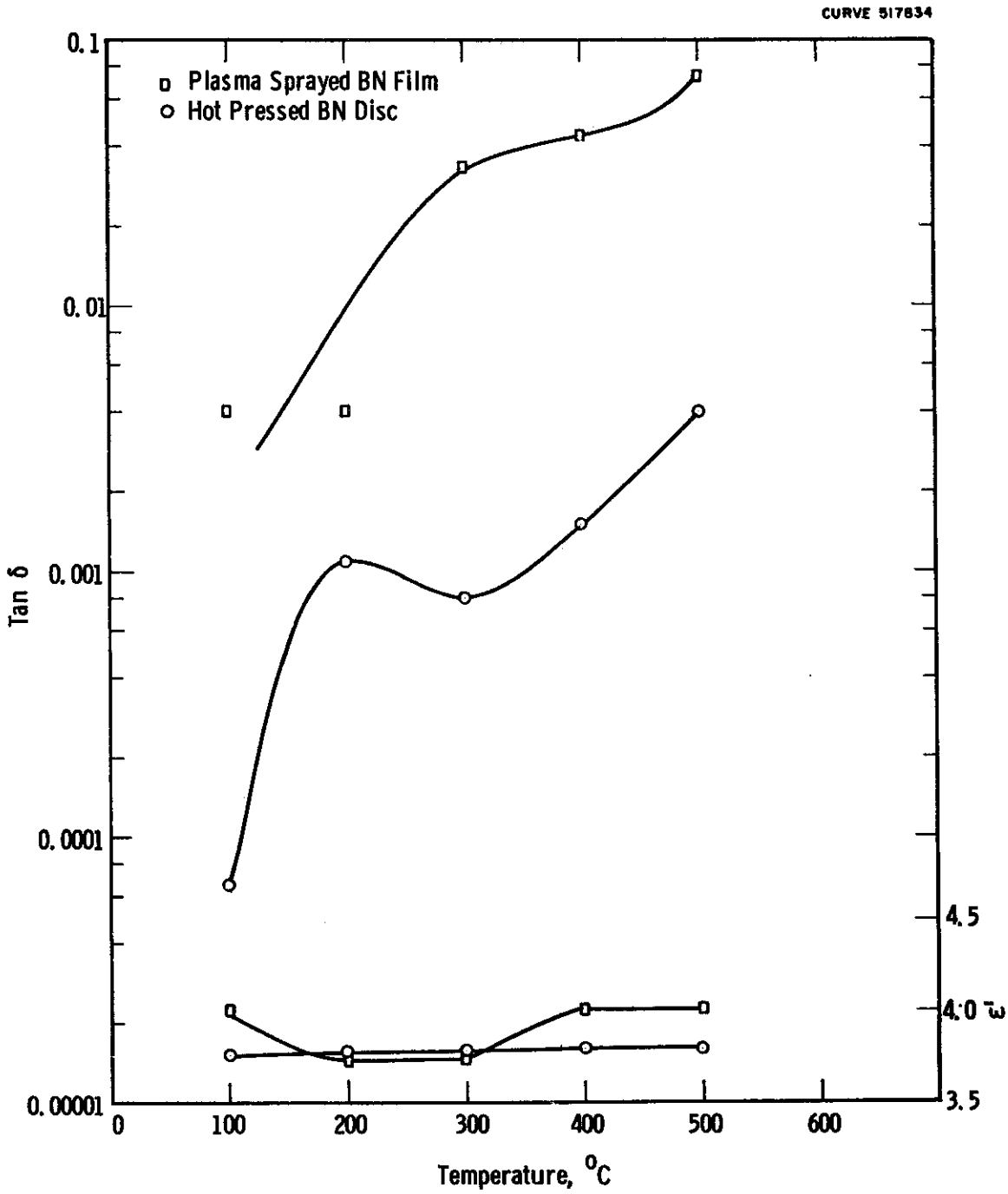

Fig. 36--Dissipation factor and dielectric constant of hot pressed boron nitride disc and plasma sprayed film (60 cy)

Approved for Public Release

Contrails

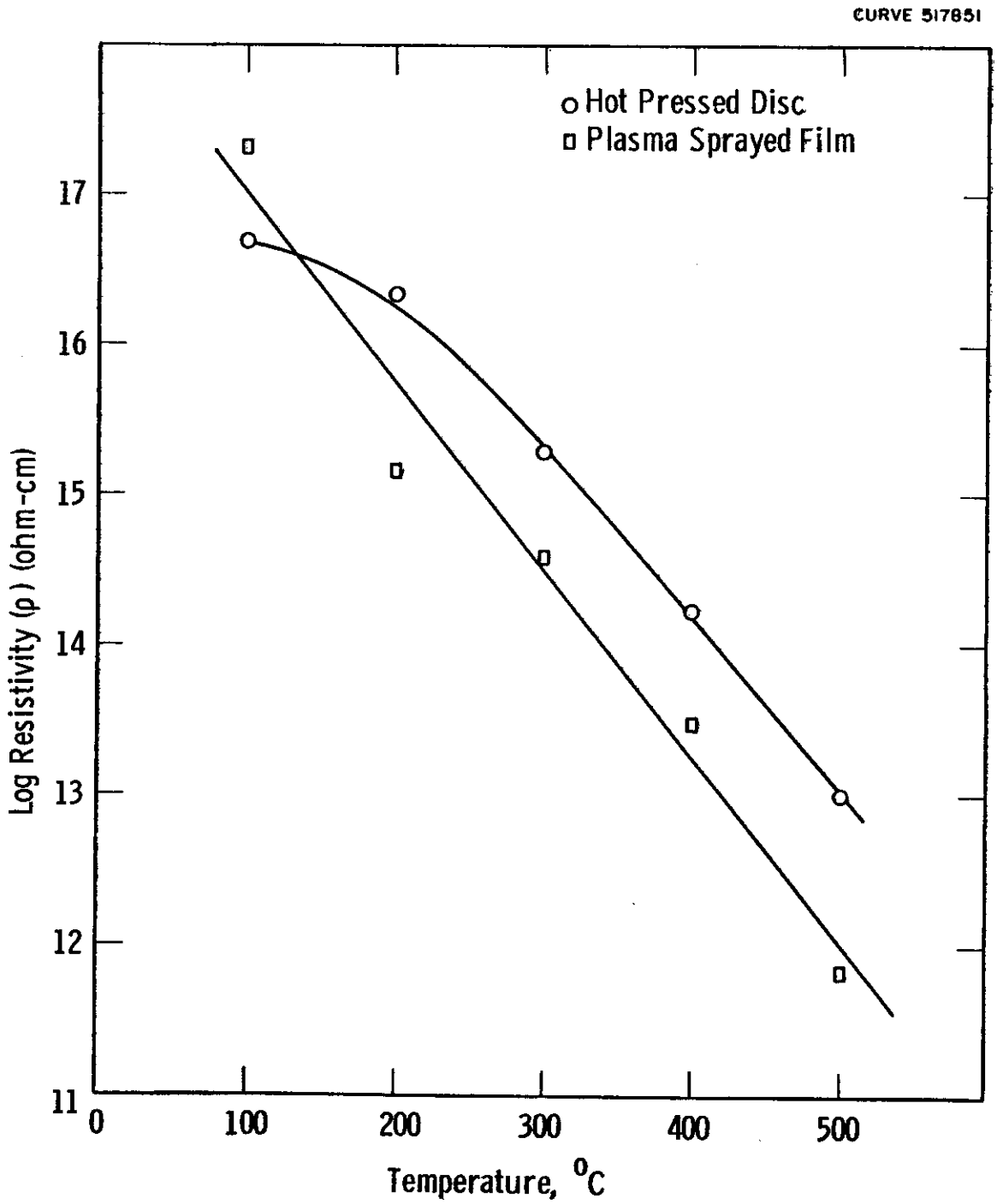

Fig. 37 --Two minute resistivity of hot pressed disc and plasma sprayed film composed of 70% boron nitride and 30% cabal glass

Approved for Public Release

Contrails

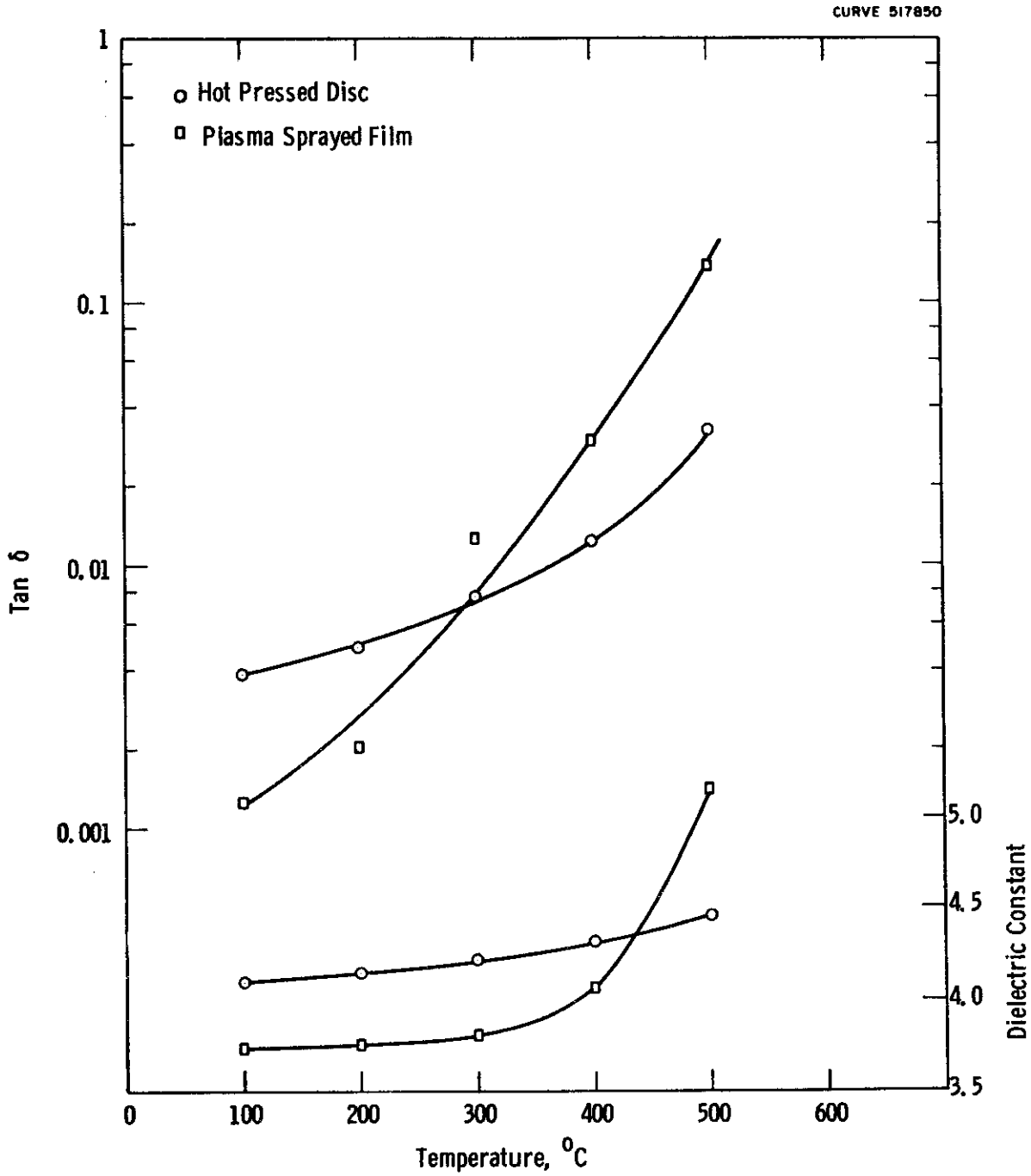

Fig. 38--Electrical properties of hot pressed disc and plasma sprayed film composed of 70% boron nitride and 30% cabal glass (60cy)

Approved for Public Release

Contrails

SECTION IV. ANODIZED ALUMINUM

(W. C. Divens and D. H. Hogle)

A. INTRODUCTION

High purity alumina was shown in previous reports under this contract (WADC TR 59-337, Part I) to have excellent dielectric properties at 500°C. To obtain alumina of high purity in a thin film useable as a capacitor dielectric, the properties of high purity anodically formed alumina have been investigated during the later stage of this contract.

Electrolytic capacitors have long utilized this form of dielectric. Extremely high capacitance per unit area is obtained in electrolytic capacitors, due to the thinness of the oxide film and the intimate contact provided by the conducting electrolyte. The thickness of the oxide film (and inversely the capacitance) is proportional to the final anodizing voltage. A barrier oxide layer thickness of about 6 to 13 angstroms is developed per anodizing volt, depending on the electrolyte. Anodizing voltages can reach a maximum of 500 to 1000 volts, also depending on the electrolyte. The maximum operating d-c voltages of electrolytic capacitors are close below the final anodizing (forming) voltage. The oxide dielectric of electrolytic capacitors is extremely sensitive to the polarity, having a much lower resistance with the polarity reversed from the anodizing direction. These capacitors are commonly operated in the electrolyte from which they were formed, with the electrolyte being the counter electrode.

To utilize such a dielectric at very high temperatures, it is obvious that the conventional electrolyte solutions must be abandoned. Furthermore no solid or paste electrolytes or semiconductors have so far been found suitable for very high temperatures in this application. Changing from the electrolyte counter electrode to a metal electrode, and operation of the anodic oxide as a dry dielectric, offers both advantages and disadvantages. It offers the potential reduction, if not the complete elimination, of polarity effects and the capability of operating at much higher temperatures. On the other hand, it presents a problem of maintaining the continuity and the electric strength of the film over large areas.

This is partly due to the difficulty of handling the thin dry films without puncturing them and partly due to the elimination of the anodizing film forming capability of the counter electrode.

It has been found, (cf also J. Burnham and P. Robinson, Ann. Report, N.R.C. Conference on Electric Insulation, p. 68 (1948)) that the capacitance per unit area of the dry oxide films is essentially the same as that in an electrolytic capacitor with the same oxide thickness, providing an intimate contact metal electrode is applied to the dry films, such as an evaporated or sputtered metal film.

The use of thin evaporated or sputtered metal electrodes also helps to overcome the problem of defects in the dry film: the defect-shorts are

Approved for Public Release

Contrails

isolated by the local current melting of the metal which flows away from the defect spot. This still does not, however, permit the application to appreciable areas of these films of voltage stresses comparable to those used with the anodizing electrolyte as the counter electrode. With very small areas, the electrolytic capacitor voltage can be approached on the dry film.

It has been found that the voltage capability of these dry films can be improved substantially by increasing the film thickness but with a corresponding reduction in capacitance. This has been accomplished with two anodizing steps by growing a protective porous layer of oxide of controllable thickness above the barrier oxide layer. The capacitance of the dry films decreases inversely as the total thickness of the porous layer and barrier layer. Practical values of this thickness reduce the capacitance per unit area two or more times below that obtained with high voltage electrolytic capacitors.

During this last period of the contract, the principal goal has been to improve the electrical properties of the anodically formed alumina film capacitors and to establish procedures which would lead to more uniform results. In practice, it has been found difficult to separate these objectives, since, in many cases a change of one variable has also affected the others.

Many factors have been studied; some are a continuance of work described in previous reports, and others were initiated during this period. In the latter category, increasing the thickness of the porous layer has been responsible for a marked improvement in the electric strength and the attainment of reasonably long life at 500°C. In principle, the use of different electrolyte compositions and anodizing conditions which lead to dense films with very small pores should lead to improved electrical properties, but in practice the observed effects have not been as large as had been expected.

B. APPARATUS

1. Anodizing Equipment

a. Protective enclosure

Earlier in the program it has been shown that the purity of the anodizing electrolytes had to be maintained in order to produce satisfactory oxide films. Preparation of pure electrolytes has been achieved, but it became apparent that the electrolyte had to be protected against air borne contaminants, because of the ventilating system used in the laboratory. A transparent enclosure was made from Plexiglas sheet. This enclosure was made large enough so that it could be used for storage of materials as well as carrying out the anodization process without crowding. Figure 39 shows this enclosure with its contents. The temperature controlled bath container is the rectangular transparent container on four wooden supports. The bath is a mixture of glycerine and water which can be heated or cooled. A 500 watt immersion heater is used to heat the bath for anodization above room temperature, and a copper coil in the same bath is connected to an external refrigeration unit, for anodizations below room temperature. A stirrer in the bath continually circulates the bath liquid to

Approved for Public Release

Contrails

maintain high heat transfer. A round polyethylene container is used to hold the anodizing electrolyte and it is immersed into the temperature controlled bath. Also, a magnetic stirrer driver is positioned underneath the bath and a Teflon coated stirrer is placed in the electrolyte container to provide constant agitation of the electrolyte.

b. Anodizing cells

During the program, several types of anodizing cells have been used. Most of them were discarded because of some suspected adverse effects each would have on the anodized film. The ideal electrolyte container or anodizing cell is one which has the following features:

1. Non-metallic and electrically non-conducting
2. Chemically inert
3. Absolutely liquid tight
4. Thin walled
5. Good thermal conductivity
6. A physical shape which permits efficient stirring

The cell which is presently being used is a molded polyethylene container which is about 4 inches in diameter. So far, this cell has been the most satisfactory one used. This is shown in Figure 40.

c. Cell screens

During the anodizing process, hydrogen gas is profusely evolved at the cathode and is dispersed throughout the electrolyte. Even with rapid stirring, many bubbles can cling to the anode. It has been noted that under such conditions poor anodic films are produced. It was imperative that preventative measures be taken to restrict the bubbles from the anode region. Most of the methods tried centered around the idea of separating the cell into two compartments by a fine material which would not pass the bubbles, yet would permit conduction through the electrolyte. Fine glass cloth was tried but was discarded because contaminants were being continuously leached from the cloth. Nylon cloth was also tried, but poor films were produced and it too, was discarded. Moderate success was achieved by using a fine nickel mesh which had been gold plated. However, with time it was noted that poorer and poorer films would result. After a sufficiently long time, it could be seen that the gold was being removed from the screen and the bare nickel was exposed to the electrolyte. See Figure 41. It was suggested that since this screen was floating electrically, it became a bipolar electrode and may have caused deposition of gold on the anode in small quantities. The present system in use utilizes a regenerated cellulose sleeving which is normally used for electro-dialysis work. The sleeving is placed around the cathode and is very effective in eliminating any bubbles from the bulk of the electrolyte.

d. Power supplies

Two power supplies were constructed for the anodization process. Because of the wide range of current and voltage necessary, two small supplies were used rather than one large one which could cover the necessary range.

Approved for Public Release

Contrails

Both supplies utilized silicon rectifiers in conjunction with replacement type radio transformers. Voltage was controlled with an autotransformer at the input and appropriate voltage and current measuring instruments were used. One supply had a voltage range of 0-800V and a current range of 0-400 ma with power restriction of 40 watts maximum. The other supply had a voltage range of 0-120V, a current range of 0-1.6 amperes with power limited to 160 watts. Neither supply used any filtering of the rectified a-c.

2. Test Facilities

a. Testing ovens

The ovens which were used for routine evaluation of test capacitors have had no major revisions since the last report. Two ovens which are identical have been used exclusively for testing and have proved to be entirely adequate. These ovens are capable of temperatures up to 900°C but are limited to 600°C for making electrical measurements by components of the electrical measurements systems. Temperature controllers used with these ovens control the temperature to within plus or minus 3°C at any given setting. There is, however, a temperature gradient within the ovens themselves of as much as 15°C from one position to another. This is of little consequence since the actual sample temperature is measured by a separate thermocouple which senses the temperature of the stainless steel plate on which the sample capacitors are placed for measurement. Figure 42 shows the placement of test capacitors and associated leads. Platinum foil is used to make connection between the bare aluminum of the sample and the stainless steel plate. Contact is maintained by pressure applied through weights. A gold foil is used to make contact to the gold electrode of the sample capacitor by pressure contact also. Inherent electrical losses of the measuring leads are negligible. The measured stray capacitance of the leads is approximately 20 picofarads. Shunt losses are less than 0.1% since all solid insulation is Teflon, located outside the hot region of the oven. Both of these values are considerably smaller than those which are being measured, hence they are ignored.

b. Life test oven

Figure 43 shows the arrangement which was used to life test sample capacitors. This oven essentially has all the features of stray capacitance, shunt loss, etc. as the routine testing ovens. The major difference is that space is provided for testing up to 8 samples. A recorder was used to indicate a failure of any sample being tested. This was done by placing a 10,000 ohm resistance in series with the test capacitor and placing a millivolt recorder across a proportionately small part of this resistance. Under normal conditions, the IR drop across this resistor is small compared to that of the sample. However, when the test capacitor failed due to shorting, the test voltage would appear across the 10,000 ohm resistor and the recorder would show the proportionate voltage increase on the chart.

c. Measuring instruments

The majority of the testing involved the evaluation of individual capacitors as to their tan δ - frequency and resistance - temperature characteristics. A General Radio Type 1650-A Impedance Bridge was used in conjunction with a variable frequency voltage source to evaluate the tan δ-frequency properties of samples. This instrument had a usable frequency range of 20 to 20,000 CPS and a tan δ range of 0.1 to 100 depending upon the frequency used.

Approved for Public Release

Contrails

D.C. resistance measurements were made with a Keithley Electrometer and a variable voltage battery source. Figure 44 shows a typical set up for routine testing.

C. FOIL PREPARATION

Throughout the program, attention has not been entirely centered on the preparation of electrolytes and their application. Much effort has been expended in the study of the starting aluminum foil and the effects of various treatments given them. Three characteristics of the Al foil have been investigated as to their effect on the electrical properties of the anodic film, namely,

Purity of the aluminum
Grain structure
Surface condition resulting from chemical polishing

Each of these characteristics is somewhat dependent upon the other. For example, it is known that the resulting grain structure is dependent upon the purity of the aluminum. Also, the surface roughness is dependent upon the grain size and structure and such surfaces respond differently to chemical polishing. Because of these closely related conditions, isolating the effect produced by any one was difficult and in the end, conflicting data did not permit making any definite conclusions. However, an examination of the overall data does seem to show trends favoring certain types of aluminum conditioning.

1. Chemical Polishing

Almost all of the aluminum foil used during this program was 0.002 inches thick and of 99.99% or better purity.

Polishing of the foils prior to anodization was done mainly for two reasons. First, any surface contamination would be removed and secondly, any existing surface roughness would be eliminated. Removal of surface contamination was considered important since the existence of such areas would prevent film formation at these sites. Each defect site is a potential point for electrical conduction to increase, resulting in higher electrical losses.

Keeping the surface as smooth as possible is equally as important because of the high fields to which these films are subjected. Fields approaching 10^6 volts per centimeter are quite common for the films involved. Although the anodization process has a tendency to smooth the surface as it progresses, the film developed does retain much of the contour of the aluminum substrate. This is apparent as is shown in Figure 45. This picture shows the normal cross section of a sample capacitor and some sharp points on the aluminum surface are visible. Figure 46 shows a thickly anodized section and it is very noticeable how the aluminum substrate has been smoothed by the anodization. This particular sample had not been polished and will be discussed later in this report. Experimentally, samples of aluminum have been anodized in which the controlled variable has been the chemical polish. The electrical properties of such polished and unpolished samples have shown very little change on an average. It is believed that polishing may have negligible effect because of the surface condition of the starting aluminum. The aluminum as received has a highly reflective surface indicating that such a surface is very smooth and in some cases attempts to polish may result in actual etching rather than polishing. The

Approved for Public Release

Contrails

polishing solution consists of 112 parts ortho-phosphoric acid, 8.5 parts nitric acid and a trace of cupric sulfate all held at 95°C. A differential spectral analysis was made on polished and unpolished aluminum as well as the aluminum obtained from the two suppliers. The analysis results are tabulated below in percentages of impurities.

	Cu	Mg	Mn	Fe	Si	Ag
Polished - Supplier A	.02	.002	.0002	.002	.002	<.0001
Polished - Supplier B	.02	.002	.0002	.002	.002	<.0001
Unpolished - Supplier B	.005	.0008	<.0001	.002	.002	<.0001

This data indicates that the polishing process increases the impurity level of Cu and Mg. This is probably due to the presence of cupic sulfate in the polishing solution. It is doubtful whether the small increase of these impurities has any adverse effects on the overall properties of the anodic films.

2. Heat Treating of Aluminum Foil

Aluminum foil, as it is received from the manufacturer, has some cold working in it due to the final rolling process. Heating the foil to 500°C results in complete recrystallization of the material within a very short time - possibly less than one minute. Just how the recrystallization would effect the anodic film was not known and as a result some studies were made with regards to it. Earlier in the program, the porous oxide film was formed on the aluminum directly from the supply roll without any annealing. The subsequent heating of the sample prior to the second anodization in tartaric acid may have caused some cracking or fissures due to the annealing. This was of little concern since the tartaric anodization would, so to speak, heal such defects. Experiments have been carried out where sample capacitors have been made with both the porous and non-porous anodizations being completed before any heating of the aluminum. Also, samples were prepared from aluminum which had been first annealed prior to any anodization. Here again, electrical measurements revealed little or no significant difference as a result of the two types of processing.

Studies were then started on the effects of the grain size relative to the formed oxide films and their resulting electrical properties.

During annealing, grain structure and crystal sites develop, their physical nature depending upon the degree of cold working and heat treatment given. Attempts were made to choose the proper conditions which would result in the development of large grain and fewer grain boundries. It is known that electrical conduction is more pronounced at grain boundries and that the oxide films which are produced are replicas of the aluminum surface. Hence it was reasonable to expect that fewer grain boundries would result in lower conduction through the oxide film.

For aluminum there are two conditions which are conducive to the formation of large grains. The amount of cold working has to be in a region below 3% or up to the vicinity of 98%. Obviously when using 2 mil foil to start with, the 3% region is the only one useable. The foil is first completely annealed at 500°C for a short period of time. It is then given 3% cold working

Approved for Public Release

Contrails

by stretching until the cross-sectional area is reduced by 3%. The strip of foil is then suspended so that it is lowered into an oven which has its temperature set slightly below the melting point of aluminum. The temperature which was used was 630°C. The condition which is best suited for formation of large grains is to have the foil subjected to a steep thermal gradient. This is accomplished by having the foil enter the oven through a thin slit and on the outer portion a cold stream of vaporized liquid N_2 is played over the surface of the foil. The foil is then lowered into the oven at a rate of 5 cm. per hour. With this technique, individual grains were produced with areas up to several square inches. Unfortunately, the shape of these large grains did not permit the fabrication of a sample capacitor from one individual grain. Figure 47 shows a capacitor made from such aluminum and the grain boundary is quite evident. The reverse side of this sample is a mirror image of the front side, showing that the grain boundries propagate through the sample.

Samples were fabricated to evaluate the films made from large grain aluminum. As a comparison, a sample which had only been annealed, was given the same treatment as the larger grained one with one exception. That exception was the "annealed only" sample (OT-27) which was anodized with 93 coulombs, instead of 69 coulombs. The capacitance and loss as a function of frequency is shown in Figure 48. Several unique properties are evident from the data. First, the change in tan δ with frequency is not great. This is to say that there is no sharp dispersion peaks present. Second, the loss, in general, seems to be lower than most previously prepared samples, and third, the change in capacitance with frequency is considerably less than has been noted before. The curve marked as OT-28 (compensated) is the same as the OT-28 capacitance curve except the capacitance has been decreased by a 69/93 ratio. This is valid if the sample thickness is proportional to the number of coulombs used. For any given set of conditions, this proportionality has been found to be correct.

Data from these tests revealed a condition which was not expected, in that the D.C. resistance was no better than previous samples. The R.C. value for sample OT-28 was about 8.8 ohm farads. It is believed that the cause of such behavior lies in the structure of the aluminum. It has been pointed out previously that the formed film is a replica of the aluminum surface and it is believed that oxidation takes place more readily at grain boundries. It is conceivable that under certain conditions, where minute grains exist, that oxidation could proceed around such a boundry and result in the isolation of small aluminum particles. Also, with small grain size, random boundry paths through the aluminum would provide a longer path from the surface of the oxide to the aluminum substrate. Whereas in the large grained samples, the path would be much shorter and could possibly contribute more to the D.C. conductivity. There has been some indirect evidence to support this theory obtained through tests made on aluminum foil from another manufacturer. The foil was guaranteed to be better than 99.99% pure and it was proposed that, if the purity level of the aluminum was a major contributing factor to the overall electrical properties of the anodic film, some changes should become apparent. Sample capacitors made from this foil were tested and they showed decidedly poor properties in all respects. Examination of the samples showed that the aluminum had developed many grain boundaries. Attempts to anneal and rework the aluminum were futile. The aluminum as received was quite hard indicating a rather high percentage of cold working due to rolling. Upon annealing such aluminum, grain structure

Approved for Public Release

Contrails

immediately developed and propagated through the foil. Attempts to grow large grains on this aluminum could not accomplished because any additional cold working on the annealed material by tensile methods place the strain on the grain boundaries rather than on the existing grains. Figure 49 shows a sample capacitor made from this aluminum.

It seems that the ideal condition for the formation of good anodic films would be formation of the film on a single grain of aluminum where no grain boundaries exist. At present samples are being examined by metallographic techniques, but the results will not be known in time to report them.

D. ELECTRODES

1. Sputtered Gold

During the last phases of this contract sputtered gold electrodes have been used exclusively. They have been highly satisfactory with regards to thermal stability and self-healing properties. When this technique was first developed, it was thought that the gold deposited on the samples was much thicker than it actually was. Metallographic examination of a cross-section of a capacitor showed that the gold electrode was only 3500-4000 Å thick. See Figures 45 and 46. However, this thickness seems to be satisfactory.

2. Evaporated Aluminum

Several times evaporated aluminum has been tried for use as electrodes. In earlier reports it was shown that they were not feasible at 500°C. When some 200°C tests were initiated, evaporated aluminum was tried again. Under the conditions at 200°C, the aluminum was stable, however it peeled off after several hundred hours at this temperature. Such electrodes would be suitable providing methods are used to improve the adhesive properties of evaporated aluminum on anodic aluminum films.

E. ANODIZING CONDITIONS

1. The Porous Layer

There is considerable information available in the literature concerning the structure of porous anodic oxide coatings on aluminum. Perhaps the best reference is an article by Keller, Hunter and Robinson [F. Keller, M. S. Hunter and D. L. Robinson, J. Electrochem. Soc. 100, 411 (1953)] in which and electron microscope technique was used to advantage. They found that initially a barrier layer of oxide is formed, the thickness of which is proportional to the applied potential. This process is counteracted by a dissolution of oxide by the electrolyte. At isolated points of high conductivity, particularly along grain boundaries and other points where impurities concentrate, an increase in temperature greatly increases the dissolving action and a pore if formed. Pore formation continues over the surface tending to give an hexagonal close packed arrangement of pores with a pore diameter and wall thickness characteristic of the particular electrolyte and the formation conditions.

Approved for Public Release

Contrails

Tomaskov has reported that no oxygen gas layer is present in anodic oxide pores. [N. D. Tomaskov and A. V. Byalobzheskii, Trudy Inst. Fiz. Khim., Akad. Nauk S.S.S.R. No. 5, Isskdovan Korrozii Metal No. 4, 114 (1955)]. The presence of an aluminum oxide hydrate, corresponding to $Al_2O_3 \cdot 0.9\ H_2O$ along with 4-5% sulfate were reported when aluminum was anodized in a sulfuric acid electrolyte. The porosity increased with anodization time and with an increase in concentration of the electrolyte.

Russian workers have reported some effects due to orientation and pretreatment of the aluminum metal. [G. S. Vozdvizhenskii, et.al., Doklady Akad. Nauk S.S.S.R. 72, 311 (1950)]. These workers reported that porous films formed in sulfuric acid at 20°C at a low current density were less porous on faces parallel to the axis of a wire than films perpendicular to the axis of the wire. They further state that the porosity is decreased by electropolishing the sample.

In order to achieve a dielectric barrier of maximum reliability, that is with a minimum of faults, and possessing the best dielectric properties, it was felt that several critical conditions must be maintained during the porous anodization. Since, after pore formation has taken place, the anodization continues by reaction at the base of the pores, the temperature within the pore and in the immediate vicinity thereof, must increase far above ambient. It is known that pores can be sealed by placing a porous film in boiling water. Under these conditions the oxide along the walls and at the base of the pores is hydrated, expands and fills the pore. Since hydrated oxide is not a particularly good dielectric, this situation should be avoided during the anodization. Hence, efficient stirring and moderate electrolyte temperature should be maintained and excessive current densities should be avoided. Since anodization will not continue in areas where the pores have been sealed, areas of thin barrier dielectric will result. This will cause higher losses and lower breakdown at these points. That such a possibility exists is illustrated by Figures 45 and 50, which show a cross-sectional view of a finished capacitor under 1000X magnification. Uneven thicknesses of oxide are evident here even though precautions were taken to avoid the conditions just discussed.

Even though the effect of anodizing temperature has not been effectively discussed in the literature, it was felt that it has a pronounced effect on the pore structure under otherwise identical conditions. In a previous discussion (WADC TR 59-337, Part II, p. 35, June 1960), it is pointed out that: (1) the final voltage increased with a decrease in temperature, and (2) the capacitance per equivalent area under otherwise identical conditions also increased with a decrease in temperature. This effect was tentatively attributed to a change in efficiency with a change in temperature. It would appear at this time that this is an effect due to a change in porosity because of the following considerations.

It is seen from Figure 51 that when an anodic film formed at -8.5° in 2% oxalic acid in a 50% glycerol-water mixture was heated with the film in the bath, the voltage at 100 ma. steadily decreased with an increase in temperature. No voltage was applied between measurements. Since the observed voltage

Approved for Public Release

Contrails

is an indirect measure of the thickness of the barrier layer and it is known that the solubility of aluminum oxide in oxalic acid increases with temperature, one must conclude that the barrier layer beneath the pores is spontaneously dissolved by the electrolyte. That this voltage represents an equilibrium was demonstrated by the fact that the voltage remained constant with time at any given temperature, but would spontaneously drop with an increase in temperature. No spontaneous increase in voltage was noted when the bath was cooled from one temperature to a lower one. This behavior can be explained satisfactorily if one assumes that no fresh electrolyte enters the pores when no voltage is applied to the cell. The data illustrates that the size of a pore can be readily changed during the anodization, if the local temperature changes. Since the pores are propagated by anodization and dissolution in the hemispherical bottom of the pore, as depicted in Figure 52, an increase in temperature leads to a greater rate of dissolution, consequently a thinner layer of barrier oxide remains, since the rate of anodization is constant. The end result is a larger pore diameter and a correspondingly thinner cell wall, that is to say, an increase in the porosity.

It is evident that the ideal porous layer is one with an small and as few pores present that will allow a uniform layer of oxide to be formed whose thickness is proportional to the number of coulombs of anodization. Since the size and number of pores is dependent both on the electrolyte and the formation voltage, one may reason that a porous film, formed at the highest voltage possible, with an electrolyte that can be volatilized from the pores, would have the most desirable dielectric properties. This would then require an organic electrolyte such as oxalic acid, which is known to form small diameter pores and at the same time, a minimum number per unit area of surface. By lowering the temperature to near the freezing point one can attain considerable increase in the formation voltage. Using a glycerol-water solvent mixture, the formation voltage increases still further with a further decrease in temperature. A relatively large increase in formation voltage can be obtained by decreasing the concentration of electrolyte. This procedure cannot be extended to very low concentration since a point is soon reached at which insufficient electrolyte is present for proper anodization. However, if one maintains a constant supply of electrolyte for anodization and decreases the electrolyte's capacity for dissolving alumina, still further increases in formation voltage can be made. This can be accomplished by replacing a given proportion of the oxalic acid with tartaric acid which does not dissolve alumina to any appreciable extent.

Electron micrographs were made of surfaces which had been anodized by three different anodizing techniques. The effect of lowering the anodizing temperature from room temperature to near 0°C and the effect of lowering the electrolyte concentration as well as substituting tartaric acid for a portion of the oxalic acid was observed. The electron micrographs were prepared by a resin replica technique in which a thin film of resin is first laid down on the surface, stripped off and shadowed with chromium at a 30° angle. A uniform coating of carbon is then evaporated over the chromium shadow and the resin is dissolved away. The carbon replica rests on a fine copper grid during this and subsequent steps. The electron microscope photographs are then taken of the specimen. Hence depressions on the original surface show up in the photographs as protrusions which were shadowed by the chromium vapor, and appear as dark areas on the positive print.

Approved for Public Release

Contrails

The electron micrographs shown in Figure 64 are of a surface replica of a film anodized in 2% oxalic acid at 17°C and 5.8 ma/cm^2. The aluminum foil was one in which large grains had been grown and had been chemically polished prior to anodization.

Figure 65 is an electron micrograph of a surface anodized in 2% oxalic acid at 0°C and 11.6 ma/cm^2. The aluminum foil in this case had been annealed at 500°C only before anodization.

The surface pictured in Figure 66 was anodized in 0.1% oxalic acid, 0.1% tartaric acid at 0°C and 5.8 ma/cm^2. The foil was large grained and also had been chemically polished prior to anodization.

It is seen in all cases that a uniform pore diameter is not attained. There is, however, evidence that at least some of the large pores (ca. 1000 Å as compared to 170 Å reported by others) are funnel shaped as a result of the dissolving action of the electrolyte. In Figure 66, particularly at the higher magnifications, this effect can be seen quite clearly on some pores. The presence of pores several times larger than normally encountered could also be interpreted as an effect similar to that recently reported by Renshaw (J. Electrochem. Soc. 108, 185 (1961)) in which hemispherical colonies of pores were formed under the surface from single pores in an otherwise barrier oxide.

The number of pores visible in a given area is somewhat contrary to what one would expect on the basis of the observed formation voltage. One must tentatively conclude that there are pores present in the 0°C, 2% oxalic acid film that are not visible in the photographs, since fewer pores are apparent here than in the mixed oxalic-tartaric acid film which was formed at an appreciably higher voltage.

Comparing Figures 64 and 66, in which only the temperature of anodization differs, it can be seen that the low temperature anodization produces an uneven distribution of visible pores as well as a fewer number of them as was predicted. It is felt, however, that considerably more work in this area would be necessary to elucidate the true differences in the microstructure of these oxide films.

Initial formation voltage curves as a function of time for several anodizing conditions are shown in Figure 53. The formation of the porous structure is clearly indicated on the curves after a period in which the voltage increases linearly with time. The roughly linear decrease in voltage after the pores have been formed may be attributed to a further dissolving action on the walls of the pores. The initial linear portion of the curves is no doubt the time in which the barrier layer is growing prior to pore formation. At any given current density, it should be noted that the initial slopes of the lines are roughly equal, indicating a nearly constant growth of barrier oxide. As the current density is increased, the slope increases, indicating a greater anodization efficiency. This may be done in part to the fact that dissolution

Approved for Public Release

Contrails

of oxide from the surface is less, because of the greater rate of oxide formation. For example, at 200 ma in the 0.1% oxalic acid, 0.1% tartaric acid solution, twice as much oxide has been formed at any given time as the same process at 100 ma, such that the maximum voltage is reached in 1.75 minutes, whereas the 100 ma process requires 4 minutes. The proportionately greater time in the latter case possibly represents the amount of alumina dissolved from the surface in the last 2.25 minutes of the anodization.

Some of the curves do not extrapolate through the experimental zero time on the graph. This is more evident for the cases of moderate current density and low electrolyte concentration, indicating that the internal resistance of the cell may be significant in such cases. Any oxide present on the aluminum before anodization, that is, room temperature thermal oxide, would cause some error also.

The dielectric properties of the porous layer and its varying thickness of barrier layer has been evaluated. Table 7 compares the properties of an anodic film formed at 56°C in 2% oxalic acid with one formed at 0°C in a mixture of 0.1% oxalic and tartaric acids. It is seen that the anodic oxide formed at high voltage has considerably better properties as well as a smaller effective thickness as indicated by a larger capacitance. Any interpretation of these facts is complicated by a large difference in barrier layer thickness of the two samples. The barrier layer thickness is assumed to be proportional to the formation voltage, which is different by a factor of 18 in these two cases. It is apparent, however, that the anodic oxide with the thickest barrier layer has dielectric properties that are considerably closer to those with a two stage anodization. The larger equivalent capacitance may be due to the decrease in porosity of this oxide.

TABLE VII. DIELECTRIC PROPERTIES OF POROUS LAYER ALUMINA AT 500°C WITH SPUTTERED GOLD TOP ELECTRODES

Sample	Capacitance Equiv. Coul.	100 tan δ, 1 Kcy.	Resistance Ω@ ~ 5V
56°C, 2% oxalic, 9V	0.119	100	3.7×10^4
0°C, 0.1% oxalic + 0.1% tartaric, 160V	0.147	17.5	1.8×10^6

2. The Barrier Layer

Since the porous layer and its concurrent barrier layer are formed prior to anodization in tartaric acid, the latter process merely increases the thickness of the already present barrier layer to a standard thickness. The behavior of the anodization is, however, quite dependent on the pore structure of the previously anodized layer since this anodization takes place, as before, at the base of the pores. Therefore it is important not to use an excessive current density which will form hydrated oxide and seal the pore from further anodization. Hence it has been found necessary to limit the power input to about 0.7 watt/cm^2 during the anodization of films whose porous oxide had been previously formed at high voltages. This is generally accomplished by appropriately

Approved for Public Release

Contrails

reducing the anodization current as the voltage rises. Using this technique, it has been found that current levels of 3.5 $\mu a/cm^2$ @ 500V are readily obtainable when the anodization is carried out in a well stirred electrolyte at near 0°C. The use of the low temperature allows a somewhat higher maximum formation voltage, an effect quite parallel to the effect of concentration discussed in an earlier report. (This contract, WADC Tech. Report 59-337, part II, p. 37).

The dielectric properties of the barrier oxide alone has also been evaluated. In this case, only the heavy tab section was formed in oxalic acid prior to anodization in tartaric acid. After clearing at 22.5V d.c., 500°C it was found that the losses were quite normal. The capacitance was of the order that one would expect, i.e. .093 μF/sq. in., which is about twice the value normally measured on the composite dielectric. The resistance, however, was approximately two orders of magnitude lower than normally measured on a composite sample, and corresponded roughly to that obtained with the porous layer anodization at low temperature reported in Table 7. These samples would not withstand continuous application of 45V dc. After only 1.5 hours of life under this applied stress, the capacitance was only 10% of the initial value. It appears that the a.c. loss of the composite anodized film is controlled by the barrier layer to a greater degree than the porous layer, although the porosity of the porous layer seems to have some effect. The d.c. resistance, and the electric strength appear to be functions of the combination.

F. DIELECTRIC PROPERTIES

Measurements have been made of some 300 anodized aluminum samples prepared in different ways. A majority of the measurements have been made with samples having an active electrode area of 1.5 in^2 with a porous oxide layer of about 0.7 microns thick over a barrier layer of about 0.6 microns the latter being formed at about 500 volts in tartaric acid. The capacitance of these samples is about 0.04 μF/square inch.

Samples prepared in duplicate procedures have shown appreciably different dielectric properties, particularly in regard to d-c resistance-temperature dependence. The a-c characteristics are much more reproducible, particularly the capacitance and its frequency and temperature characteristics as shown in Figure 64. The tan δ level is fairly consistent, varying between 0.05 and 0.20 at 500°C and with distinct maxima which shift regularly upward to higher frequency with increasing temperature. Both the capacitance and tan δ variations with frequency and temperature are fairly typical of a Maxwell-Wagner ionic polarization phenomena. Mobile ions are limited in the distance they can move within the film. As they reach this limit they are polarized, contributing to the capacitance. At higher frequencies, the cycle time decreases, and fewer ions have time to reach their limit of motion causing a decreasing capacitance with frequency. The frequency of the maximum tan δ, which is related inversely with the average ion transit time in its available space for migration, is not very reproducible from one film to another.

The wide variations in d-c resistance characteristic from one sample to another, without a corresponding change in tan δ level is believed to be due to the presence of a few lower resistance spots in the area of the film. These would affect the d-c resistance measurement greatly, but not the a-c

Approved for Public Release

Contrails

dissipation factor nearly as much.

Figures 64 and 65 illustrate the typical dielectric characteristics of a somewhat better than average capacitor with about a 0.7 micron porous oxide film over a 0.6 micron barrier layer film.

Some of the abnormal properties which have been encountered are best described by referring to the curves presented. Figure 54 is a plot of loss versus frequency for various DC bias voltages applied during loss measurements. This particular sample is one with a thicker than normal anodic film and the loss is considerably higher than normally encountered. It can be seen that with increasing bias voltage the dispersion peak is successively lowered. Also there is a time dependence present. At 180V bias the loss is lowered even further if the sample is left with the voltage applied for a length of time. In this case, after one hour it is clear that the loss was significantly decreased. Figure 55 is a plot of the capacitance as a function of frequency for the same capacitor and it can be seen that increasing the bias voltage decreases the sample capacitance. These phenomena could be attributed to Maxwell-Wagner polarization of ionic impurities within the oxide film, and in this case they seem to be rather abundant because of the high, broad dispersion peak present. Progressive application of higher d-c fields would cause ions to be polarized at one of the oxide-electrode interfaces. Since the a-c measurement voltage is only about 1 volt, this gradient will not displace the ions which are polarized by the much higher d-c voltage. A similar effect is noted in liquid impregnated paper capacitors. The contribution to the a-c capacitance by ion movement would be expected to be greatest at low frequency, where there is more time for polarization to occur in the half cycle period. Superposition of a high d-c gradient essentially prevents a-c polarization. Examination of the curve will show that such is the case. As was mentioned before, the sample of Figures 54 and 55 under consideration was one in which the oxide film was approximately four times as thick as what is termed a normal thickness of 1.3 microns. However such phenomena were noted on thinner films but to a much lesser degree.

Another test capacitor which exhibited unusual properties is that one whose characteristics are shown in Figures 57, 58 and 59 and Table 8. In this case the resistance showed an increase during the time which the sample was under voltage stress.

The reason for this behavior is not known for sure, but it is suggested that it could be due to one or two effects. It is well known that ions can be removed from films by electrolytic polarization. Another effect which could occur here is the clearing isolation by the sputtered gold electrode of low resistance spots in the film. However, it does show that anodic films with RC values of more than 100 at 500°C are possible. These results have not been duplicated and hence would be viewed with suspicion if it were not for the fact that the capacitance and loss values remained normal. This is a dramatic example of the departure from the more usual correlation of decreasing tan δ with increasing d-c resistance. The relation of the a-c test frequency to the frequency of the Maxwell-Wagner tan δ maximum at this temperature could account for this behavior. If the frequency of maximum tan δ is above 1 Kcps and is shifting downward with aging time this result could occur.

Approved for Public Release

Contrails

TABLE VIII. DIELECTRIC PROPERTIES OF CAPACITOR LT-2C AT 500°C

Time in hours at 45V D.C.*	Capacitance (μf)	100 Tan δ (1 KC)##	RC(ohm-farad)#
0	0.090	2.5	7.5
1	0.091	4.1	34.5
6	0.091	5.3	61
19	0.092	5.6-6.0	92
25	0.090	5.2	214
90	0.096	6.8-7.4	121

*Polarity the same as during anodization.
##Measured with less than 1V. rms.
#Measured at 10V DC.

Resistance measurements of all samples, with a few exceptions, have shown a decrease in value with increasing field.

The increasing current or decreasing resistance with increasing voltage is most suggestive of an increased number of charge carriers, probably electrons from the electrodes. However, a potential barrier to charge movement in the oxide film, which barrier is reduced by the electric field, could also be a possible mechanism. Here again, no single conduction mechanism fits the data obtained. Both ionic and electronic conduction mechanisms are probably contributing to the overall conduction and it would be expected that, due to the high fields, some field enhanced emission of electrons from the metal should be present. Figures 56 and 58 are resistance-voltage curves of the two previously mentioned samples and it can be seen that both have an appreciable slope. It has been observed that samples showing high RC values at 500°C do not have as steep a voltage dependence as the poorer ones.

A comparison has been made of the electrical properties of identically prepared samples except for the anodizing temperature. This data is shown in Figure 60. It was expected that due to the structure of the porous layer as described earlier, a difference would be noted. However, it is seen that the tan δ values are not significantly different. One difference that is apparent is that the capacitances are of the same order despite the fact that the number of coulombs used was different for each sample.

This is inconsistent with the usually observed dependence of capacitance on oxide film thickness, which is in turn proportional to the applied coulombs.

The electric strength of a self clearing capacitor has a somewhat different meaning than when applied to capacitors of conventional construction. In a self clearing capacitor, a localized fault draws a high current which melts or evaporates the electrode away from the fault. Hence, a localized fault does not cause a failure, but only a momentary current surge. If a sufficient field is applied to such a capacitor, however, there will be a voltage at which clearing becomes continuous and the capacitor does not stabilize. This rather uncertain point, then, represents the practical electric strength of the unit.

Approved for Public Release

Contrails

The electric strength of an anodized aluminum capacitor has been found to be mainly a function of the thickness of the oxide layer when it is operated at 400°C or below. In other words, it is more or less directly proportional to the electric field across the dielectric. At 500°C, the electric strength is much lower with the field reversed from the anodizing direction as discussed in a previous report (This contract WADC Tech. Report 59-337, Part II pp. 43-44, Sept. 1960). No further insight into this phenomenon has been attained.

Capacitors with film thicknesses of the order of 1.3 μ will stabilize for short periods of time, at least, at approximately 100 V d.c. Under extended life test conditions, they have not been stable at 500°C for any length of time. Thicker films (ca. 5 μ) have survived over 300 hours of d.c. voltages of 100V at 500°C, as will be described in the discussion of life tests. These capacitors were tested after completion of such life test as illustrated in Figures 54, 55 and 56. Table 9 summarizes the dielectric behavior of these units during the life test. The dielectric loss was fairly high at the conclusion of the life test. The effects of d.c. bias are quite dramatic in both the dissipation factor and the capacitance behavior. It should be noted that the capacitors were stable at a bias voltage of 225V.

The behavior of the resistance as a function of bias voltage as illustrated in Figure 56 is reminiscent of the behavior of a capacitor whose leakage resistance was measured after anodization and while still in the electrolyte bath. (This contract, Annual Report WADC Technical Report 59-337, Part II).

G. LIFE TESTS

Considerable difficulty has been experienced with life tests at 500°C. Capacitors with porous anodic layers of the order of 1.3 micron thickness which consistently stabilize at 400°C and give indications of a long life would rapidly fail when the temperature was raised to 500°C. In one such case, capacitors which had run for 357 hours at 30 volts d.c. with little change in their dielectric properties quickly failed or rapidly deteriorated when the temperature was raised to 500°C. After removing these units from test, it was noted that a deposit had formed, particularly on the underside of the capacitors. A spectrographic analysis of both the oxide film and the aluminum substrate revealed that a high concentration of silver was present. Since silver leads were utilized in both the life test oven and the preliminary test ovens, it was necessary to replace these with gold wire tipped with gold foil in order to obtain a simple pressure contact. Furthermore, silver paint had been used to prevent a high resistance contact at the aluminum foil connection. This also has been replaced with a thin film of sputtered gold.

Several unusual effects have been noted with certain specific capacitors. The behavior in each of the following instances could not be related to the previous history of the sample involved.

In the case of capacitor LT-2C, whose behavior on a short life test is summarized in Table 8 and previously discussed, the varying behavior of the resistance (and RC) appears to be unique, since no subsequent life test has shown a similar effect of this magnitude. The general increase in the dissipation factor, however, appears to be normal at higher voltage stresses.

Approved for Public Release

Contrails

Two effects which occurred randomly from time to time are illustrated in the photographs in Figures 61, 62 and 63. The strain lines which developed in the anodic film, Figure 61, seemed to have no relation to grain structure or possible grain growth after anodization, as one might suspect. These lines did not appear to be cracks or crazes in the oxide, since no general clearing of the gold counterelectrode occurred along the lines. Instead, it appeared that a severe stress caused a wrinkle to form in the finished capacitor. The pattern in all cases was identical on both foil faces and seemed to occur only in areas under a voltage stress, that is, areas with a sputtered gold counterelectrode. The same pattern of behavior applied to the bubbles illustrated in Figure 62 and 63. In this case, one may postulate that a gas was generated in the aluminum (perhaps hydrogen), causing a bubble to form. Both phenomena occurred only after the capacitor had been under stress for a fairly long time at high temperature.

Extended life tests have been conducted on capacitors with porous layer thicknesses of the order of 5μ. These capacitors have been run at 200°C, 100V, 60 cycles a.c. for nearly 1000 hours with only minor changes in their dielectric properties. Capacitances of the order of 0.025μf/in.^{2} and dissipation factors of 0.002-0.005 have been maintained. Series construction units with one half the capacitance have withstood 200V, 60 cycles a.c. for the same period with similar losses.

Similar single units with ca. 5μ thickness of porous layer have been life tested at 500°C with varying d.c. voltage stresses applied. The dielectric properties as a function of time and voltage are summarized in Table 9. Although the major portion of the life test was conducted at 180 volts, it is seen that the capacitors appear quite stable below 180 volts. At 180V and 500°C, apparently some chemical process is generating ions in the dielectric since both the dissipation factor and the capacitance increases considerably. The d.c. resistance also increases, perhaps indicating a large degree of polarization under these conditions.

TABLE IX. LIFE TEST OF A 1.5 SQ. IN., 5μ FILM CAPACITOR AT 500°C UNDER VARYING DC VOLTAGE STRESS

Voltage	Total Time (Hrs.)	100 Tan δ**	Capacitance (μf)	Resistance (Ω)##	RC
10V	0	5.7	0.0186	5 x 10^8	9.3
45	0.5	11.0	0.0213	4.3 x 10^8	9.1
45	2.0	14.0	0.0217	3.0 x 10^8	6.4
*10V	2.0	25.0	0.025	4.3 x 10^8	10.7
45	3.0	25.0	0.026	5 x 10^8	13.0
45	7.5	25.0	0.026	6.6 x 10^8	17.2
90	9.5	12.0	0.0215	4.0 x 10^8	8.6
90	26.0	29.0	0.0225	4.3 x 10^8	9.7
135	29.5	10.8	0.020	2.1 x 10^8	4.2
135	31.0	10.2	0.023	1.6 x 10^8	3.7
135	86.25	20.0	0.027	1.4 x 10^8	3.8
135	88.5	11.5	0.021	2.5 x 10^8	5.3
135	97.5	13.2	0.021	3.1 x 10^8	6.5
180	100.5	12.5	0.021	2.8 x 10^8	5.9
180	326.5	39.0	0.031	1 x 10^{10}	310
180#	326.5	46.0	0.045	1.3 x 10^9	59
180	330	34	0.030	---	---

\# No voltage applied for 24 hrs. * Sample removed from oven for examination.
Measured at 10V. ** Measured at ca. 1V, 1 Kcy.

Approved for Public Release

Contrails

H. SUMMARY

A certain degree of success has been achieved in fabricating high temperature anodic alumina capacitors. These have voltage capabilities of 50 to 100V with about 1.3 micron films and capacitances of about 0.04μf/sq. in. Films with this thickness have been stable in life tests at 400°C, but so far not at 500°C. Thicker films of about 5 microns with correspondingly lower capacitance have been stable for 300 hours at 500°C with 180V d-c. Similar units have shown no change in more than 1000 hrs. at 200°C with 100V 60 cy. applied continuously. RC factors of 5 to 10 and tan δ values of .05 to .20 at 500°C can be produced fairly regularly. Occasionally much higher RC values have been obtained.

Approved for Public Release

Contrails

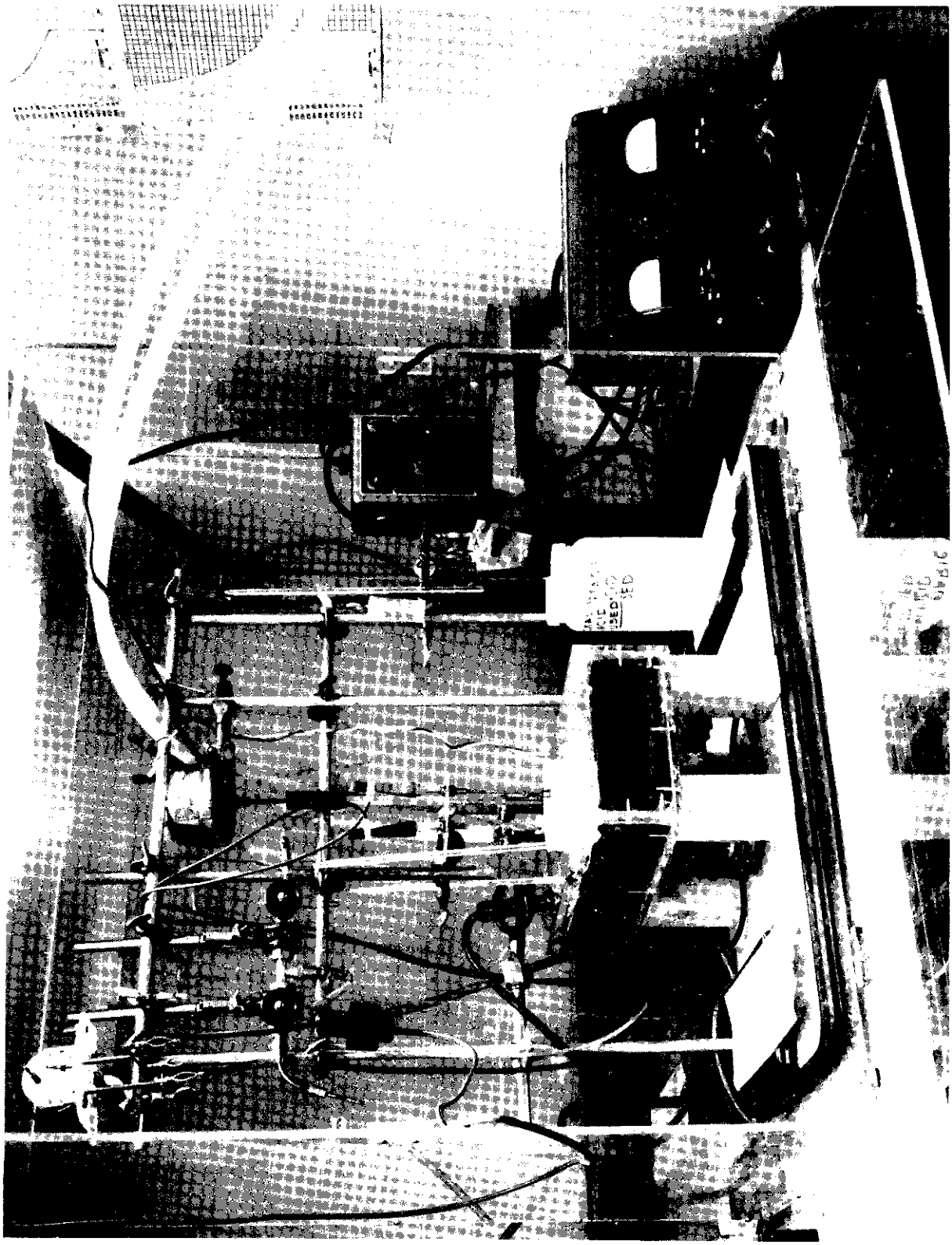

Fig.39—Anodizing equipment.

Approved for Public Release

Contrails

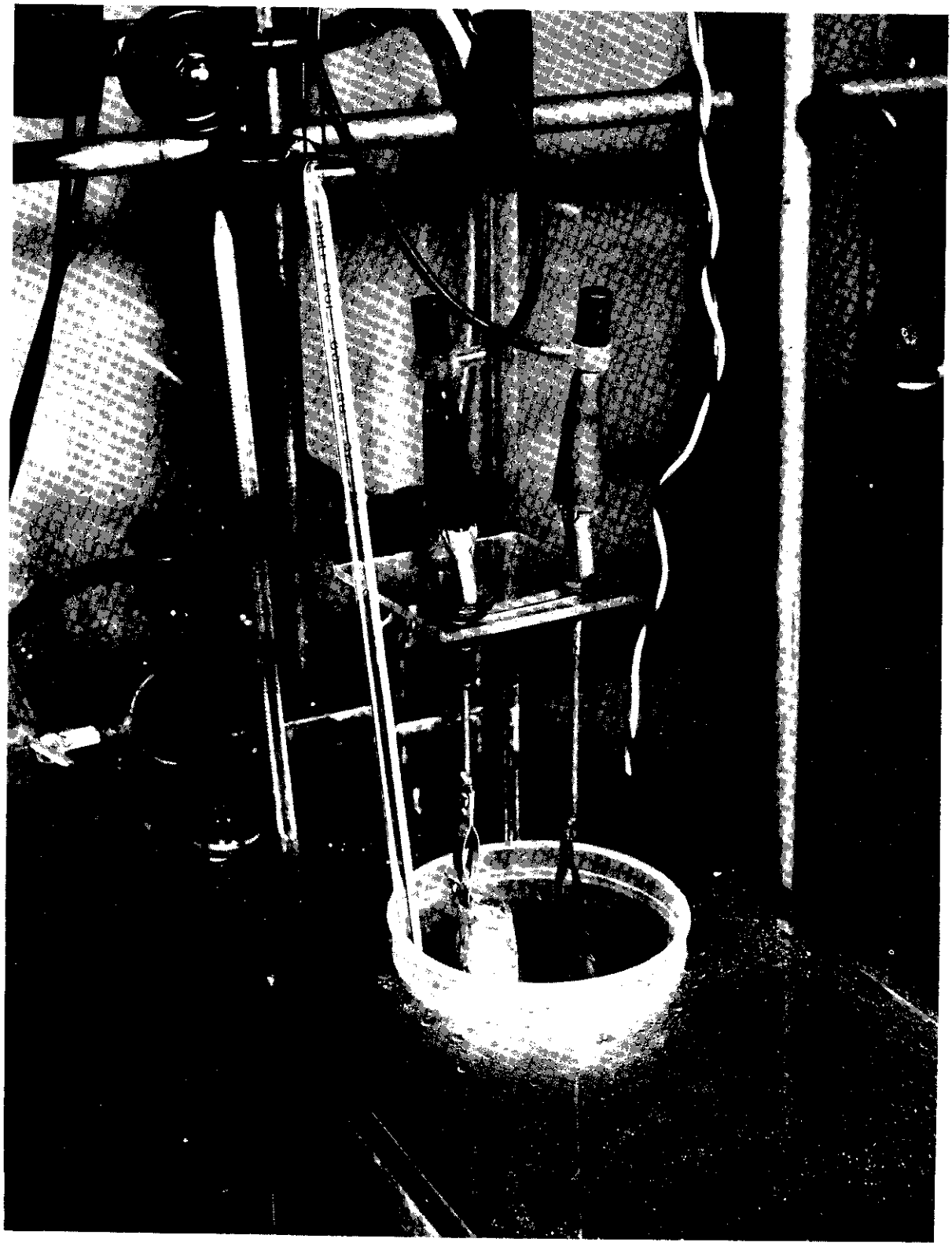

Fig. 40- Anodizing cell.

Approved for Public Release

Contrails

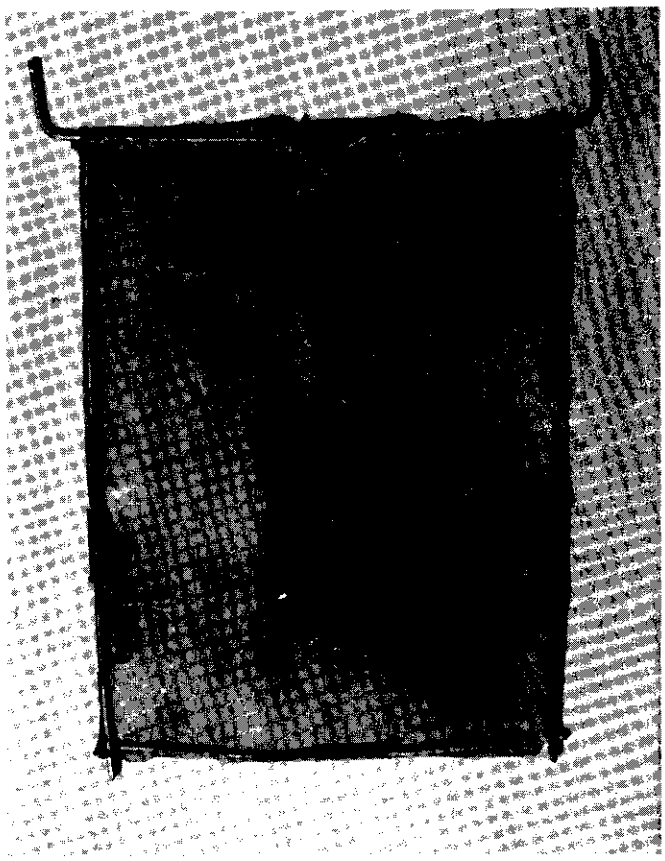

Fig. 41 Screen Separator Used in Cell.

Approved for Public Release

Contrails

Fig.42-- Placement of test capacitors in oven.

Approved for Public Release

Contrails

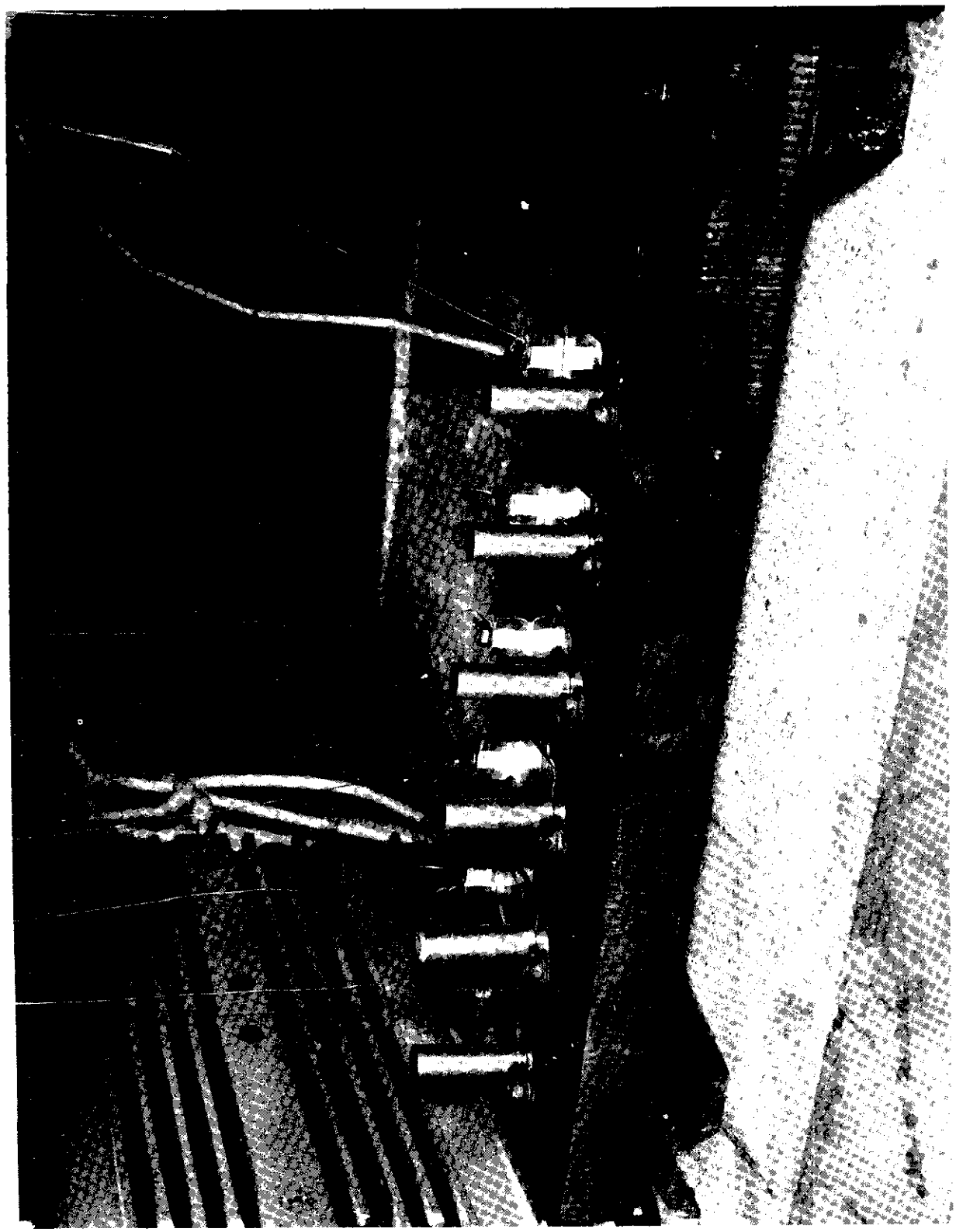

Fig. 43— Life test oven and samples.

Approved for Public Release

Contrails

Fig. 44 – Test equipment.

Approved for Public Release

Contrails

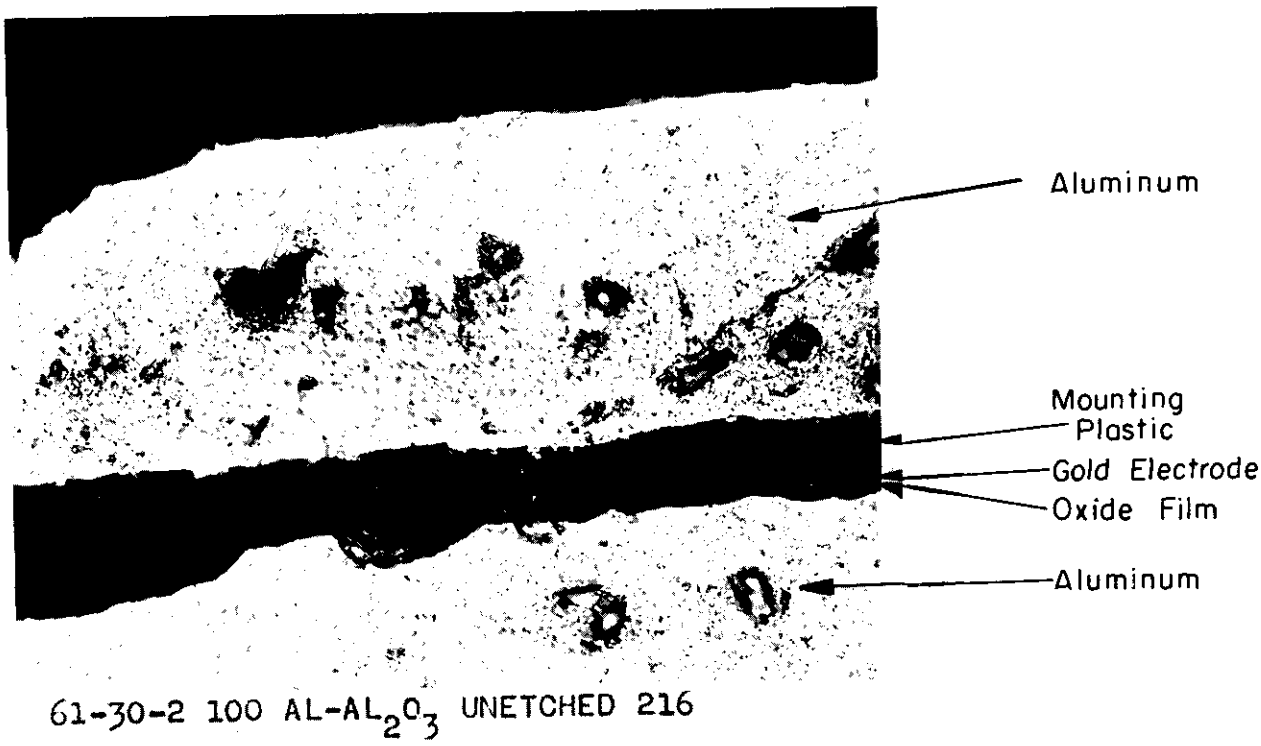

Fig. 45— Cross section of sample capacitor (X1000)

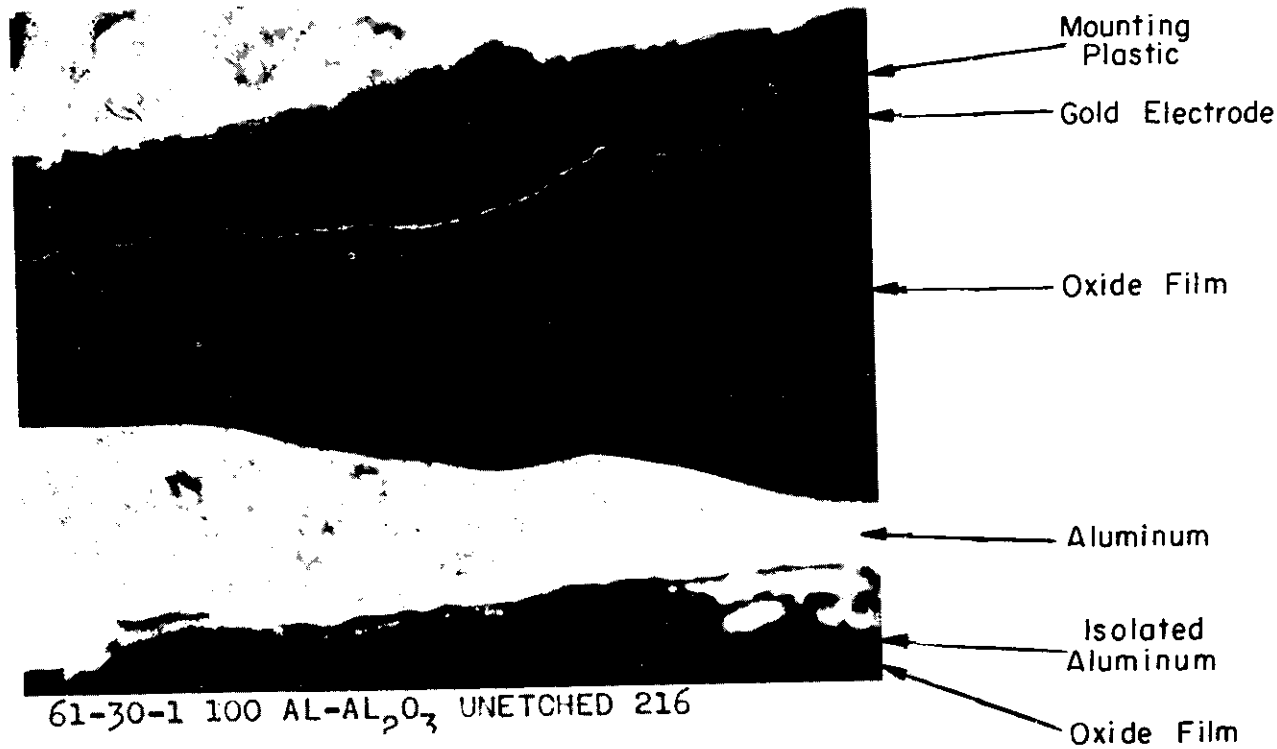

Fig. 46— Cross section of thick oxide section of capacitor in fig. 45.

Approved for Public Release

Contrails

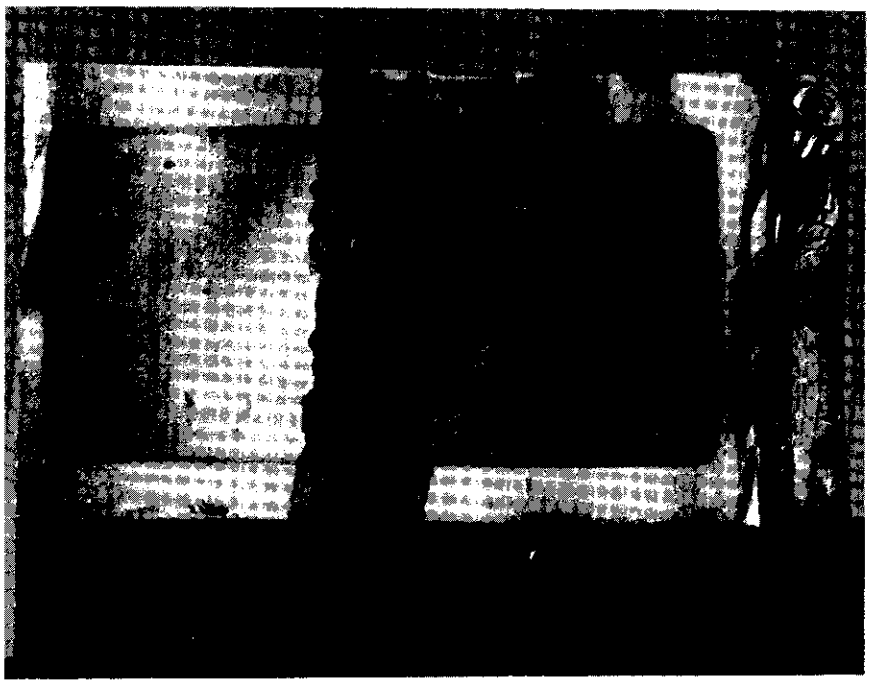

Fig. 47 Large Grain Capacitor.

Approved for Public Release

Contrails

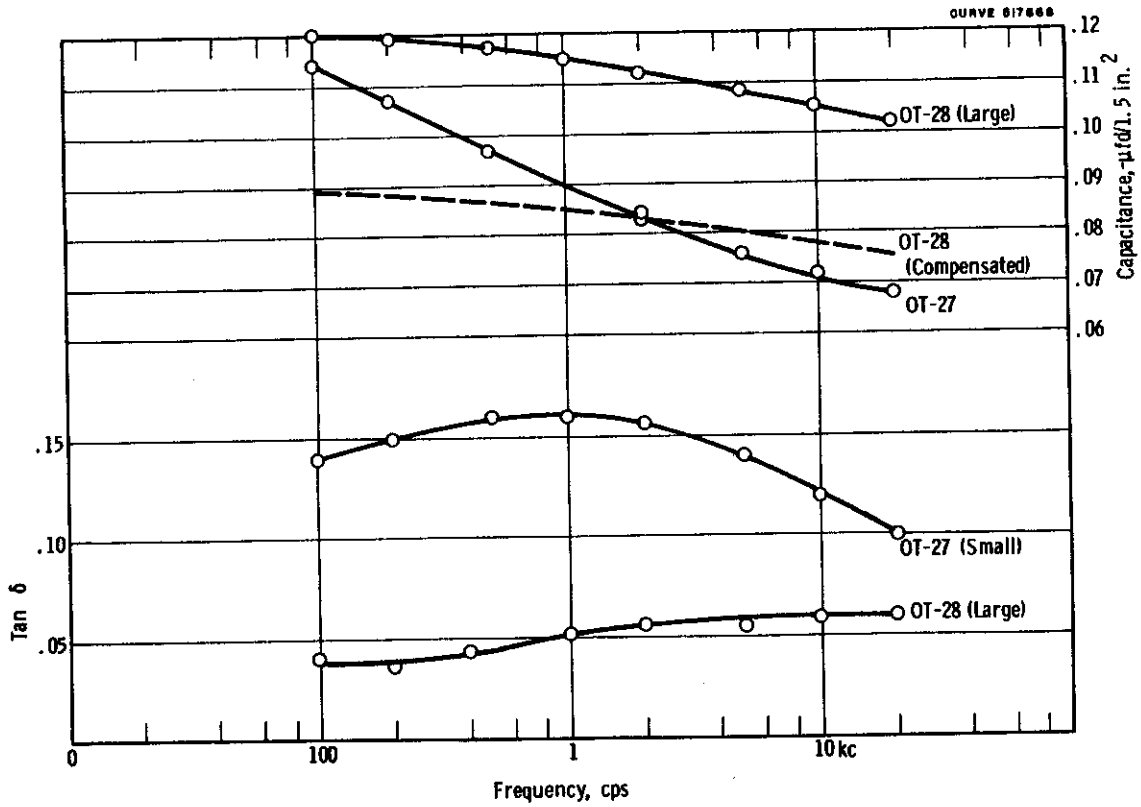

Fig. 48--Effect of grain size on the electrical properties of anodically formed Al_2O_3 film capacitors

500°C

Approved for Public Release

Contrails

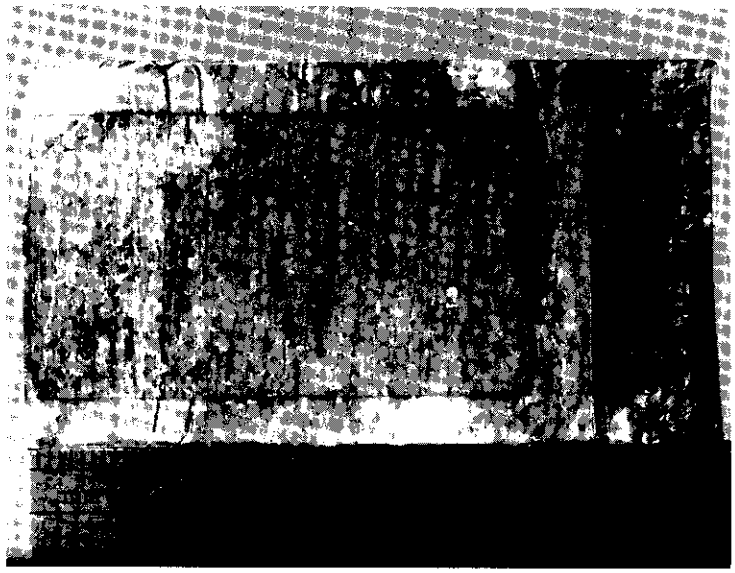

Fig. 49--Capacitor made from highly cold worked aluminum

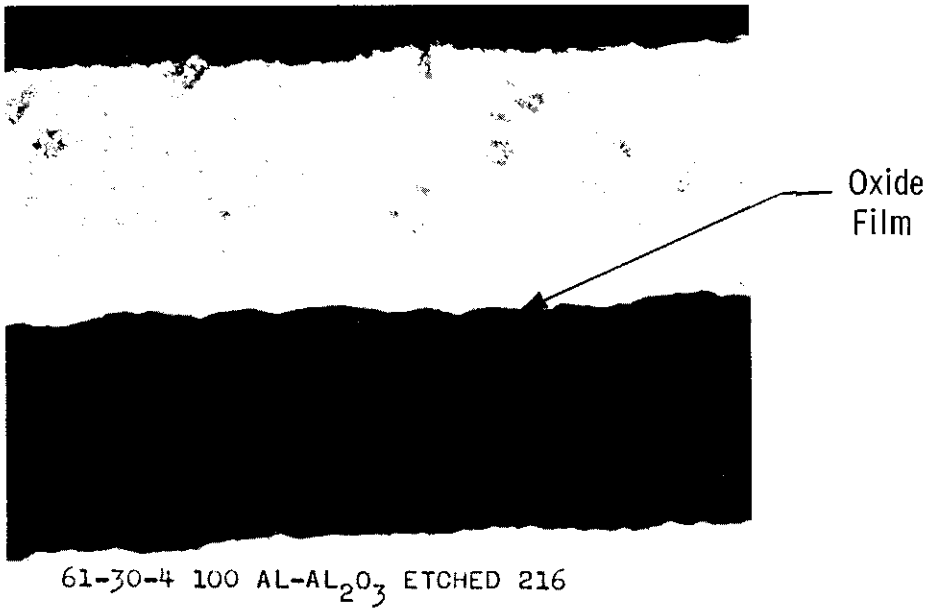

Fig. 50--Cross section of sample capacitor showing uneven oxide film (X 1000)

Approved for Public Release

Contrails

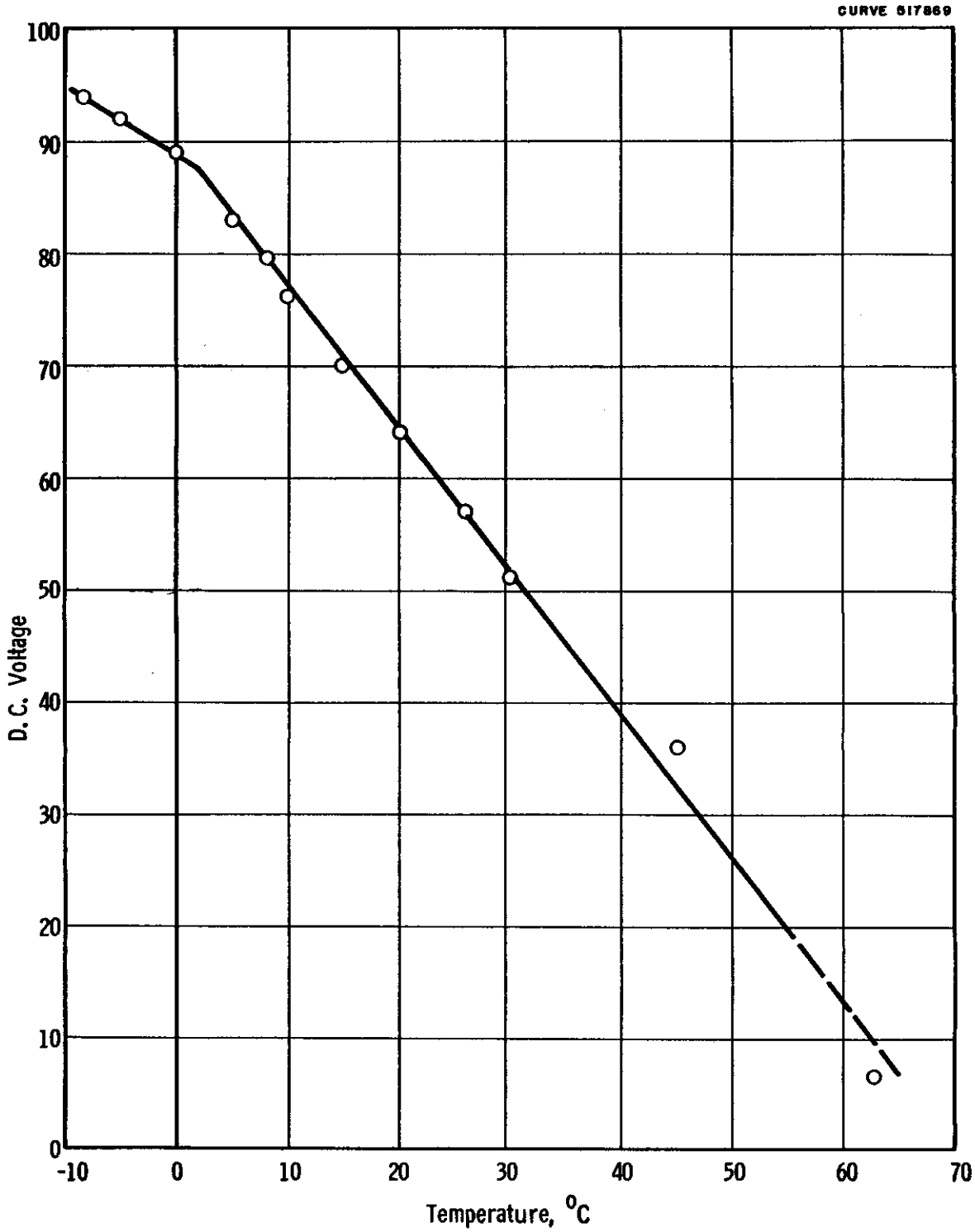

Fig. 51--Temperature effects on the solvation of the oxide barrier layer

Approved for Public Release

Contrails

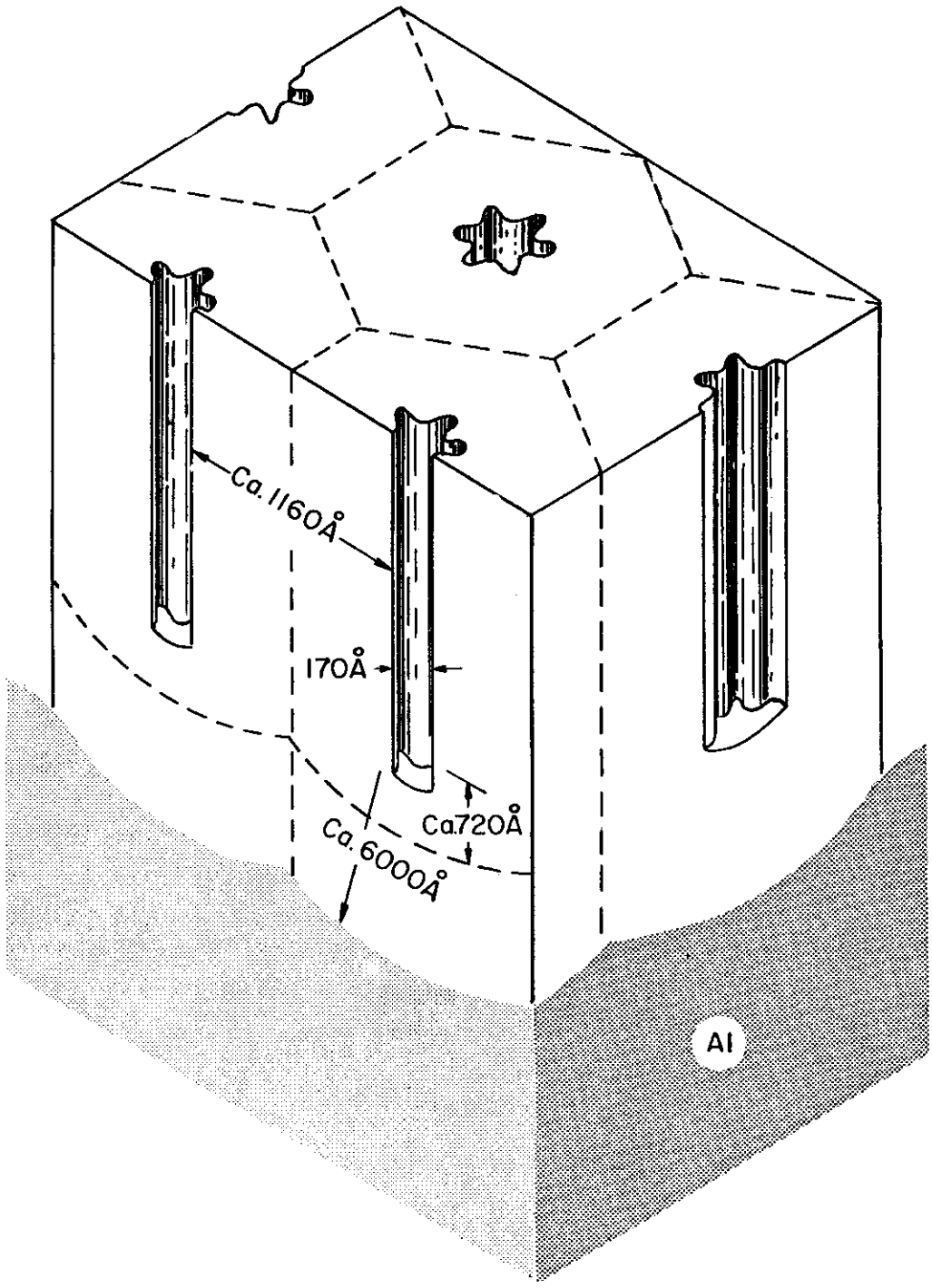

Fig. 52--Schematic cross section of cell base pattern for 60 volt, 2% oxalic acid solution at 23°C and 500 V tartaric anodization. [After Keller etal., J. Electrochem. Soc. 100, 411 (1953).]

Approved for Public Release

Contrails

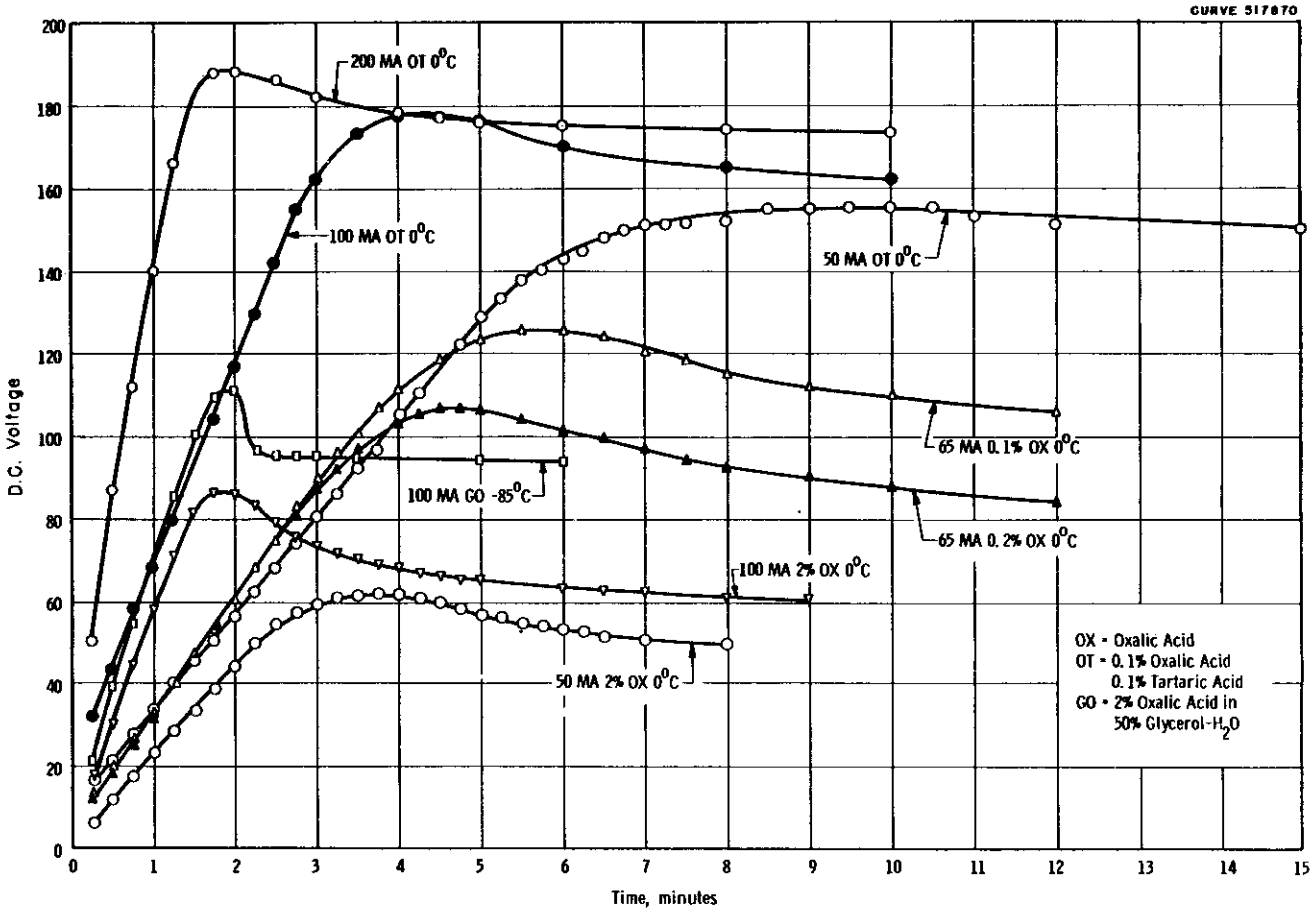

Fig. 53--Initial formation voltage - time behavior with various anodizing conditions

Approved for Public Release

Contrails

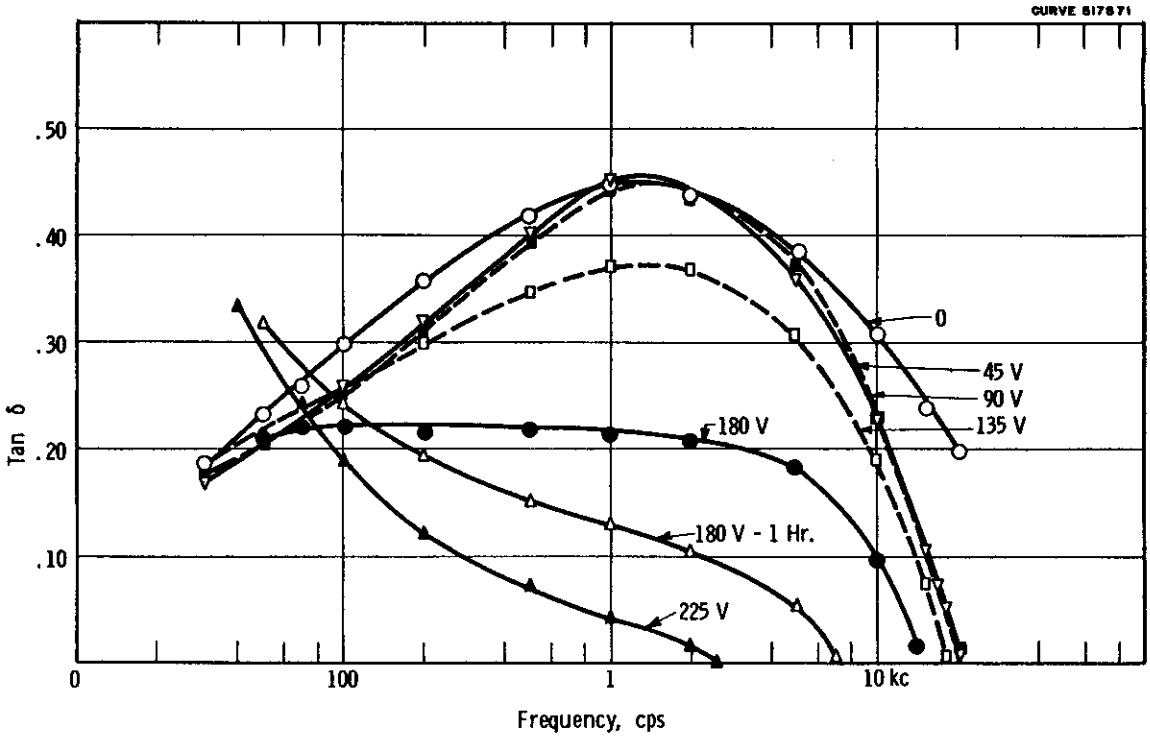

Fig. 54--Dielectric loss as a function of frequency and D.C. bias voltage of a 5 micron oxide film capacitor
500°C

Approved for Public Release

Contrails

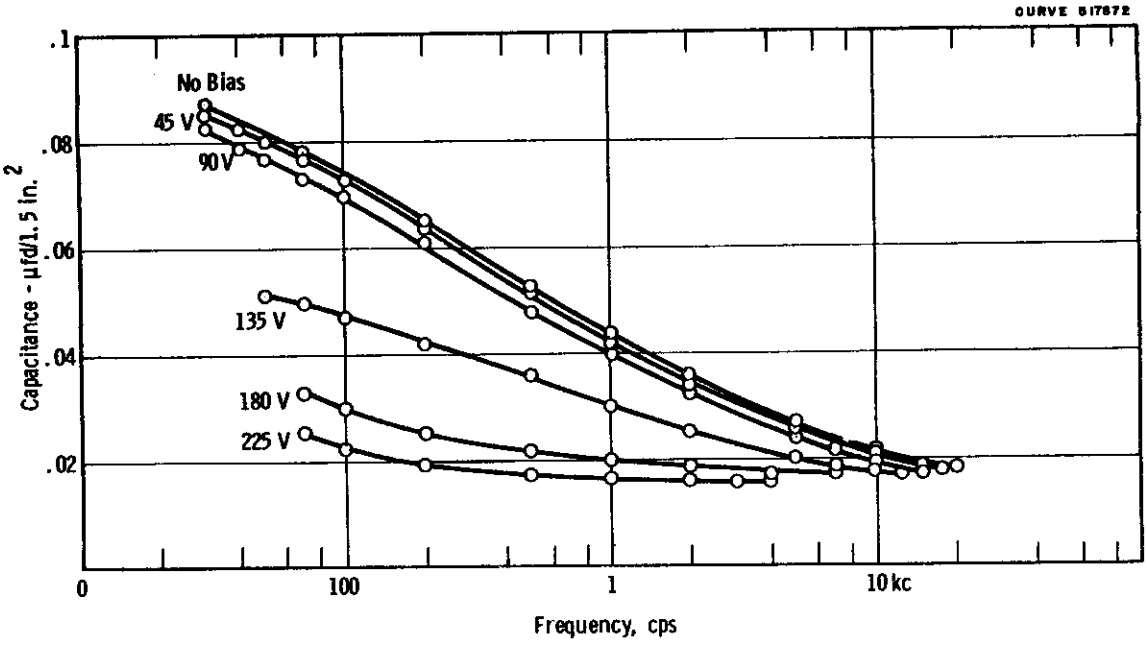

Fig. 55--Capacitance as a function of frequency and D. C. bias voltage of a 5 micron oxide film capacitor 500°C

Approved for Public Release

Contrails

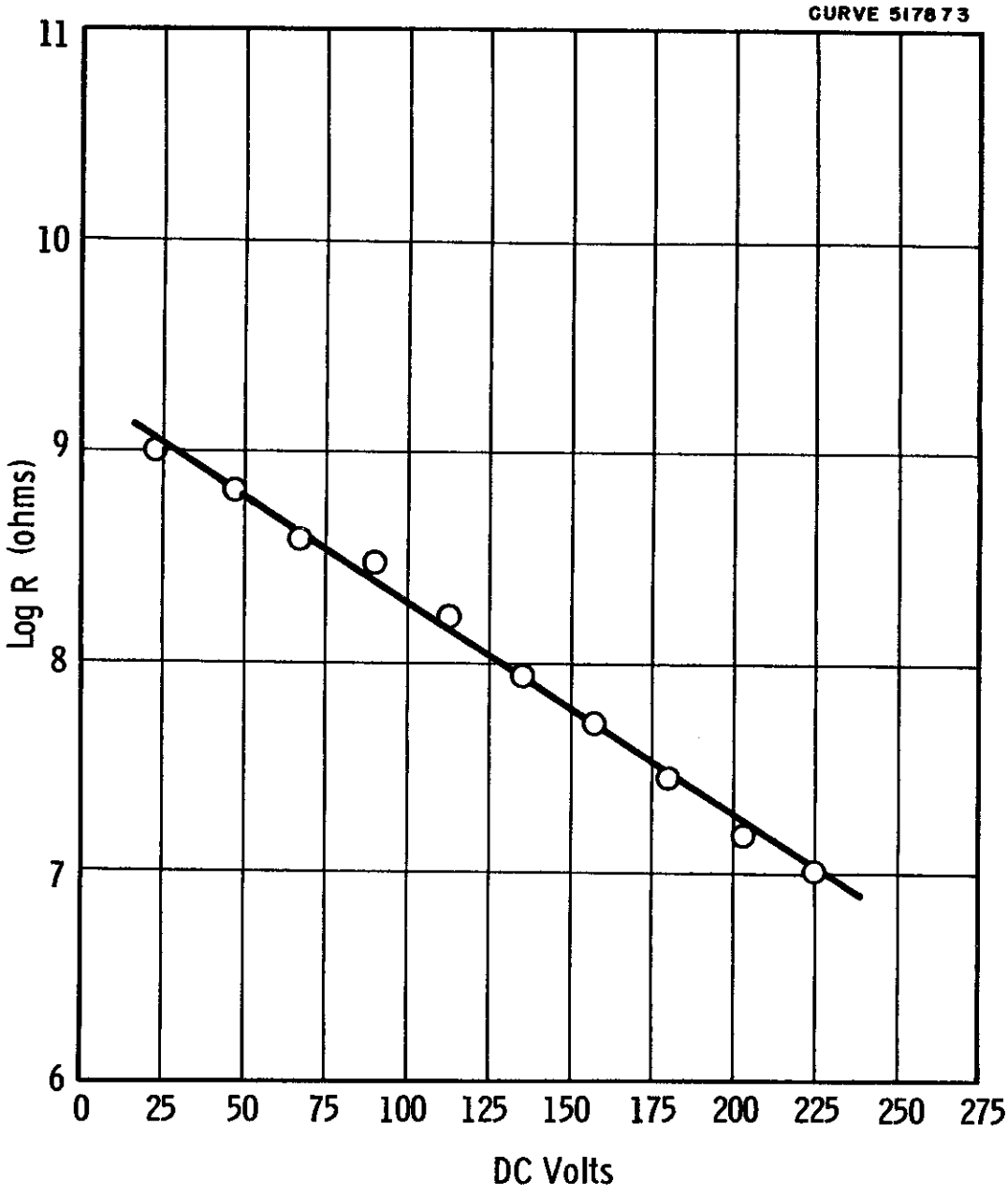

Fig. 56--Resistance-voltage characteristics of a 5 micron oxide film capacitor

Approved for Public Release

Contrails

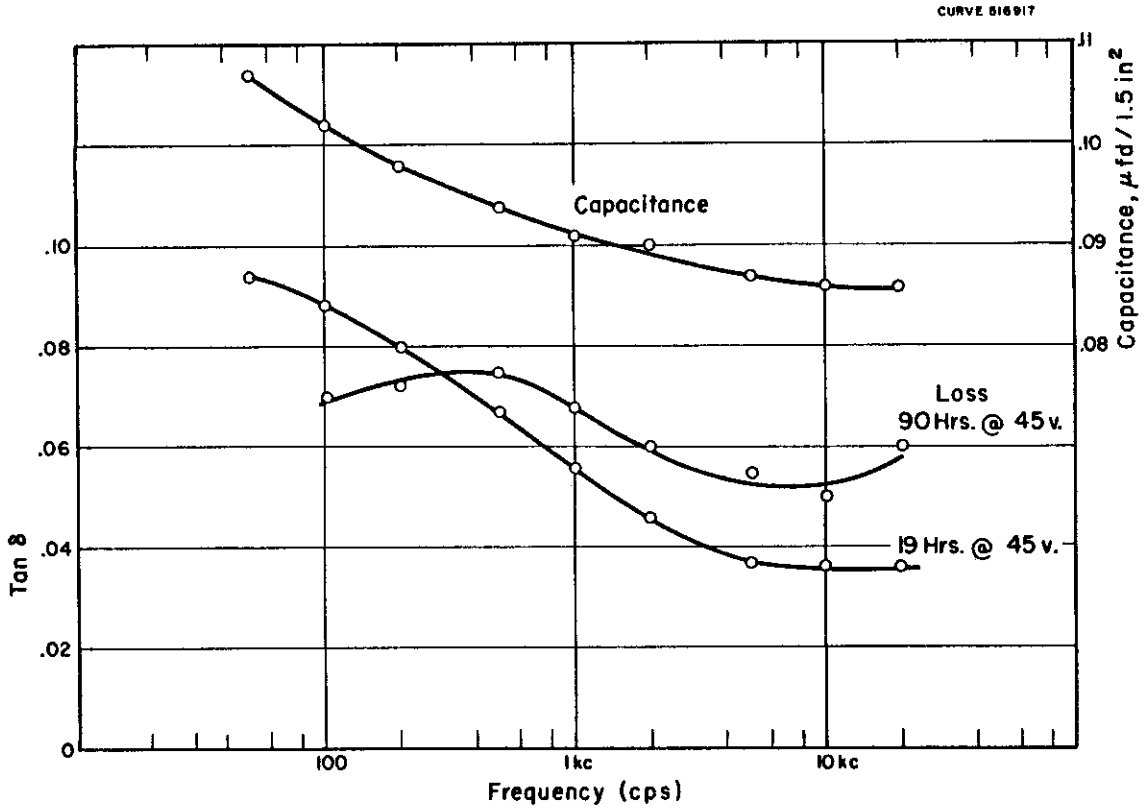

Fig.57-Frequency characteristics of loss and capacitance for capacitor LT-2C at 500°C.

Approved for Public Release

Contrails

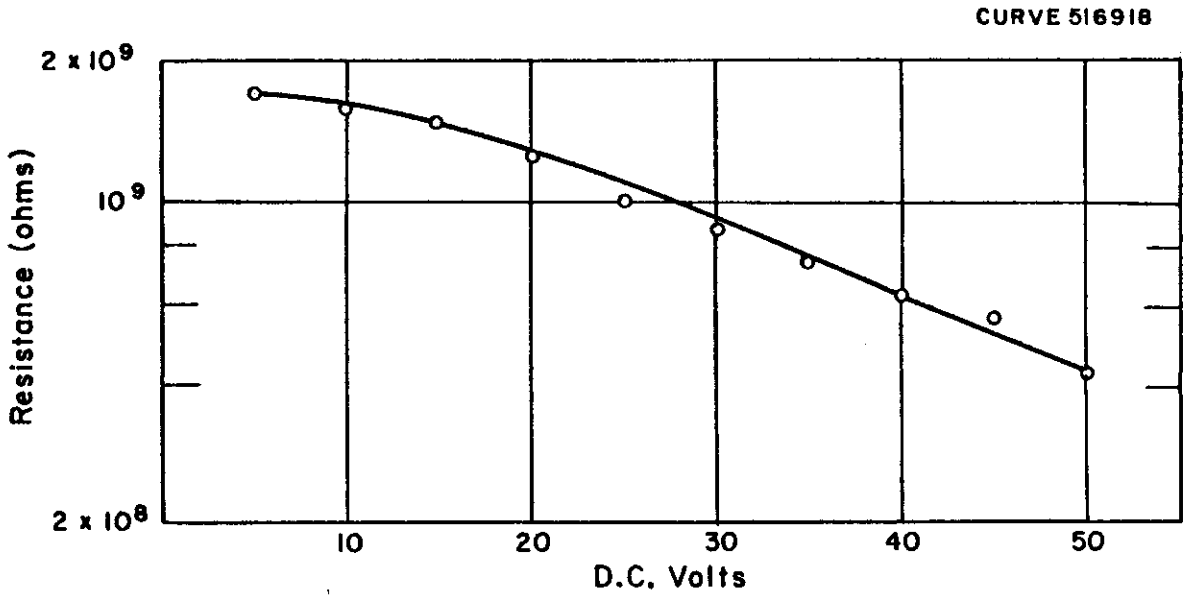

Fig.58- Resistance voltage characteristics of capacitor LT-2C at 500° C.

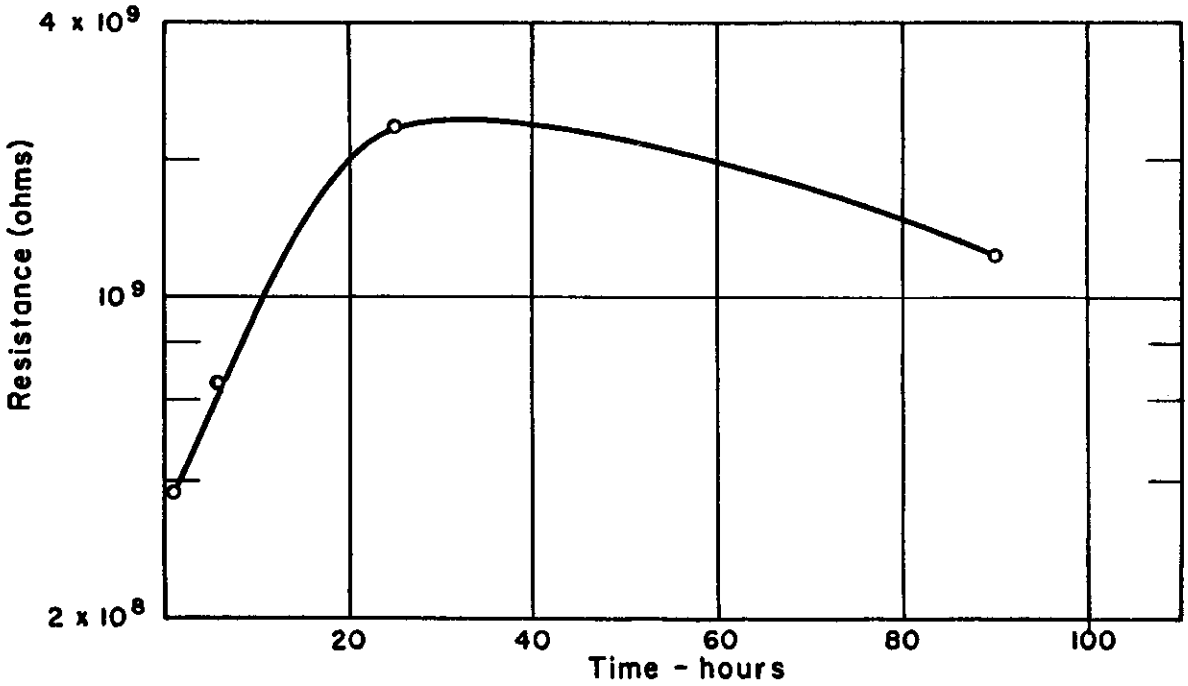

Fig.59-Effect of aging time under a voltage stress of 45 volts for capacitor LT-2C at 500° C.

Approved for Public Release

Contrails

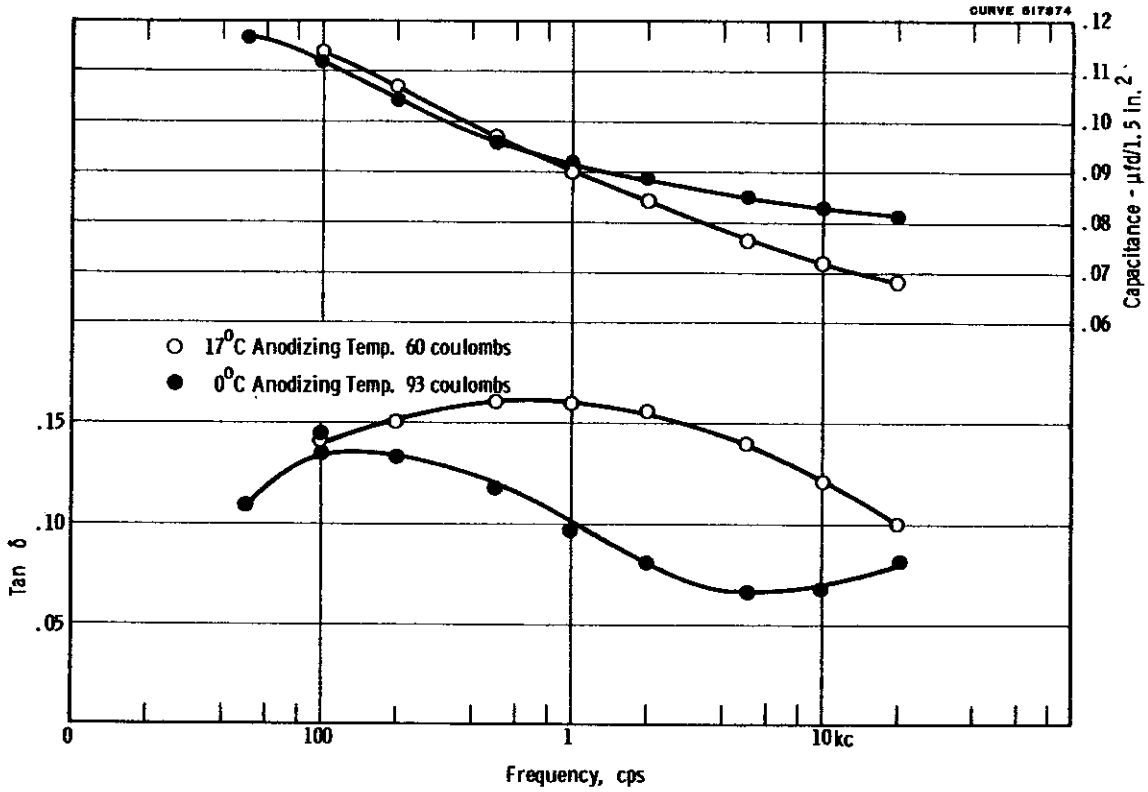

Fig. 60--Effects of anodizing temperature on the electrical properties of anodized aluminum capacitors

500°C

Approved for Public Release

Contrails

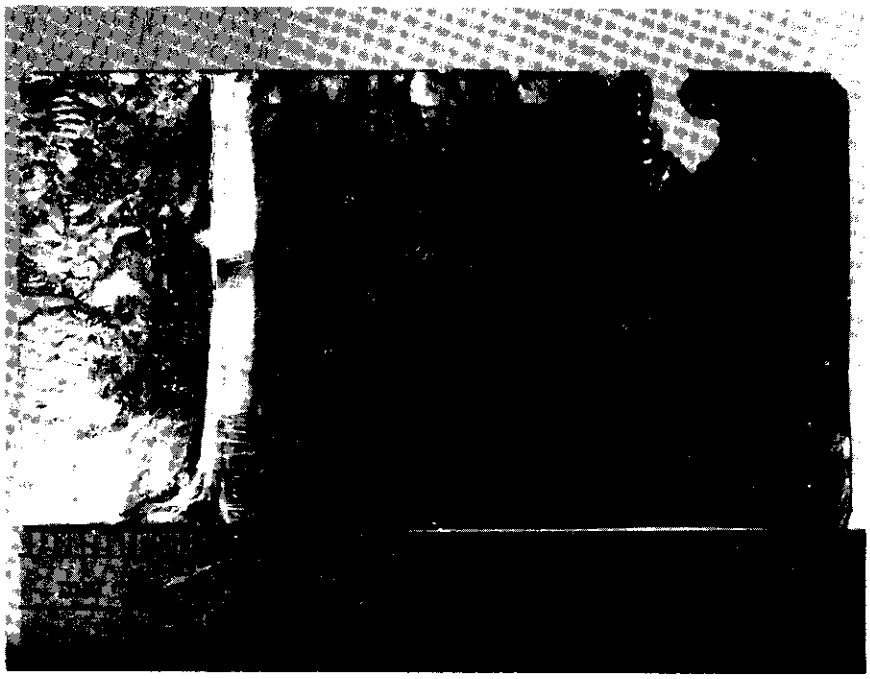

Fig. 61 Development of Apparent Strain Lines Under the Counterelectrode of a Sample Capacitor Aged Under Electrical Stress.

Approved for Public Release

Contrails

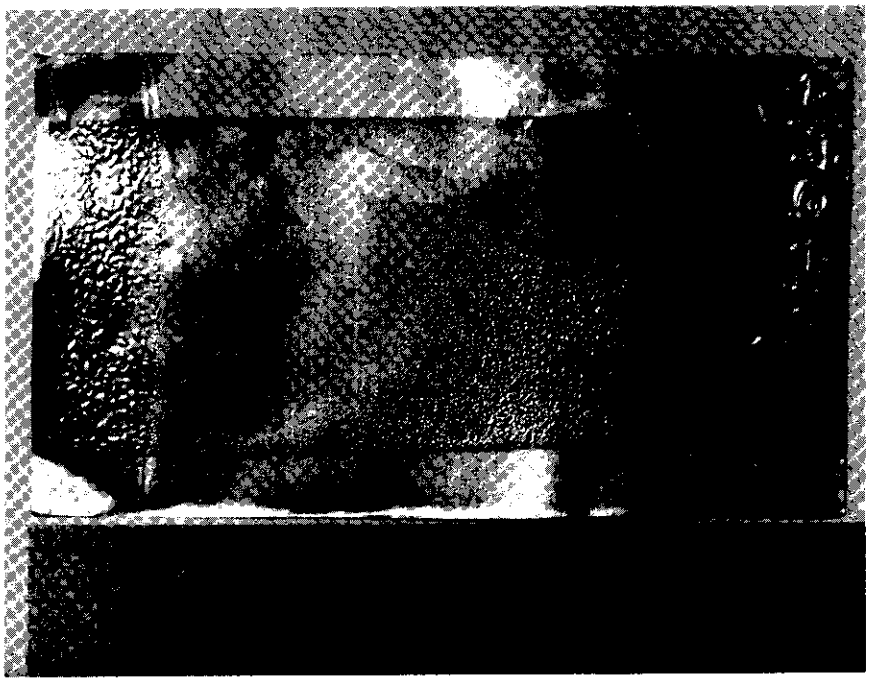

Fig. 62 Development of Bubbles Under the Counterelectrode for a Sample Capacitor Aged Under Electrical Stress.

Fig. 63 Reverse Side of Capacitor in Figure 62.

Approved for Public Release

Contrails

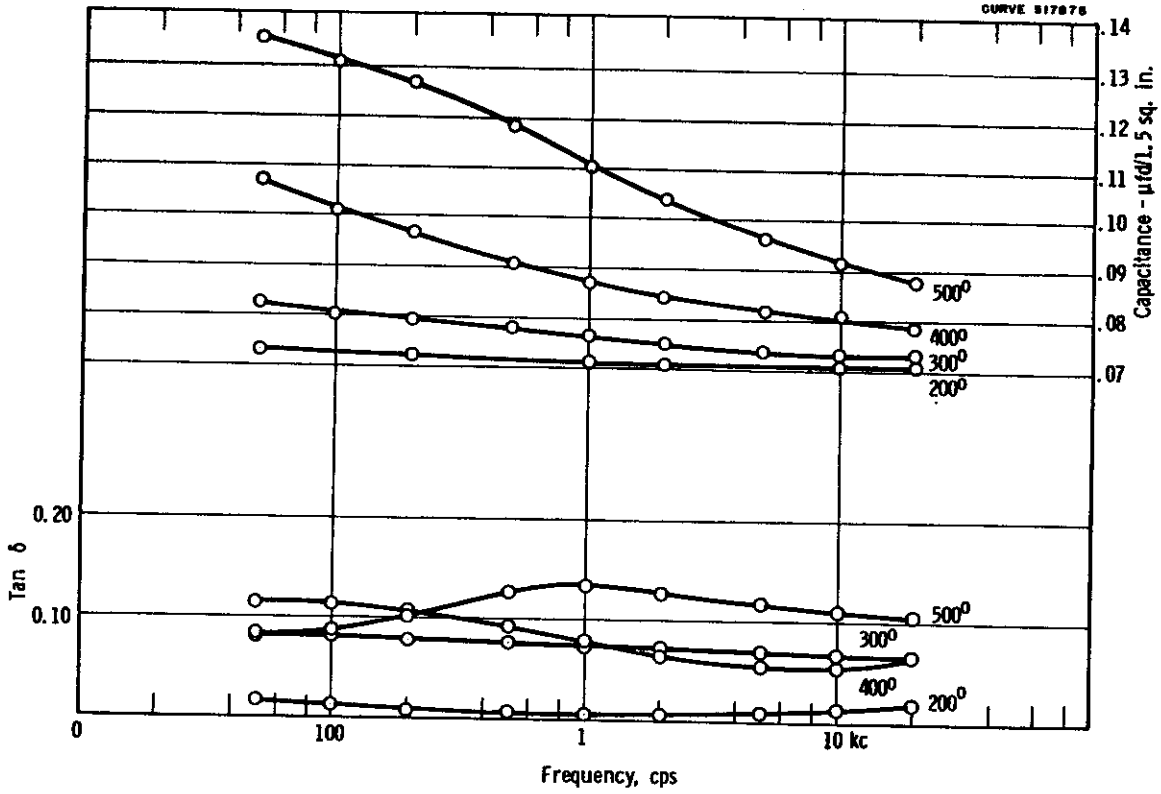

Fig. 64—Dielectric properties of a 1.3 micron anodized aluminum capacitator (No. 02)

Approved for Public Release

Contrails

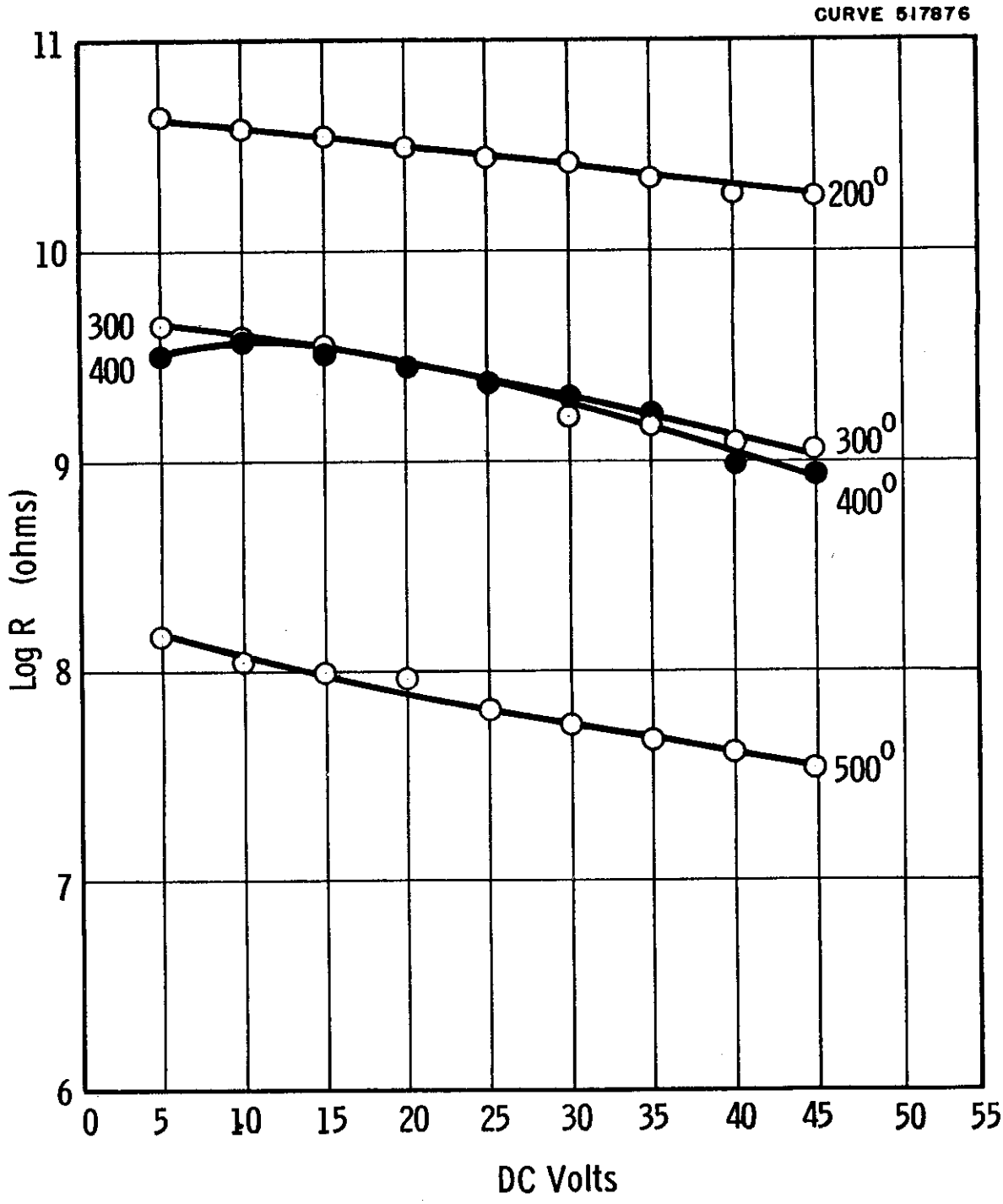

Fig. 65--Resistance-voltage temperature characteristics of 1.3 micron anodized aluminum capacitor (No. 02)

Approved for Public Release

Contrails

33,000 X 5965 A

1 μ

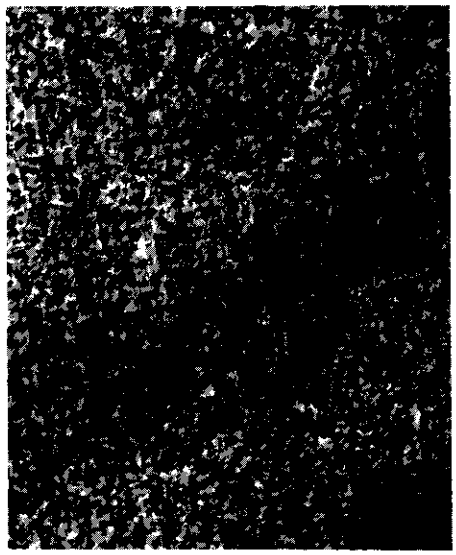

18,000 X 5965 B

1 μ

5,900 X 5965 C

3 μ

Fig. 66--Electron micrograph of high purity, large grained and polished aluminum anodized in 2% oxalic acid at 17°C and 5.8 ma/cm^2

Approved for Public Release

Contrails

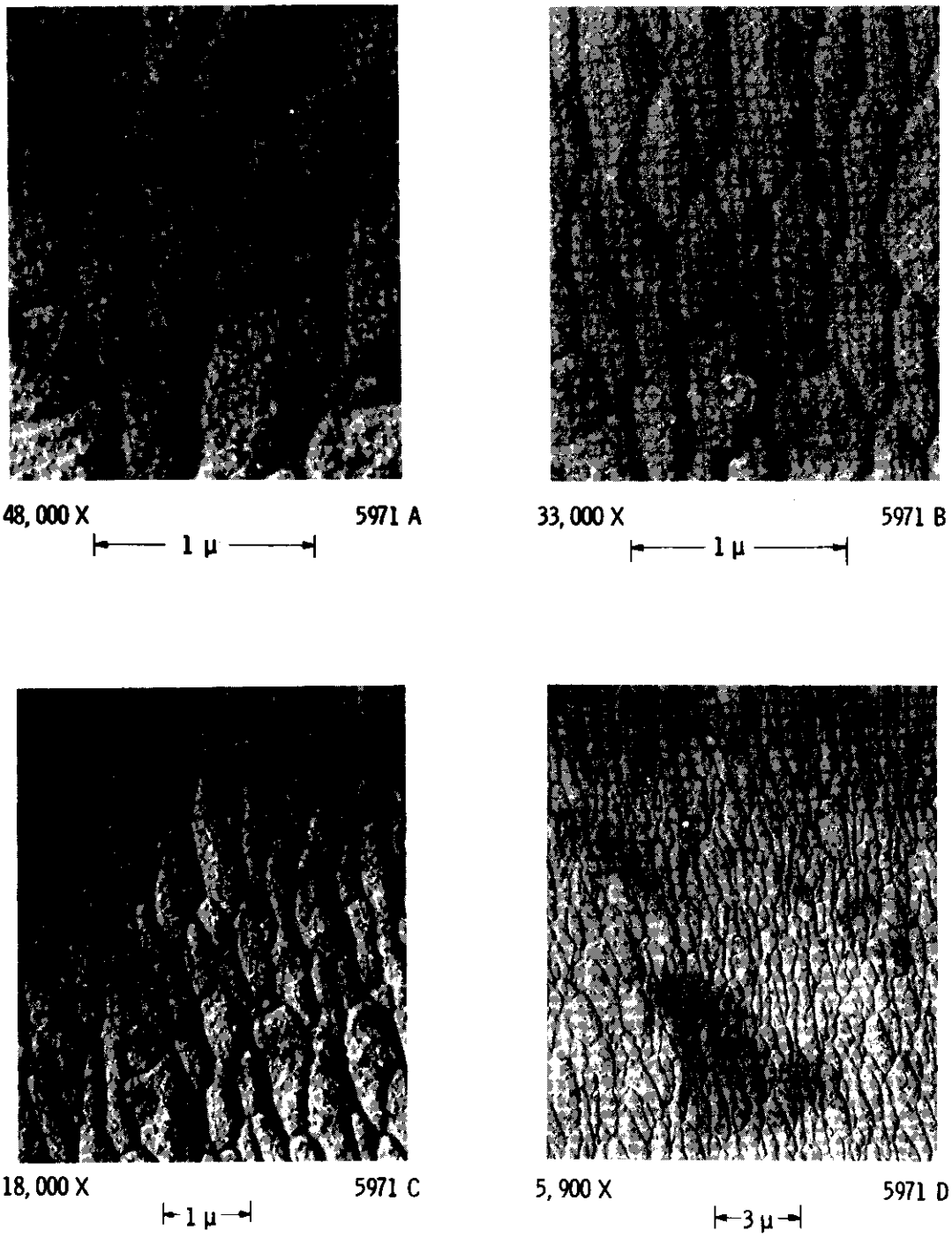

Fig. 67--Electron micrograph of high purity, annealed and polished aluminum anodized in 2% oxalic acid at 0^{0}C and 11.6 ma/cm^{2}

Approved for Public Release

Contrails

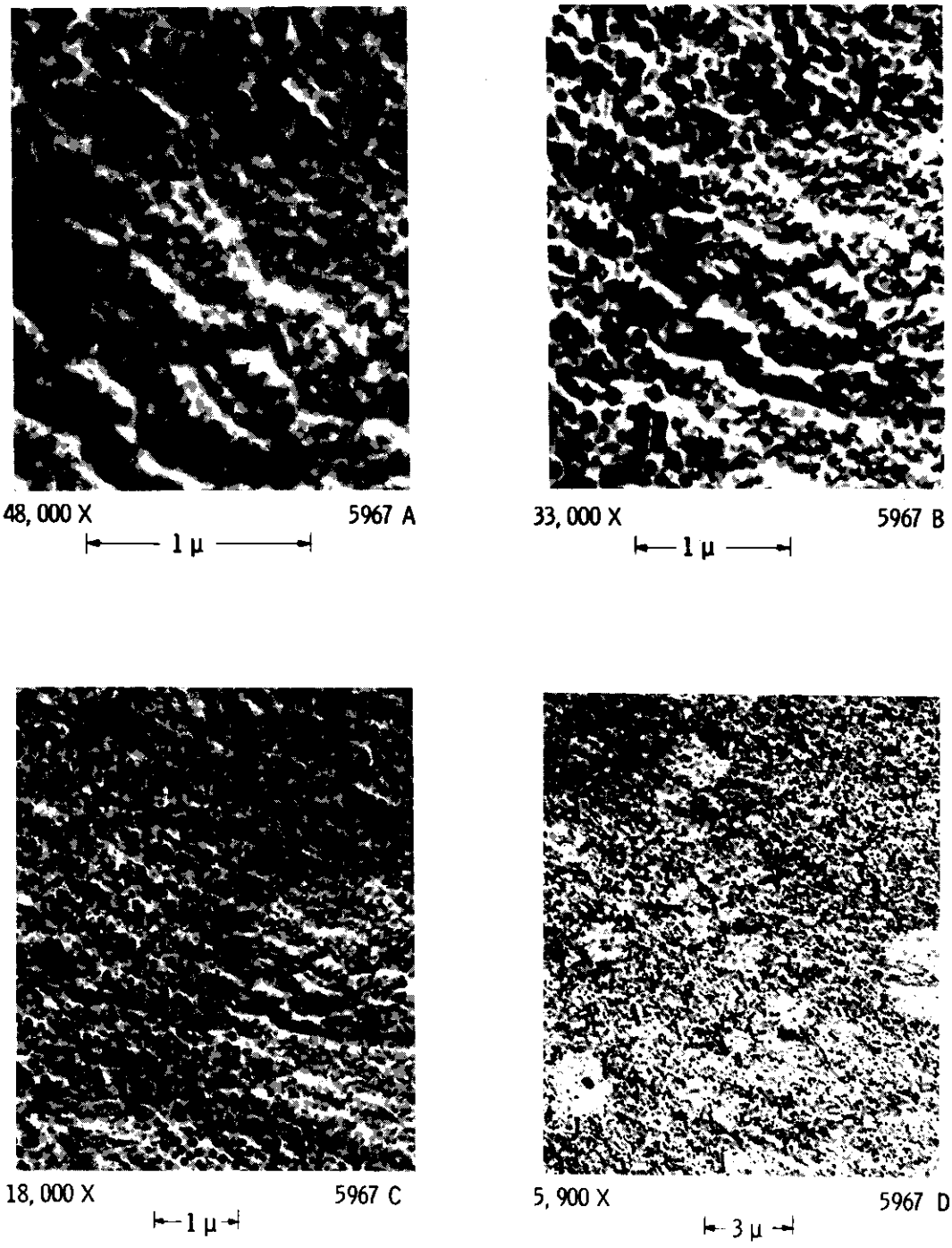

Fig. 68--Electron micrograph of high purity, large grained and polished aluminum anodized in 0.1% oxalic acid, 0.1% tartaric acid at 0^{0}C and 5.8 ma/cm^{2}

Approved for Public Release

Contrails

GENERAL CONCLUSIONS AND SUGGESTIONS FOR FUTURE WORK

The research program under this contract has repeatedly confirmed the importance of eliminating impurities to obtain the best dielectric properties in inorganic materials for high temperature use. The elimination of impurities from the starting materials as well as the prevention of their introduction during fabrication of the materials into useful forms have both been emphasized. Following these principles, good high temperature dielectric properties have been produced both in molded or sintered blocks of alumina and boron nitride and thin films of these same materials. The feasibility of forming satisfactory thin film high temperature capacitors of boron nitride and alumina has been demonstrated.

Syntheses of boron phosphide have demonstrated that this compound is not a good insulator.

Preparation and evaluation of films of a number of good dielectric materials by arc plasma jet spray has revealed that this process introduces contamination into the materials, which seriously detracts from the high temperature dielectric properties.

It is suggested that future work be continued to further perfect the anodized aluminum films for high temperature capacitor and other insulation applications. While good properties have been obtained with these films fairly regularly, superior properties have been obtained occasionally, indicating that proper control of impurities and fabrication techniques could result in a much better dielectric film than has been achieved regularly so far. Further basic investigation of the mechanism of conduction and polarity and voltage effects in these dry anodized films should also give results leading to further improvement of these films, possibly in the area of higher breakdown voltage.

So far, the program of preparation of very pure inorganic dielectric materials has centered around a few rather simple compounds. There is a large area of more complex ceramic and glass compositions which could very likely give many improved high temperature dielectric materials of different and desirable properties if a similar approach of purification were pursued with those materials.

Approved for Public Release